Characteristics and origin of the Weldborough sapphire, NE Tasmania

Brendan Michael McGee
BSc.

UNIVERSITY OF TASMANIA
School of Earth Sciences

CODES
ARC Centre of Excellence in Ore Deposits

A research thesis submitted in partial fulfilment of the requirements for an Honours degree at the School of Earth Sciences, University of Tasmania.

November 2005

Abstract

Alluvium and colluvium in the Weldborough area, NE Tasmania, yield sapphire, zircon and spinel, corroded by magma and abraded by alluvial transport. Drainage patterns and inferred palaeodrainage indicate the Weldborough basalts are the primary source. The Weldborough intraplate alkali basalts are fine-grained, olivine- and/or clinopyroxene-phyric with varying content of mantle and crustal xenoliths and xenocrysts. Despite extensive study, no sapphire or zircon megacrysts are found in the basalt or related clastic rocks. The Weldborough sapphires are blue (80%), yellow and green (20%) with rare pink sapphires. They contain olivine, feldspar, spinel, zircon, molybdenite and Nb-Ta-rich phases as mineral inclusions. The composition of zircon inclusions indicates the parental melt was highly evolved. Secondary olivine mineral inclusions are present. Primary fluid inclusions indicate a minimum trapping pressure of 4.5 kbar at 1000 to 1200ºC. LA-ICPMS analysis indicates the sapphires have iron (2590 ppm), titanium (383 ppm), gallium (258 ppm) and tantalum (186 ppm) as the most abundant trace elements. Niobium, beryllium, magnesium, vanadium, chromium and tin are low level trace elements in the Weldborough sapphires. Beryllium, titanium, niobium and tantalum are enriched in the cores of the sapphires. Two element associations were recognised in the sapphires: an Fe-V-Ga association and an Nb-Ta-Be association. The Nb-Ta-Be association is typical of input by an incompatible-element rich melt such as a granite pegmatite or a carbonatite. The sapphires have O-isotope values of + 4.4 ‰ to + 6.3 ‰, indicating they are in O-isotope equilibrium with rocks of mantle O-isotopic compositions and little or no crustal interaction is inferred in the source. The zircon inclusions in the sapphires have a U-Pb age of 47 ± 4 Ma which is identical to the age of the Weldborough basalts (46.8 ± 0.6 Ma). The zircon inclusions have been reset during entrainment in basaltic magma. The Weldborough sapphires were entrained and brought to the surface by the Weldborough basalts 47 million years ago. The Weldborough basalts are the source of sapphire, spinel and zircon found in the Ringarooma, George and possibly the Boobyalla River catchments. The broad range of trace element and inclusion data reported here support an origin for the sapphire in shallow parts of the underlying mantle.

Acknowledgements

I would like to thank the following many people who have helped me a various ways throughout the year. In particular, I would like to thank my father, Michael, for his understanding support throughout the year.

My supervisor Dr. Khin Zaw, for making this type of project possible. His guidance, support and humour is very much appreciated.

My co-supervisor Dr. Ron Berry, for his extensive assistance in my attempt at unravelling the corundum conundrum.

My co-supervisor and company liaison officer, Dave Duncan, for invaluable field assistance, discussions, advice and accommodation.

Neil Kinnane and Van Dieman Mines for generous logistical support.

Mineral Holdings Australia - the company which started the sapphire project in 1995.

Almost all of the academic staff at the School of Earth Sciences and CODES at UTAS, especially Dima Kamenetsky and Sebastian Meffre.

Simon Stephens for his enthusiasm, important discussions, technical advice and assistance.

Ralph Bottril, Marcus McClenaghan and John Everard (Mineral Resources of Tasmania) for providing Tasmanian-based expertise.

Terry Mernagh (Geoscience Australia) and Tzen-Fu Yui (Academia Sinica, Taiwan) for assistance with foreign analytical techniques.

Honours soldiers Adam (Adamathon) King, Sam (Samathon) Ekins, John (Oh Jonathon) de Little, Kim Hurd, Katherine Harris, Melanie (Melathon) Sutterby and Corey (The Superfly) Jago. Joel (Ball and Chain) Kitto must be recognised for setting the pace early.

My friend Paul (Maths is a beer) Burch for field assistance, data analysis and logistical support. Al Chambers for keeping the home fires burning. Gordon Williams, Nathan Turner and Douglas Beattie for field assistance.

My brother Zac for not asking about my thesis in times of stress and, of course, Natalee for her support and friendship.

TABLE OF CONTENTS

TITLE PAGE..... *i*

ABSTRACT..... *ii*

ACKNOWLEDGMENTS..... *iii*

TABLE OF CONTENTS..... *iv*

LIST OF FIGURES..... *vii*

LIST OF TABLES..... *ix*

CHAPTER 1: INTRODUCTION **10**

1.1 Sapphire and Ruby **11**
1.1.1 Introduction 11
1.1.2 Variation 11
1.1.3 Occurrence 12
1.1.4 Corundum from alkali basalt terrains 14

1.2 Tasmanian Sapphires **16**

1.3 Previous exploration **17**

CHAPTER 2: BACKGROUND GEOLOGY **18**

2.1 Location **18**

2.2 Climate **18**

2.3 Relief **18**

2.4 Geology **18**
2.4.1 Mathinna Beds 18
2.4.2 Devonian granites 20
2.4.3 Parmeener supergroup 21
2.4.4 Jurassic and Cretaceous igneous activity 21
2.4.5 Tertiary basalts and associated sediments 21
2.4.6 Quaternary 22

2.5 The source of the sapphire – a review **22**
2.5.1 Potential host rocks in north eastern Tasmania 23
2.5.2 Present day drainage and paleodrainage 23

2.6 Review of potential corundum sources **27**
2.6.1 Silurian-Devonian Mathinna Beds 27
2.6.2 Cretaceous Lamprophyre Dykes 27
2.6.3 Devonian Granite pegmatites 27
2.6.4 Sediment hosted corundum 27
2.6.5 Tertiary alkali basalts 28

2.7 Conclusion **28**

CHAPTER 3: FIELD OBSERVATIONS, BASALT PETROGRAPHY AND GEOCHEMISTRY 29

3.1 Previous Work Summary 29
3.1.1 The Weldborough basalts 29
3.1.2 Greys Hill 30
3.1.3 Mutual Hill 30

3.2 Field Observations 30
3.2.1 The Weldborough basalt 31
3.2.2 Basaltic agglomerate 32
3.2.3 Polymict conglomerate 32
3.2.4 Greys Hill Basalt 33
3.2.5 Mutual Hill basalt 34
3.2.6 The Gardens 35
3.2.7 Discussion 36

3.3 Petrography 36
3.3.1 Basalt 36
3.3.2 Agglomerate and conglomerate 37

3.4 Geochemistry 38

CHAPTER 4: THE CHARACTERISTICS OF THE WELDBOROUGH SAPPHIRE 39

4.1 Introduction 39
4.1.1 Experimental Techniques 39

4.2 General characteristics of the Weldborough sapphire 43

4.3 The mineral and fluid inclusions of the Weldborough sapphire 44
4.3.2 The mineral inclusions of the Weldborough Sapphire 48
4.3.3 Inclusions detected by LA-ICPMS 48
4.3.4 Fluid inclusions in the Weldborough Sapphire 60

4.4 The mineral chemistry of the Weldborough Sapphire 64
4.4.1 Trace element chemistry of corundum 64
4.4.2 Trace element chemistry of the Weldborough sapphire 65
4.4.3 Results 67
4.4.4 Discussion 75

4.5 Oxygen isotopes 78
4.5.1 Results 78
4.5.2 Discussion 79
4.5.3 Conclusion 83

4.6 Geochronology 83
4.6.1 Introduction 83
4.6.2 Previous Work 84
4.6.3 Results 85
4.6.4 Discussion 85

CHAPTER 5: SUMMARY AND EVALUATIONS 90

5.1 The characteristics of the Weldborough Sapphire 90

5.2 Evidence for sapphires being basalt hosted 90

5.3 Evaluation of the primary source 91

5.4 Sapphire genesis implications 91
5.4.1 Evaluation of contemporary sapphire genesis models 92

5.5 Recommendations for future work 94

CHAPTER 6: REFERENCES 95

Appendix 1: Basalt Petrography
Appendix 2: Photomicrographs of basalt
Appendix 3: Geochemistry of basalts
Appendix 4: Laser Raman Spectra
Appendix 5: LA-ICPMS Results
Appendix 6: Literature review: "Corundum Occurrence"

List of figures

Figure 1. Tasmanian corundum localities (after Bottril, 1990)…….…...…….…… 12
Figure 2. Geology of NE Tasmania (modified from Moore, 1991)…….……. 19
Figure 3. Present day catchment boundaries (modified from Jordan, 1975)...…….. 23
Figure 4. Distribution of the Weldborough sapphire (modified from Yim et al., 1985 and Jordan, 1975)…….…….. 25
Figure 5. Improved geological map of the Weldborough area (modified from Moore, 1991)…… 31
Figure 6. A – Photograph of columnar jointing (Fieldwicks Quarry)
B – Photograph of basaltic agglomerate (Fieldwicks Quarry)…….…. 34
Figure 7. A – Photograph of polymict conglomerate outcrop
B - Photograph of polymict conglomerate…….. 35
Figure 8. Crystal habit of corundum (After Guo, 1993)……...….. 44
Figure 9. Physical features of the Weldborough sapphire (Six photographs)…… 45
Figure 10. LA-ICPMS detected inclusions (Four LA-ICPMS spectra)…….. 50
Figure 11. Photographs of mineral inclusions (Eight photomicrographs)…….. 52
Figure 12. Photographs of mineral inclusions (Four photomicographs)…… 53
Figure 13. Photomicrographs of CO_2 –rich fluid inclusions (includes temperature data)….. 61
Figure 14. Temperature-density diagram for a pure CO_2 system. Used for determination of fluid inclusion density (After Roedder, 1984)……. 62
Figure 15. Temperature-pressure-density diagram for pure CO_2 system. Data from this study included (after Roedder, 1984)…… 63
Figure 16. LA-ICPMS spectra with analytical spikes…… 66
Figure 17. LA-ICPMS spectra exhibiting inclusions…….. 66
Figure 18. Fe v Ga/Mg discrimination diagram (Data from this study included, after Peucat et al., 2005)……..... 68
Figure 19. Trace element discrimination diagram (after Sampinpanya et al., 2003)……. 69
Figure 20. Explanation for rim and core values in detrital grains (after Guo, 1993)……. 72
Figure 21. Rim and core plots for four Weldborough sapphires (this study)……. 73
Figure 22. Fe, V, Mg and Ga in rims and cores of sapphires (this study)…….. 74
Figure 23. Nb, Ta, Ti and Be in the rims and cores of sapphires (this study)……74
Figure 24. Nb-Ta-Be correlation plot for the Weldborough sapphire (this study) …… 76
Figure 25. V-Fe-Ga correlation plot for the Weldborough sapphire (this study)……....77

Figure 26. Oxygen isotope values of the Weldborough sapphires: Histogram (this study)…80
Figure 27. Corundum O-isotope values for different host rocks (after Giuliani et al., 2005 including the Weldborough sapphires (this study)…….……..…….. 81
Figure 28. Corundum O-isotope values for sapphires from basaltic hosts (after Giuliani et al., 2005) including the Weldborough sapphire (this study)…..……..…… 82
Figure 29. Zircon inclusion reverse U-Pb concordia plot (Khin Zaw, submitted)……. 86
Figure 30. Detrital zircon U-Pb concordia plot (this study)……..…….. 87
Figure 31. Comparison of zircon ages (this study) with rocks from NE Tasmania…… 88

List of Tables

Table 1. Major occurrence of corundum in different rock types (after Guo, 1993)…….13
Table 2. NE Tasmania Quaternary stratigraphy (McClenaghan et al., 1984)…….. 22
Table 3. Summary of potential sapphire sources for NE Tasmania……. 26
Table 4. Sample locations and characteristics of sapphires for inclusion studies…….40
Table 5. Hand specimen characteristics of sapphires for LA-ICPMS…….. 42
Table 6. Mineral inclusions reported in corundum (multiple references)…….46
Table 7. Summary of inclusions in the Weldborough sapphires (this study)……48
Table 8. Zircon inclusion chemistry (this study)……54
Table 9. Elemental chemistry of Nb-Ta bearing phases known to occur in corundum….. 59
Table 10. LA-ICPMS results summary (this study)…….……..…….67
Table 11. Trace element chemistry comparisons of corundum (this study)……...…….70
Table 12. Correlation table of trace elements (this study)……...……70
Table 13. The Weldborough sapphire rim and core data (this study)……...……...71
Table 14. O-isotope compositions of the Weldborough sapphire (this study)…….78
Table 15. Summary of ages and geochronology for NE Tasmanian rocks……..……84
Table 16. Zircon inclusion U-Pb ages (this study)……...86
Table 17. Detrital zircon U-Pb ages (this study)……..86
Table 18. Sapphire genetic evidence obtained through this study……...91
Table 19. Characteristics of the Sutherland et al. (1998a) and the Guo et al. (1996a) genesis models for corundum from alkali basalt terrains…… 92

Chapter 1: Introduction

Gem corundum (sapphire and ruby) occur in placer deposits in many areas of Tasmania (Figure 1), with the most promising area for fossicking and exploration being in the states north east (Bottrill, 1996). In this part of Tasmania, cassiterite placers and certain sediments contain the minerals monazite, ilmenite, zircon, corundum, pleonaste (Mg-Al-Fe spinel) and rare chrysoberyl (Yim et al., 1985). The corundum ("The Weldborough sapphire") is present in low quantities and the primary source of this occurrence remains an enigma, although, on the basis of detrital sapphire distribution, it has long been believed that the Weldborough Basalts are the source of the sapphires. On this basis, Totteny Pty Ltd explored for primary sapphire deposits in 1988 which resulted in failure (Morrison, 1989). Until now, only minor research had been done into the characteristics of the sapphires or the nature of their primary source.

The first aim of this research thesis is to determine the macroscopic, microscopic and chemical characteristics of the Weldborough sapphires. Features such as the physical characteristics (i.e. colour and shape), mineral chemistry, oxygen isotope chemistry, the mineral/fluid inclusion types and geochronology of the sapphires will be examined. This will be used to contrast the sapphires with literature examples and evaluate modern sapphire genesis models. Microanalytical techniques such as Laser Ablation Induced Coupled Plasma Mass Spectrometry (LA-ICPMS) and Laser Raman Spectroscopy (LRS) are used to analyse the trace and minor element chemistry and the fluid and mineral inclusions in the sapphires. Laser fluorination is used to determine the oxygen isotope compositions of sapphires and U-Pb dating is performed on zircon inclusions and detrital grains. Information recovered from this study will add to the growing database on world wide sapphire characteristics.

The second aim of the thesis is to determine the type and location of the primary source of the Weldborough sapphires. As mentioned above, the sapphires occur in placer deposits in low concentrations. To establish the location of a concentrated primary source would allow for further investigation of economic sapphire recovery. Sapphire characteristics, stream sediment heavy mineral analysis and a palaeodrainage study will be used as tools to predict the primary source location.

This chapter (Chapter 1) contains introductory material on this research project, corundum, Tasmanian sapphires and previous exploration. Chapter 2 contains

background information on the geology of NE Tasmania and a review of potential sources for the Weldborough sapphire. Chapter 3 contains information on the study area, field observations and petrography of the basaltic units. Chapter 4 contains the characteristics of the Weldborough sapphires, i.e. the physical characteristics (i.e. colour and shape), mineral chemistry, oxygen isotope chemistry, the mineral/fluid inclusion types and geochronology. Chapter 5 contains the geochemistry and petrography of basaltic rocks from the field area and discusses potential host units in the study area. Chapter 6 will contain the conclusions of the study and recommendations for further work.

1.1 Sapphire and Ruby

1.1.1 Introduction

Sapphire and ruby are varieties of corundum (Al_2O_3) and are highly valued as two of the four "precious" gem stones (plus diamond and emerald). Natural corundum (α-Al_2O_3) belongs to the trigonal crystallographic system. β-Al_2O_3 (hexagonal) and γ-Al_2O_3 (cubic) are synthetic polymorphs that, along with heating, convert to α-Al_2O_3 and therefore not found in nature (Deer et al., 1992).

The physical properties of corundum include an extreme hardness (9/10 on Moh's Scale), high specific gravity (3.98-4.02), a distinctive basal parting {0001}and is insoluble in all acids.

Corundum has a hardness of nine on Moh's scale and hence can also be used as an abrasive (commonly in the form of emery), although the artificial production of corundum (dehydration of bauxite) is now favoured.

1.1.2 Variation

Substitution in the lattice of aluminium with Fe^{2+} or Ti^{2+} is responsible for the variety of blue hues exhibited in sapphires whilst Cr^{3+} causes the red tint of rubies. Substitution of Fe^{3+} into the lattice produces a yellow tint and combinations of these impurities are responsible for the other colours known in gem corundum (eg. green, purple and black). It is important to note that only red gem corundum is referred to as ruby whilst yellow, green and blue corundum is known as sapphire. Synthetic gems can be produced by the Verneuil process, with chromium or ferric ion being added for colour.

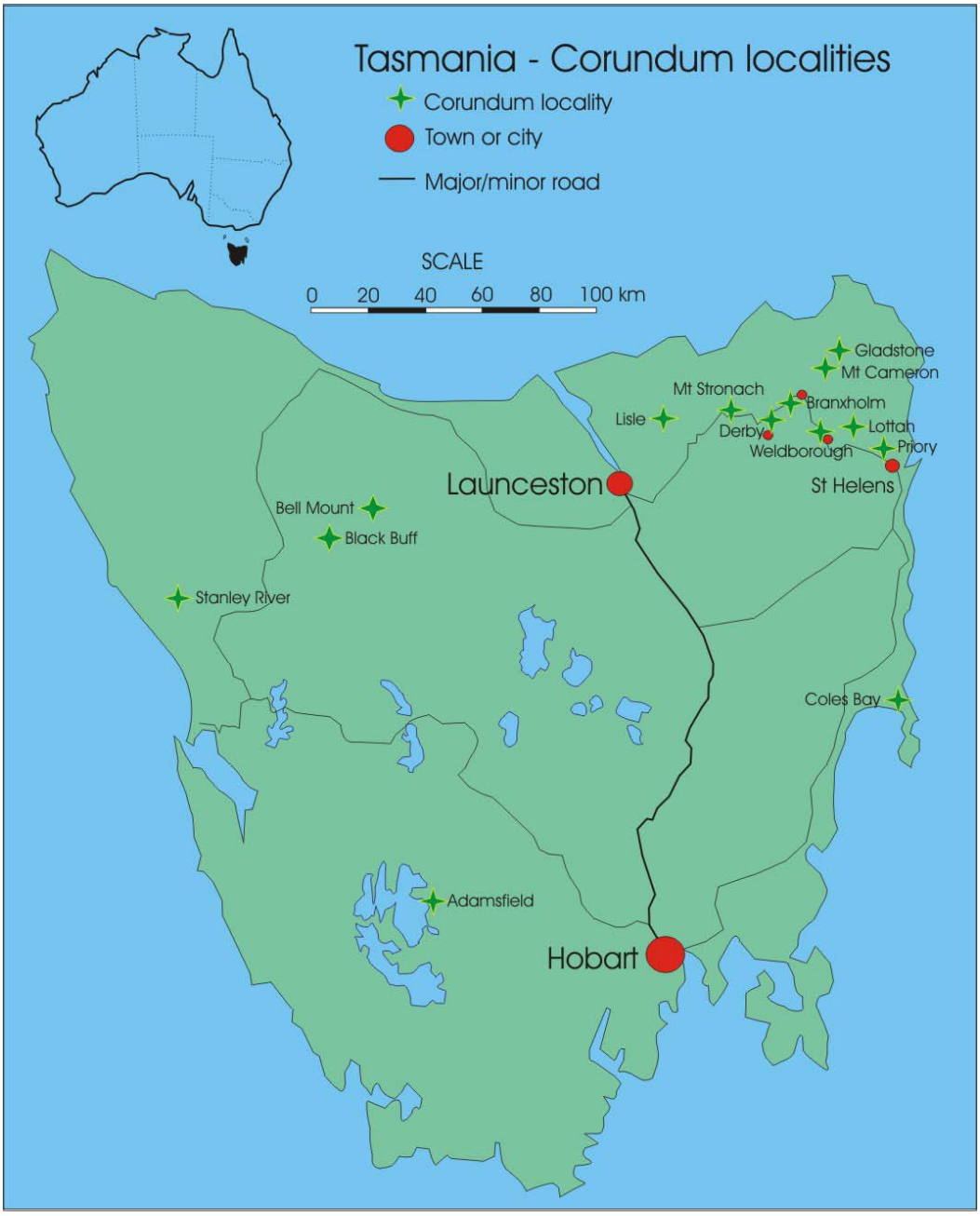

Figure 1. Tasmanian corundum localities (after Bottril, 1996). Dark green stars denote corundum occurrences.

Star sapphires occur when titanium impurities in corundum crystallise as rutile needles in three directions at 120º and perpendicular to the *z*-axis. This affect can be created synthetically.

1.1.3 Occurrence

Corundum occurs in alluvial deposits and wide variety of metamorphic and igneous rocks, where it indicates a silica undersaturated-alumina rich genesis (Table 1).

Table 1 - Major occurrence of corundum in different rock types (Modified from Guo, 1993)

Occurrence classification	**Group**	**Subgroup**	**Geological occurrence**
Metamorphic	1	1.1	Si-poor hornfels within the aureole of igneous intrusions (Evans, 1964; Smith, 1965; Ferguson and Al-Ameen, 1985; Riesco, Stuwe et al., 2004; Grant and Frost, 1990)
Metamorphic		1.2	Various types of gneisses, schists and granulites in metamorphic terrains as porphryroblasts (e.g., Clabaugh, 1952; Wells, 1956; Cooray and Kumarapelli, 1960; Lawrence et al., 1987; Grant and Frost 1990; (Kerrich et al., 1987); (Mercier et al., 1999)) or as corundum rich bands within normal metasediments (Coetzee, 1940; Golani, 1989; Feenstra, 1985, 1996)
Metamorphic		1.3	Al-rich xenoliths enclosed in mafic and granitic intrusive rocks (Thomas, 1922; Hall and Nel, 1926; Read, 1931; Murdoch and Webb, 1942)
Metamorphic	2	2.1	Marbles interbedded with other metasediments (Okrusch et al., 1976; Guberlin, 1982; Bender, 1983; Keller, 1983; Bowersox, 1985; Pecher et al., 2002; Garnier, Giuliani et al., 2002)
Metamorphic		2.2	Skarns developed between limestones and granitic intrusion (Silva and Siriwandena, 1988)
Accessory phase in igneous rocks	3		Syenites, nepheline syenites and associated pegmatites (e.g. Du Toit, 1918; Wells, 1956; Carlson, 1957; Kerr, 1977)
Accessory phase in igneous rocks	4		Plagioclase pegmatite (Sokolov, 1931; Tomlinson, 1939; Rose, 1957; Solesbury, 1967; Petrussenko, 1981; Atkinson and Kothavala, 1983; Simonet, 2003), oligoclase pegmatite (Lawson, 1904; Oftedal, 1963) and albitite veins (Larsen, 1928)
Accessory phase in igneous rocks	5		Altered igneous rocks in association with mineralisation (Schwartz, 1982; Steefel and Atkinson, 1984; Wojdak and Sinclair, 1984)
Accessory phase in igneous rocks	6		Alkremite xenoliths (Exley et al, 1983) and ecologitic xenoliths in kimberlites (Sobolov et al., 1968; Dawson, 1980; Kornprobst et al., 1982; Hill and Haggerty, 1989)
Discrete crystals or simple intergrowths in mafic\ultramafic dikes and basaltic rocks	7	7.1	Ultramafic dyke as discrete crystals (Claubaugh, 1952; Brownlow and Komorowski, 1988; Meyer and Mitchell, 1988)
Discrete crystals or simple intergrowths in mafic\ultramafic dikes and basaltic rocks	7	7.2	Basaltic rocks as large discrete crystals or simple intergrowths with other phases (McNevin; 1972, Stephenson, 1976; Upton et al., 1983; Guo 1993, 1996; Sutherland, 1996, 1998ab , 2002; Garnier, 2005; Saminpanya, 2003; Aspen, 1990; Khin Zaw, 2002; Limutrakun, 2001; Yui, 2002; Sutthirat; 2001)

Exploitable deposits of gem quality corundum tend to form as alluvial deposits sourced from the erosion of alkali basaltic rocks (Table 1, Subgroup 7.2). Other economic deposits of gem quality corundum are rare, but include corundum hosted in ultramafic dykes (Yogo, Kashmir) and corundum formed due to isochemical metamorphism of carbonates (Thai and Myanmar marble hosted rubies).

1.1.4 Corundum from alkali basalt terrains

Corundum is found in certain alkali basalt fields and their associated alluvial deposits. This occurrence is significant due to the large number of associated economic gem corundum deposits (sapphire and lesser ruby). Corundum is considered a xenocryst phase of the associated basaltic rocks but controversy exists over the origin of the corundum-bearing xenocrysts and their relationship with alkaline basaltic volcanism. One critical issue is whether mantle-derived magmas at depth can evolve to compositions peraluminous enough to crystallize significant amounts of corundum without contamination of an Al-rich crustal rock (Upton et al., 1999).

1.1.4.1 Occurrence

Corundum in alkaline basaltic terrains is commonly observed in alluvial placer deposits or much less commonly as in situ megacrysts.

The weathering and erosion of basaltic lavas, pyroclastics, plugs and diatremes has created economic deposits of gem-quality sapphire in eastern Australia, eastern China, Thailand, Vietnam, Cambodia, Kenya and Nigeria (Guo 1996b). Lesser deposits exist in Madagascar and Europe (Sutherland 1998).

Although rare, corundum xenocrysts have been reported in situ in basaltic rocks: MacNevin (1972), Stephenson (1976) and Vichit (1978) all reported occurrences of corundum or corundum-composite megacrysts in basalts. Guo et al. (1993) reported the occurrence of an alkali basalt breaking down to form alluvial material containing gem-quality corundum. Other evidence associating alluvial corundum with corundum from basaltic terrains includes corundum colour, trace element patterns, crystal habits and corrosion textures.

1.1.4.2 Genesis Models

With corundum being unable to crystallise out of basaltic magmas, current understanding of the topic calls for a two-stage process. The first stage involves the magmatic/metamorphic **generation** of corundum at crustal/mantle depths followed by a

second stage of alkaline intraplate basaltic **incorporation and transport** of the xenocrysts. This implies that the generation of corundum has to occur at levels higher than the magma generation.

It is noted that many of the models suggest origins for either sapphire generation or ruby generation. More recently papers have been published which attempt to constrain the origins of the multi-modal gem suites (eg. Sutherland, 2002; Saminpanya, 2003).

The currently postulated models for metamorphic/magmatic generation of corundum can be divided into three groups (after Khin Zaw et al., 2002):

Plutonic crystallisation at high pressures

a. Plutonic crystallisation from highly evolved alkaline melts derived by the crystallization of intraplate (nephelinite, basanite etc.) magmas at mantle and lower crustal pressures (Irving, 1986)

b. Plutonic crystallisation from syenitic melts that are the result of high temperature crystallization of anhydrous trachytic magmas at deep crustal level or the upper mantle (Aspen et al., 1990)

c. Plutonic crystallisation from primary alkaline melts which are produced by low to moderate degrees (6-14 wt%) of partial melting of amphibole-metasomatised mantle, or alternatively partial melting of a lower crustal amphibole bearing assemblage (e.g. amphibole pyroxenite; Sutherland et al., 1998).

d. Plutonic crystallisation from syenitic melts originating from partial melting of a metasomatised mantle, but with aluminous character developed by the loss of alkalis and carbonatitic fractions (Upton et al., 1999).

e. Plutonic crystallisation from a fractionated partial melt from a metasomatised mantle interacting with a lower-crustal Al-rich rock (Khin Zaw et al., 2002).

f. Plutonic crystallisation in a deep magma chamber, at the lower continental lithosphere and upper mantle boundary, in evolved melts issued from the fractionation of alkali basaltic magmas contaminated with lower crustal fluids (Garnier et al., 2005).

The plutonic crystallization models of corundum genesis are very similar in that they require a highly aluminous volatile and trace element rich alkaline parental magma. They only differ in how such a magmatic melt composition was produced.

Corundum generation by magma mixing at mid crustal levels

Guo et al. (1996) suggests that at mid-crustal depth the interaction between a host pegmatite body and intruding carbonatitic magma causes Al-rich phases to crystallize in

the hybrid zone, including corundum. Subsequent episodes of basaltic magmatism may have carried fragments of corundum-bearing wall rocks rapidly to the surface.

Corundum generation by metamorphic recrystallisation

The generation of corundum by metamorphic recrystallisation of aluminous lower crustal rocks has also been documented.

a. Metamorphic corundum is formed the recrystallisation of Al-rich Si-poor host rocks by ocean floor subduction (Levinson and Cook, 1994).

b. Suitthirat et al. (2001) proposed that high-pressure metamorphism of Al-rich mafic rocks also crystallized corundum (ruby only).

c. The model proposed by Oakes et al. (1996) suggested that corundum was derived by the reworking of clay-altered volcaniclastic host rocks.

1.2 Tasmanian Sapphires

Tasmanian sapphires are typically a dark blue colour, but can range from yellow to green to purple. Parti-coloured and star sapphires have also been observed in Tasmanian sapphires. The largest sapphire found in Tasmania weighed 52.8g and came from the north eastern tin fields (Weld River; Department of Mines, 1970). Other localities for sapphires in Tasmania include Boat Harbour, Table Cape, Lisle, Adamsfield and Coles Bay. Sapphires in Tasmania generally originate in sediments derived from basaltic terrains, with the only notable exceptions (Adamsfield and Stanley River) occurring in areas of rapid erosion, where a basaltic source may have been totally denuded (Bottrill, 1996).

In the north east tin fields, Branxholm, Derby, Gladstone, Lottah, Main Creek, Moorina, Mt. Stronach, Mt. Cameron, Thomas Plain and Weldborough exhibit occurrences of sapphires in placer deposits (Department of Mines, 1970). The sapphires exhibit a heavy mineral association with topaz, cassiterite, zircon and spinel. The topaz and cassiterite is considered to be granite derived with the weathering of basalts providing the coarser spinel and zircon (Yim et al., 1985). It is thought that the sapphires represent the weathering of corundum-xenocryst bearing Tertiary basalts.

Two ages of Tertiary basalts have been identified, with ‘younger’ basalts present in the Ringarooma River Valley and the ‘older’ basalts present at Forest Lodge and Weldborough. The older basalts have been targeted for sapphire exploration (see below) on the basis of sapphire distribution in rivers in the area.

1.3 Previous exploration

On the basis of an analogy between gem producing areas in New South Wales, Totteny Pty Ltd investigated the possibility of a commercial sapphire prospect in the Weldborough area (Morrison, 1989). The presence of basaltic agglomerate underlying the older basalts is thought to represent a breccia dome, which suggests the presence of an eruptive centre. This is a similar sequence to that of New South Wales where tuffs and agglomerates underlying basaltic sequences have proven to be the source of sapphire, zircon and diamond (Oakes et al., 1987).

The target of the company was to detect pyroclastic rocks with evidence of zircon and/or sapphire enrichment. Investigations involved the mapping of the agglomerate basal unit via means of radiometric discrimination and heavy mineral analysis. Lack of sapphire and zircon in the mapped basal sequence led the company to conclude the sapphire and zircon host sequence was no longer preserved in the region. They further concluded that due to the historically low concentration of the stones that the only commercial production of sapphires would be as the by-product alluvial tin mining.

Chapter 2: Background geology

2.1 Location

The island of Tasmania is the southernmost state of Australia (Figure 1). The study area is shown in Figure 2 and covers an area of approximately 200 km^2 in the north east of Tasmania. The study area is centred in the Weldborough Pass, the site of the Weldborough basalts. Flanking each side of the pass is Mt. Littlechild to the north (780m) and Tower Hill to the south (760m).

2.2 Climate

The average rainfall is the highest of any Australian state, reaching a maximum of 3600mm in the west down to 500mm in the rain-shadowed zones in the east. In the area of the study, the annual rainfall is between 900 and 1800 mm (Noble in Caine, 1983). The high ground of NE Tasmania has a cool and humid climate (Gentilli, 1977). At 1200m, the approximate elevation of the tree line (Caine, 1983), there is a high frost frequency. The Blue Tier-Mt. Victoria area was found by Caine to show variability in precipitation strongly positively correlated with elevation.

2.3 Relief

With the exception of Mt Horror (pelite), part of Mt Paris (pelite), Mt Littlechild and Tower Hill (basalt), granite forms the major highland areas. Two physiographic units are recognised in the study area:

1. Highland areas rising to a maximum elevation of 900m, including the Blue Tier and
2. An intervening dissecting area of older bedrock separated by areas of dissected Tertiary sediments and basalt, which is well developed along the Ringarooma valley between Ringarooma and Derby.

2.4 Geology

2.4.1 Mathinna Beds

The term *Mathinna beds* is applied to all pre-upper Carboniferous folded sedimentary rocks in north-eastern and eastern Tasmania (McClenaghan et al., 1982). The sequence

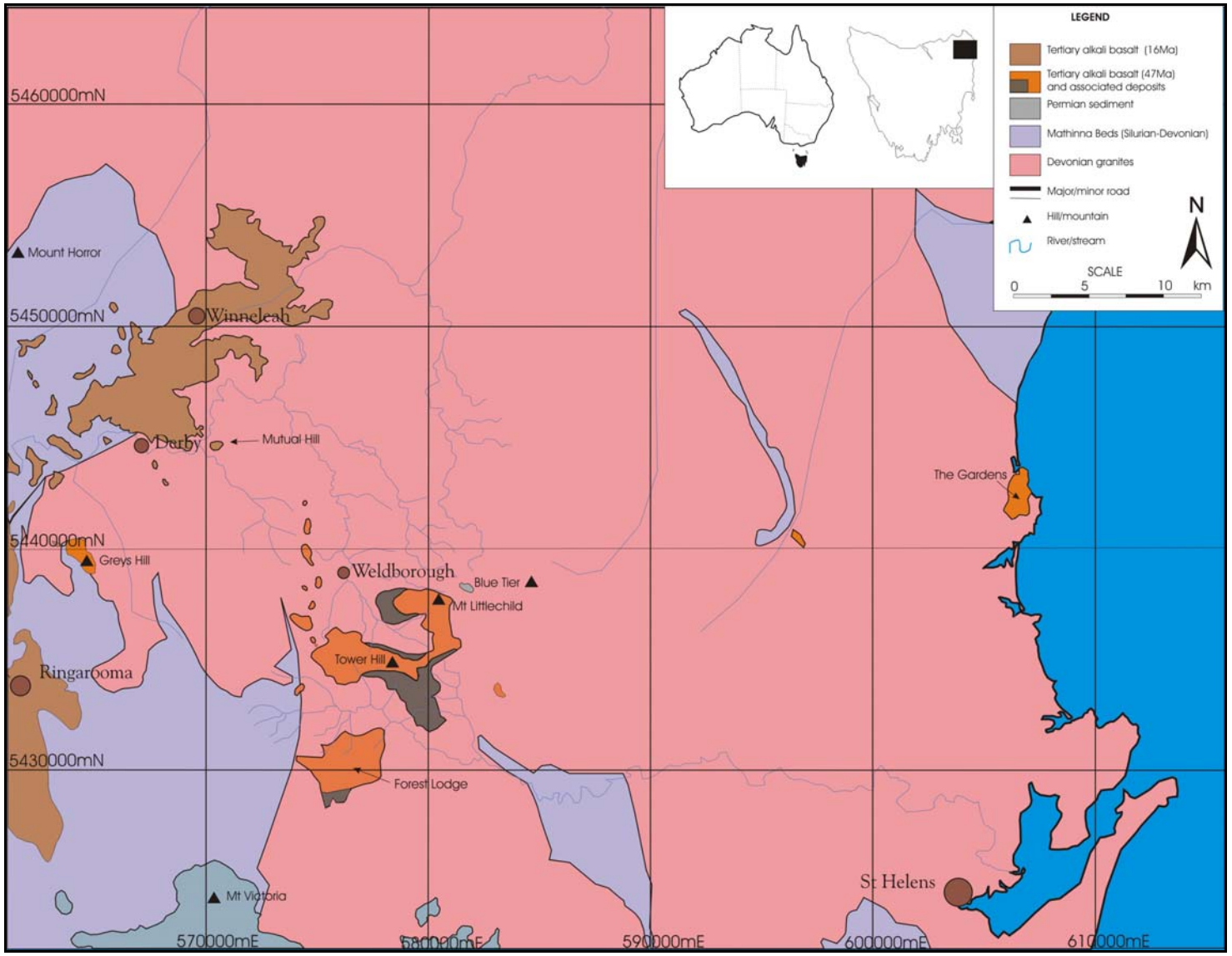

Figure 2. Geology of NE Tasmania. Modified from Moore (1991)

consists of alternating beds of poorly sorted siltstone and mudstone with textures and sedimentary structures indicative of deposition from turbidity currents.

The Mathinna beds have been divided into two groups based on palaeostratigraphy: a Lutite Association (Ordovician) and an Arenite-Lutite Association (Silurian-Devonian). The Lutite Association occurs in the west (between Lebrina and Nawbowla, Bangor, other minor areas) and is an argillaceous unit consisting of mainly lutite with an arenite component. The unit (particularly the pelites) has a distinctive strong tectonic cleavage that predates any Devonian (granite intrusion) deformation event. This first deformation event, characterised by a flat lying slaty cleavage and NNW trending folds, is dated at 416 ± 6 Ma (K/Ar) and 423 ± 22 Ma (Rb-Sr) and considered to be the probable source of the theorised Silurian unconformity.

It is now thought that the Mathinna beds were deposited in an elongate NNW-SSE basin with a quartzose cratonic source to the southwest (Burret & Martin, 1989). They occupy a foreland basin position between the Lachlan Fold Belt and the Australian Craton to the southwest.

2.4.2 Devonian granites

During the Devonian, granitoid masses with narrow contact aureoles were emplaced in folded rocks throughout Tasmania (the Mathinna beds had already undergone low grade dynamic deformation that cleaved and folded the rocks). Isotopic dating indicates the eastern Tasmanian granites are significantly older (370 to 389 Ma) than the Western Tasmanian granites (332 to 367 Ma). The granites were emplaced after the main Tabberabberan deformation event (Burret and Martin, 1989).

In the northeast of Tasmania, this is represented by high level crustal emplacement of the Blue Tier Batholith and the Scottsdale Batholith. Although these granites have some petrological differences, gravity surveys indicate they are connected at shallow depth (Leaman & Symonds, 1975).

The use of (Ti/10)-Rb-Sr discrimination was used to classify the granitic rocks of the Blue Tier Batholith into granodiorite, adamellite and alkali granite suites (McClenaghan et al., 1982). Minor intrusive bodies occur throughout the granites and include aplite, quartz-feldspar porphyry and dolerite dykes (McClenaghan et al., 1982).

There is evidence for passive emplacement of the granitic bodies (McClenaghan et al., 1982). However, at some locations the Mathinna beds have undergone local folding (Diana's Basin,

Bridport) due to intrusion, and regional doming of Mathinna beds is indicated by the subverticle axial surface of folds at the western margin of the Scottsdale Batholith.

The granites have produced narrow (<2km) contact aureoles producing hornfels from the Mathinna beds. These rocks have granoblastic textures and are generally composed of quartz, K-feldspar, cordierite, biotite and muscovite with andalusite near the contacts (Burret & Martin, 1989). Migmatite zones produced by assimilation occur in some areas, eg. Bridport.

2.4.3 Parmeener supergroup

The Permo-Triassic Parmeener supergroup crops out on the east side of Mt Littlechild as a poorly-sorted conglomerate with subrounded quartz pebbles set in a quartz-rich matrix (McClenaghan et al., 1982).

2.4.4 Jurassic and Cretaceous igneous activity

Tholeiitic dolerite was intruded into crust during the middle Jurassic as extensive sills and dikes. This dolerite was thrust into the sedimentary basins of Tasmania and Victoria Land, Antarctica and is thought to be related to the tensional stresses between continental blocks and is probably a precursor to the Gondwana break-up (Burret & Martin, 1989).

The dolerite is exposed capping Mt Victoria in the south of the field area and also as caps on hills east of Mt Littlechild.

A Cretaceous appinitic suite occurs as small flows, dykes and plug-like intrusions near Cape Portland (Burret & Martin, 1989). These andesites, lamprophyres and porphyrites have been dated at 98.7 ± 0.8 Ma (Baillie in McClenaghan et al., 1982).

2.4.5 Tertiary basalts and associated sediments

Two main basalt phases are present in the study area.

The oldest phase (46.8 ± 0.6 Ma; Sutherland and Wellman, 1986) is in the Weldborough Pass area, where the study area is focused. These alkaline basalts (alkali basalt – transitional hawaiite) are found capping Mt Littlechild, Tower Hill and Forest Lodge above 500m in altitude. Outliers occur a few km to the north east. The Greys Hill basalt, although distal, is also likely to be a part of this older association.

Below and skirting the basalt is extremely weathered basaltic agglomerate. Bottrill (1989) concluded that the rock is a highly weathered alkali basalt or basanite/nephelinite with textures indicating that it may have been an agglomerate.

Between 47 Ma and 16 Ma there were high rates of erosion (river lowerings up to 7m/my (Burret & Martin, 1989) which produced a sapphire-spinel-zircon association found in the Ringarooma deep leads.

The younger phase (16 ± 0.3 Ma; Brown, 1977) is the Winneleah-Ringarooma valley infill basalts. These flat lying basalt flows overlay Tertiary and Mathinna Beds sediments and in the Ringarooma area consist of at least two flows. The topographically higher basalt is an alkali olivine basalt with the lower basalt being an olivine nephelinite (Baillie in (McClenaghan et al., 1982).

These basalts are economically important in the genesis of the "deep lead" alluvial tin deposits.

2.4.6 Quaternary

Development of quaternary sediments, including glaciogenic, slope, coastal, Aeolian, fluvial and cave deposits are widespread in Tasmania. Table 2 is the provisional stratigraphic framework of the Quaternary in the area:

Table 2. Quaternary stratigraphy. From McClenaghan et al. (1982)

Series	**Holocene**	**Last Glacial**	**Last Interglacial**
Soils	Minor leaching, peat formation	Strong podsol, groundwater podsol development	Paleosol
Marine and related deposits	Beach sands, gravel		Sand, clay, minor peat and gravel
Aeolian	Dune sand	Lunette formation Dune sand: sheets and longitudinal dunes	
Talus and slope deposits		Talus, slope deposits	
Fluvialtile/Alluvial	Alluvium and related deposits		

2.5 The source of the sapphire – a review

In this section potential primary sources for the Weldborough sapphire will be considered. Firstly, rock types that can host corundum **and** occur in NE Tasmania will be considered. Secondly, the present day drainage and paleodrainage will be studied as to their affect on sapphire distribution in rivers.

Finally, a justification for the chosen primary target will be presented.

2.5.1 Potential host rocks in north eastern Tasmania

Corundum can occur in a wide variety of geological environments (see Chapter 1) as xenocrysts, phenocrysts and detrital grains. NE Tasmania has a number of outcropping rocks that have the potential to host corundum in a primary or secondary manner.

Table 3 is a summary of potential host rocks and includes genetic information on the corundum occurrence type and associated mineralogy.

2.5.2 Present day drainage and paleodrainage

The current and past drainage systems play an important role in the distribution of detrital sapphire in NE Tasmania. Corundum (and associated heavy minerals zircon, spinel and ilmenite) is expected to be concentrated in the river alluvium. The drainage domains in which the corundum is found can narrow down and even indicate potential primary sources.

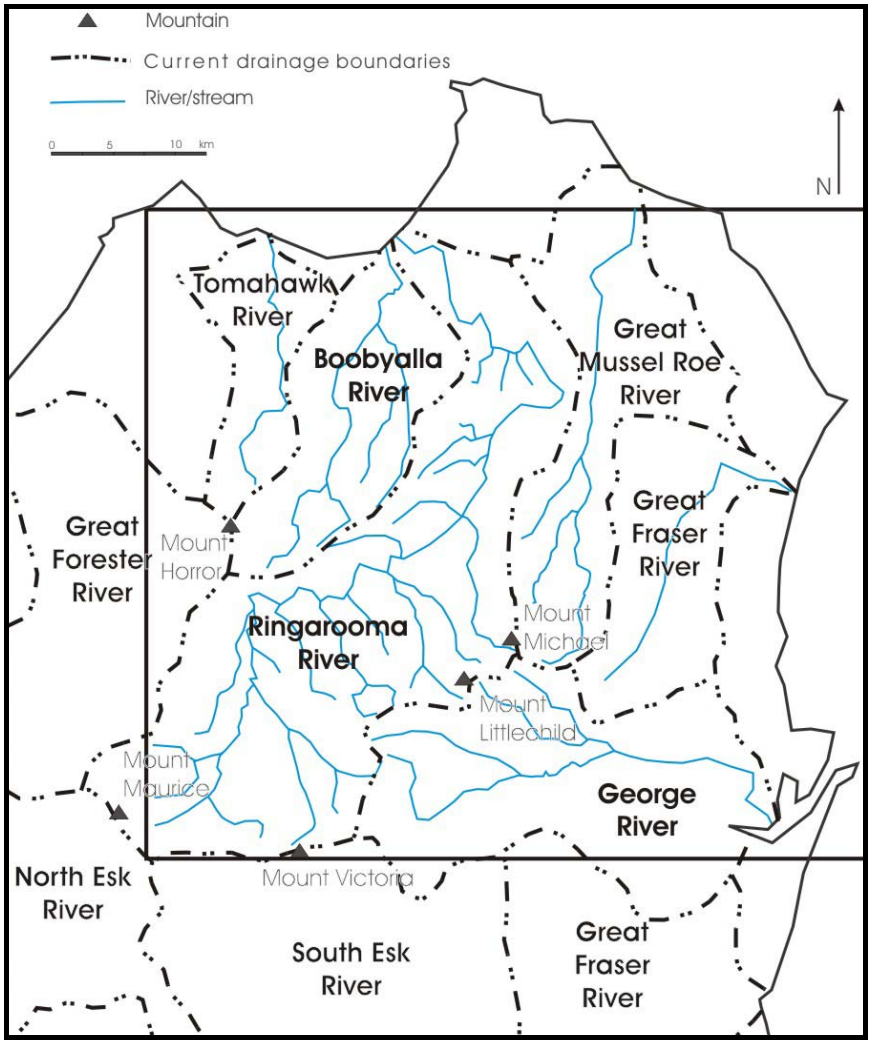

Figure 3. Present day catchment boundaries. After Jordan (1975). Inset box represents boundaries of Figure 4.

A study by Jordan (1975) delineated the present day catchments in NE Tasmania (Figure 3). NE Tasmania is dominated by the Ringarooma catchment (937km^2) with headwaters in Rattler Range, Mt Victoria and includes the Weldborough River. The Boobyalla (263km^2) and Great Mussel Roe (383km^2) catchments flank the Ringarooma catchment to the east and west, respectively. The George River catchment (no area data) has headwaters in the Forest Lodge and Mt Littlechild area.

A palaeodrainge study (Yim et al., 1985) proposed extensions to streams originating from the Blue Tier area (Figure 4). The conclusion of the study was that the deposition of the 16Ma Ringarooma-Winneleah basalts truncated these streams and diverted drainage. The drainage patterns have changed little to present day.

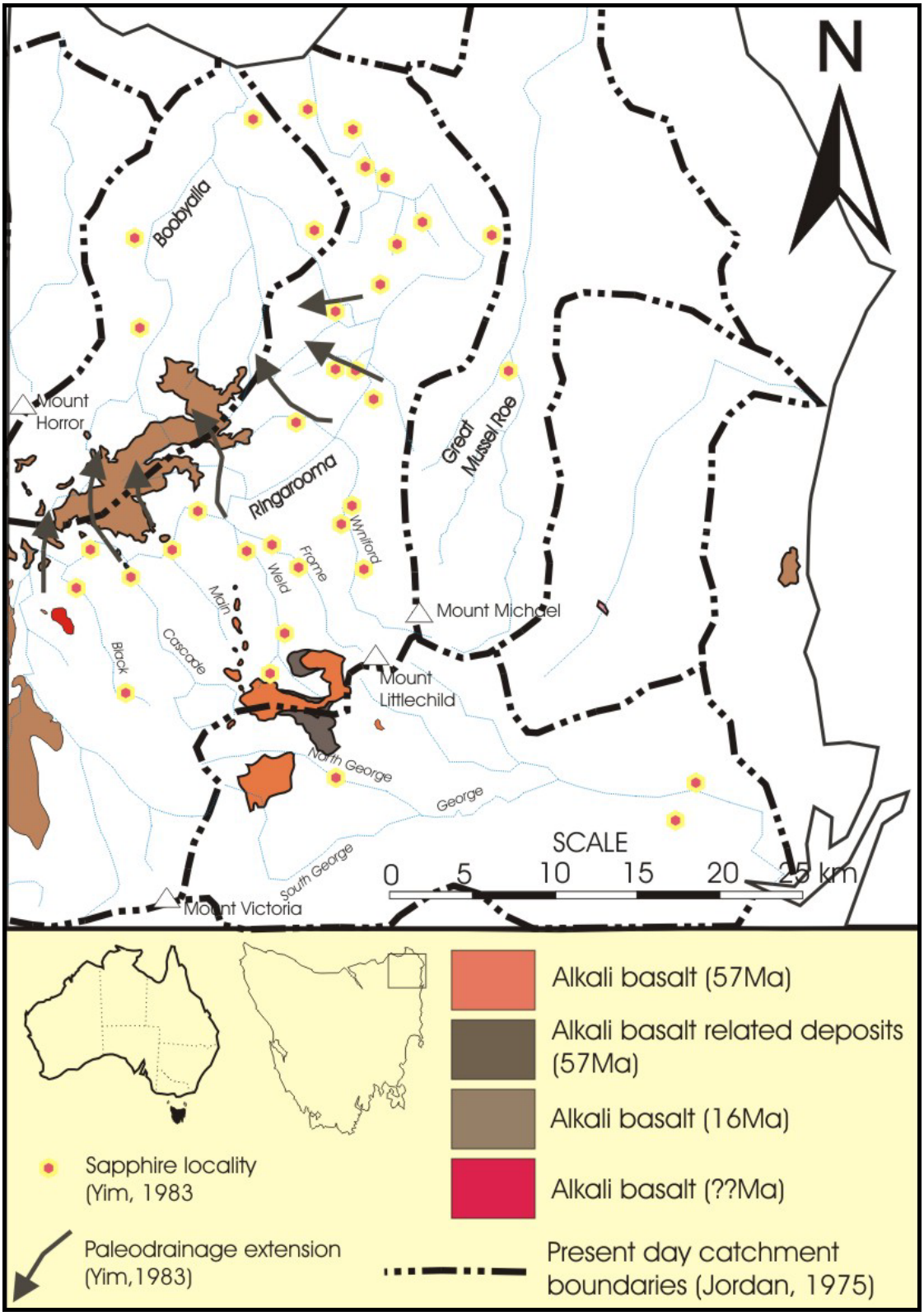

Figure 4. Distribution of the Weldborough sapphire. Present day and paleodrainage superimposed. Paleodrainage and sapphire locations from Yim et al. (1985) and present day drainage from Jordan (1975). Frome River sapphire localities from this study.

Table 3. Summary of potential sources for the Weldborough Tasmanian sapphires. Genetic origin and associated mineralogy have been included.

Potential host rock	**Potential corundum occurrence type**	**North East Tasmanian location**	**Literature example**	**Expected associated mineralogy**
Mathinna Beds (Pelite, Devonian-Ordovician	1) Partially melted pelite	1) Bridport: Assimilation of Mathinna Beds and migmatisation by Devonian granite (Burret & Martin, 1989)	1) {Lindsley, 1991}	1) K-feldspar, cordierite, spinel.
	2) Silica depleted hornfels in the aureole of an igneous intrusions	2) Diana's Basin, Bridport: Areas heavily metamorphosed by Devonian granite	2) Smith (1965); Riesco et al. (2004).	2) Sillimanite, spinel, cordierite, biotite.
Lamprophyre Dykes (Cretaceous)	Accessory mineral in an igneous rock	North of Three Mile Hill, Cape Portland	Clabaugh (1952); Meyer et al., (1988); Brownlow et al., (1988).	Biotite, pyroxene.
Devonian granite (Granite pegmatite)	Accessory mineral in an accessory rock	Mt Cameron	Wells (1956)	Feldspar, spinel, sillimanite and phlogopite.
Any sedimentary rock or material	Detrital grains	Mathinna Beds, Triassic and Permian sediments Tertiary alluvium and Quaternary sediments		Zircon, spinel, ilmenite.
Alkali basalt (Tertiary, 47Ma, 16Ma)	Corundum from Alkali Basalt Terrains	Ringarooma, Weldborough, Grey's Hill, Mutual Hill, The Gardens	Guo et al., (1996a, 1996b); Sutherland et al. (1996, 1998ab , 2002); Garnier et al., (2005); Saminpanya et al., (2003); etc.	Zircon, spinel, ilmenite.

2.6 Review of potential corundum sources

2.6.1 Silurian-Devonian Mathinna Beds

Pelitic rocks, such as the Mathinna Beds, are common host rocks to the metamorphic crystallisation of corundum. "This is because pelitic precursors that were not rich in quartz, melting and melt loss may lead to a complete exhaustion of quartz and ultimately to the formation of silica-undersaturated paragenesis including corundum" (Grant, 1985).

Although the Mathinna Beds could easily host a corundum occurrence, the level of metamorphism required (650ºC to 800ºC with a pressure of 3±0.5 kb, Lindsley, 1990) is only reached in two locations (Table 3). Given sapphire distribution and drainage patterns this type of corundum occurrence is unlikely to be the source of the Weldborough Sapphires.

2.6.2 Cretaceous Lamprophyre Dykes

Lamprophyre dykes have been known to host primary corundum, even sapphire. However, the location, mineralogy and the scale of the Three Mile Hill plagioclase-spessartites rule them out as the source of the Weldborough sapphires.

2.6.3 Devonian Granite pegmatites

Granite pegmatites, such as the aplite, quartz-feldspar porphyry and dolerite dykes from Mt Cameron and other areas in North East Tasmania (McClenaghan, 1984) have the potential to host corundum. However, as with the lamprophyric dykes, the location, mineralogy and scale of these dykes are not suitable to form the North East Tasmanian Sapphire field.

2.6.4 Sediment hosted corundum

Although not a source of primary corundum for obvious reasons, sedimentary rocks and material host corundum in many different geological terrains all over the world. The most common occurrence is that of alluvium from basaltic terrains hosting sapphires and rubies. Reworking of the sediment tends to concentrate the corundum.

Tertiary sediments eroded from basaltic terrains in Tasmania are a common source of detrital sapphires (in "deep leads" and sediment at Moorina). However, the alluvial heavy mineral association indicates the probable source of the sapphires (surficially) to be of basaltic origin.

2.6.5 Tertiary alkali basalts

Alkali basalts and their associated deposits have long been thought to host corundum, especially sapphire, xenocrysts which weather readily to form alluvial deposits. Five distinct occurrences of basalt outcrop in Tasmania's north east. Basalt from Ringarooma, the Weldborough area (includes the Mt Littlechild, Tower Hill, Forest Lodge and outlier basalts), Greys Hill and Mutual Hill are all possible sources of corundum. The Gardens basalt can be ruled out as a primary source of corundum due to its distal location.

The presence of sapphires in the George River and Ringarooma River catchments is strong evidence for a primary source being in the Weldborough region. By extending the paleodrainage to pre-16Ma it is apparent that the sapphires found in the Boobyalla catchment can also be explained by an older Weldborough region source area. However this does not imply that the Ringarooma-Winnaleah basalts are sapphire barren.

The Weldborough region hosts the older (47Ma) Mt Littlechild, Tower Hill, Forest Lodge and outlier alkali basalts and their associated deposits.

2.7 Conclusion

The only suitable target for a primary corundum deposit is one (or more) of the alkalic basalt fields that occur in NE Tasmania. This suitability is based on distribution, drainage and literature examples. By reviewing the paleodrainage of the area it is apparent that the basalts and associated basaltic deposits of the Weldborough area the likely primary source for the Weldborough sapphire. In the next chapter the Weldborough Region basalts and associated deposits will examined in order to isolate one or more lithologies as a primary source of sapphire.

Chapter 3: Field observations, basalt petrography and geochemistry

In the NE tin fields, sapphires occur in placer deposits that have been overlain by 16My basalts. These are the "younger" valley-fill basalts of Ringarooma and Winneleah. The "older" basalts (47My) may be source of the Weldborough sapphire given the "younger" basalts overly sapphire bearing cassiterite placer deposits ("deep leads"). It is for this reason that the "older" basalts suspected of being the source of the Weldborough sapphire will be investigated in this chapter.

These "older" basalts are the Mt. Littlechild, Tower Hill, Forest Lodge and outlier basalts. The Greys Hill, Mutual Hill and The Gardens basalts are also considered as sources of the sapphire because they are suspected to be "older" basalts. The Greys Hill and Mutual Hill basalts are suspected "older" because they have bases that are much higher than (up to 300m higher) than that of the nearby Ringarooma basalt. The Gardens basalt (no age) is also considered as a possible distal source of the sapphire.

The purpose of the fieldwork is to determine if the basalt or associated deposits contain or are likely to contain sapphire. The purpose of the geochemical and petrological studies is to provide a through petrographic and geochemical study of the Weldborough basalts and other possible host rocks.

This chapter will contain background information and a summary of previous work done on basalts in the field area. It will contain my field observations and hand specimen descriptions. The petrographical and geochemical nature of the basalts will be discussed.

3.1 Previous Work Summary

3.1.1 The Weldborough basalts

Work by McClenaghan et al., (1982) describes the Weldborough basalts as a lower basaltic agglomerate and tuff unit overlain by an upper basaltic lava unit. The agglomerate has a maximum thickness of 150 m on the south of the Weldborough Pass and total volcanic pile never exceeds an apparent thickness of 230 m. Small swarm-like bodies to the NE of the basalts have been interpreted as a possible feeder-dyke (Sutherland et al., 2004). The McClenaghan study indicated that Weldborough basalts and agglomerates represent small intraplate basaltic shield volcanoes.

The upper basalt unit is classified as an alkali-olivine basalt based on petrographic and chemical characteristics (McClenaghan et al., 1982). The basalts were all described as olivine-phyric porphyritic basalts. The basalts contain lherzolite, coarse-grained felsic and spinel xenocrysts and xenoliths (Bottrill, 2000). The basalts have been dated at 46.8±0.6 Ma (K-Ar; Sutherland & Wellman, 1986).

The underlying agglomerate and tuff unit has been described as "a probable basaltic agglomerate, in the alkali basalt/basanite field, but now totally altered to kaolinite, hematite and anatase" Bottrill (1989). Textures that resembled shards and pore-filling of a ropy lava were also reported. No spinel, corundum or zircon was recognised in a heavy mineral analysis of this rock (Morrison, 1989).

Based on basalt flow coverage and agglomerate dispersion, three eruptive centres have been interpreted for Weldborough area. These are centred on Mt Littlechild, Tower Hill and the Forest Lodge basalts (Sutherland et al., 2004).

3.1.2 Greys Hill

The Greys Hill basalt is described as a circular outlier of basalt. Its base is 300m higher than the nearby Ringarooma basalt (McClenaghan et al., 1982). It was also noted that the appearance of the basalt suggests it may be a remnant plug. The Greys Hill basalt has not been dated.

Petrological and geochemical analysis indicates similarities with the Weldborough basalt suggesting it may be a remnant of more extensive lava flows from the Weldborough area. (McClenaghan et al., 1982).

3.1.3 Mutual Hill

The Mutual Hill is a single circular outcrop of basalt. McClenaghan et al.(1984), stated that due to the similar petrological character, the Mutual Hill basalt is probably an outlier of the nearby "younger" Ringarooma basalts. The Ringarooma basalts are classed as olivine nephelinites and have been K-Ar dated at 15.6 ± 0.3 to 16 ± 0.3 Ma (Brown, 1977).

3.2 Field Observations

The Weldborough basalts are located around Weldborough and extend 10 km to the south. Access is gained via the Tasman Highway and outcrop accessible on foot. Basalts were sampled across a wide area including Tower Hill, Forest Lodge, Fieldwicks Quarry, Forest

Lodge and some outlier basalts. Samples were returned to the University of Tasmania where they were prepared for petrographical and geochemical analysis.

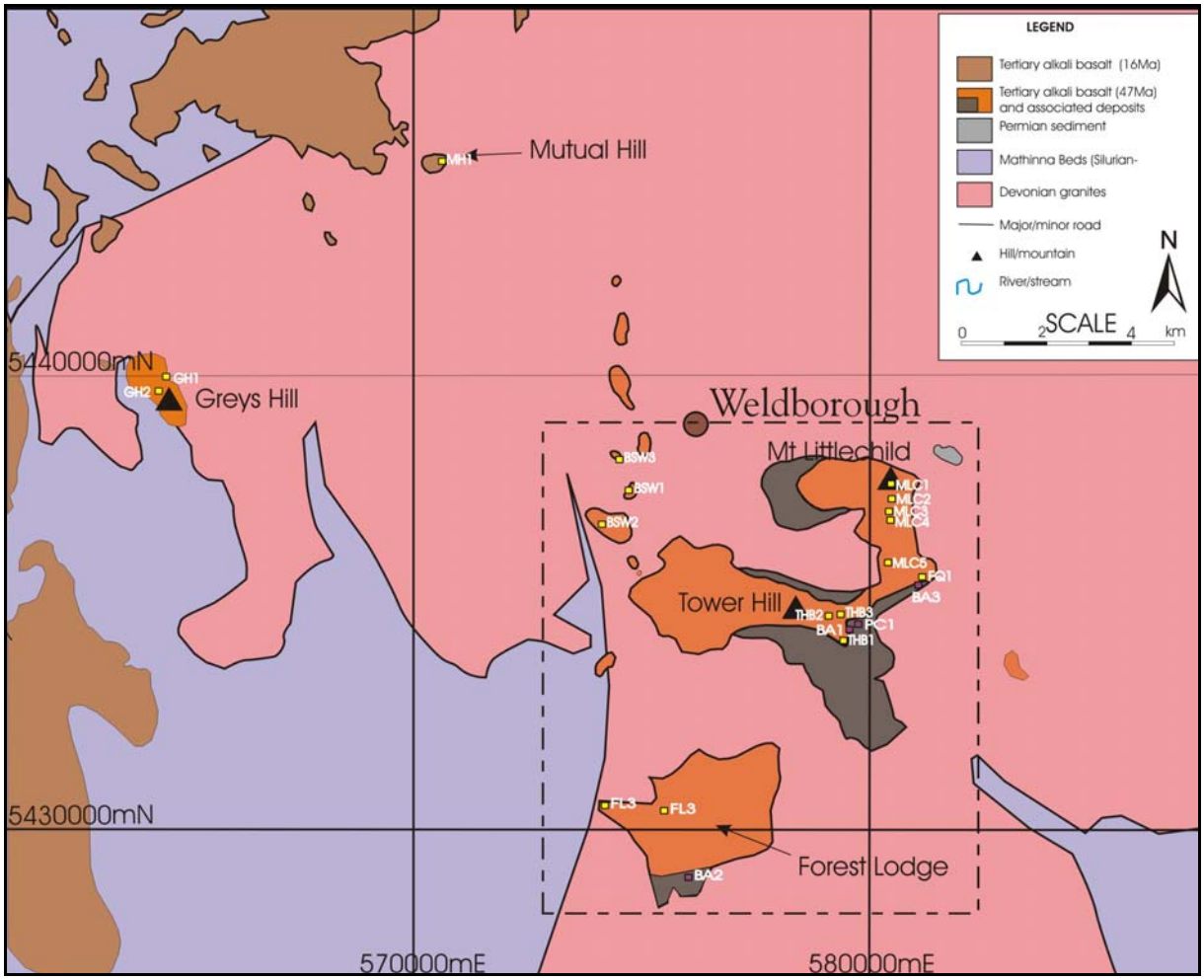

Figure 5. Improved geological map of the Weldborough area. Dashed square surrounds the Weldborough basalts, the focus of the study. Note: This study indicates that: 1. Basaltic agglomerate now outcrops south of Forest Lodge (BA2) and adjacent to Fieldwicks Quarry (BA3) ; 2. Basalt outcrop can be extended 300m on the east of Forest Lodge (FL3).

3.2.1 The Weldborough basalt

Keeping with the previous literature, the term "Weldborough basalt" encompasses the upper basalt unit and the underlying agglomerate and, now, a polymict breccia undocumented in previous literature.

The Weldborough basalt typically forms round hills will shallow to moderately dipping slopes. Mt. Littlechild exhibits benching with three obvious benches present. The upper basalt unit has spectacular columnar jointing at Fieldwicks Quarry (Figure 6A; FQ1). Columns are vertical and continuous within the quarry suggesting one "flow" (or ponded unit) is represented within the quarry. The columns are uniformly 25 - 30 cm in diameter, perfectly hexagonal and exhibit triple point junctions between columns. The column basalt is dark-

grey and aphanitic containing light coloured xenoliths of feldspathic composition (1-3 cm in diameter). The aphanitic nature of the basalt along with the suspension of xenoliths in the magma suggests it cooled quickly. However, the development of columnar jointing would indicate a period of slower cooling followed.

The dominant basalt lithology of the area is a dark-grey, olivine and clinopyroxene-phyric to aphyric basalt containing mantle and crustal xenoliths. Xenoliths are typically subrounded to subangular and 3 – 8 cm in diameter. Xenoliths of spinel-lherzolite, feldspar and spinel composition are typical, and more abundant at Tower Hill. Areas of high vesicularity are present at Fieldwicks Quarry and Tower Hill. Vesicles range from 2 – 3 mm in diameter and are filled with zeolitic material. The basalts from the Weldborough area are olivine- and clinopyroxene-phyric to aphyric. The basalts show varying degrees of vesicularity and contain varying amounts of mantle and crustal xenoliths.

At field location MLC2, a coarser grained basalt dyke crops out and contains abundant crustal xenoliths is present. The xenoliths have a gabbroic texture and are composed of quartz, feldspar and pyroxene. The xenoliths have knife-edge contacts with the dyke-rock suggesting a short residence time or chemical equilibrium with the magma. The orientation of the dyke is E-W.

3.2.2 Basaltic agglomerate

The agglomerate crops out at three locations (Figure 5; BA1, BA2, BA3). Outcrops have orange, red and yellow hues (Figure 6B), whilst hand specimens exhibit a patchy red and orange colour. The agglomerate consists of large, subangular to subrounded clasts of fine-grained basalt (10 – 20 cm in diameter) in a fine-grained matrix of soft clay. Small (1 – 4 cm in diameter) pale-grey clasts are present which are now totally altered to clay minerals.

Recent road construction has revealed a new outcrop (Figure 5; BA3) indicating that the agglomerate unit is much more widespread than previously suggested.

3.2.3 Polymict conglomerate

This rock is best described as a carbonate altered massive clast-supported crystal-, lithic- and pumice-rich conglomerate. This previously undocumented rock was found at the base of Tower Hill (5434461N, 579720E, Figure 5; PC1) and occurs as a single discrete outcrop set into the hill (Figure 2B). The outcrop of yellow to brown conglomerate has dimensions 5m x 2m x 2m (Figure 7A). At outcrop scale the rock appears to be massive, although a distinct plane, dipping towards 208 degrees at 11 degrees, is present at the top of the rock. From the

exposure it was difficult to tell the lateral extent of the package, if any, and the occurrence of this rock may represent a single megaclast.

Fresh surfaces of the rock are generally dark grey to black depending on clast composition. The rock is clast supported, with little or no matrix material between adjoining clasts. Polymict clasts, ranging from granule to boulder (1mm- >64mm), are composed of up to three different varieties of basalt, granite, pumice and pelite (Figure 6B). Crystal shards ranging from 1-10mm are present and consist of angular to rounded quartz, K-felspar, spinel, spinel lherzolite and anorthoclase megacrysts.

Basalt clasts (granule to boulder) range from olivine-, clinopyroxene and plagioclase-phyric to glassy and highly vesicular. Some of the basalts contain quartz xenocrysts with reaction rims. Larger basalt clasts tend to be sub-angular to sub-rounded with the smaller basalt clasts, especially pumice, tending to be extremely angular. A black, glassy, finely vesicular basalt clast was distinctive in hand specimen, as this clast type does not appear as a primary unit anywhere else in the Weldborough area.

The granite clasts (granule to cobble) tend to be rounded, as with the pelite clasts (granule to cobble) which are rounded to sub-angular. The light to dark grey pelite clasts are composed of fine-grained quartz. The granite is feldspar-quartz-biotite-mica-phyric and porphyritic in texture.

3.2.4 Greys Hill Basalt

The Greys Hill basalt is located 12 km west of Weldborough. Access is gained via access road from Branxholm (Figure 5; GH1 and GH2). The Greys Hill basalt is a dark-grey olivine-phyric to aphyric fine-grained basalt. At the base of the basalt sequence (Figure 5; GH1) large xenoliths are abundant (< 12cm in diameter), but at higher levels (Figure 5; GH2 GH2) the xenoliths are far less abundant and much smaller. This can be due to xenolith sinking within a single flow during slow cooling or magma fractionation over a longer period of volcanism. At the lower levels, the rounded to elongate xenoliths are up to 12cm in diameter and consist of olivine, pyroxene and spinel. At higher levels, only xenocrysts of olivine <7mm were observed. No other basalt-related units were observed in the area. Because we are unable to determine the nature of the flows from these outcrops, we cannot tell which scenario is likely.

3.2.5 Mutual Hill basalt

The Mutual Hill basalt is located 8 km north west of Weldborough (Field location MH1). Access is gained via private road from Derby (Figure 5; MH1). The Mutual Hill basalt is grey rock with a porphyritic texture. The olivine is present in two size ranges; <1mm and 2-3mm indicating a possible xenocrystic and phenocrystic phase. Subangular to rounded xenoliths of olivine and spinel composition are sparse and up to 3 mm in diameter.

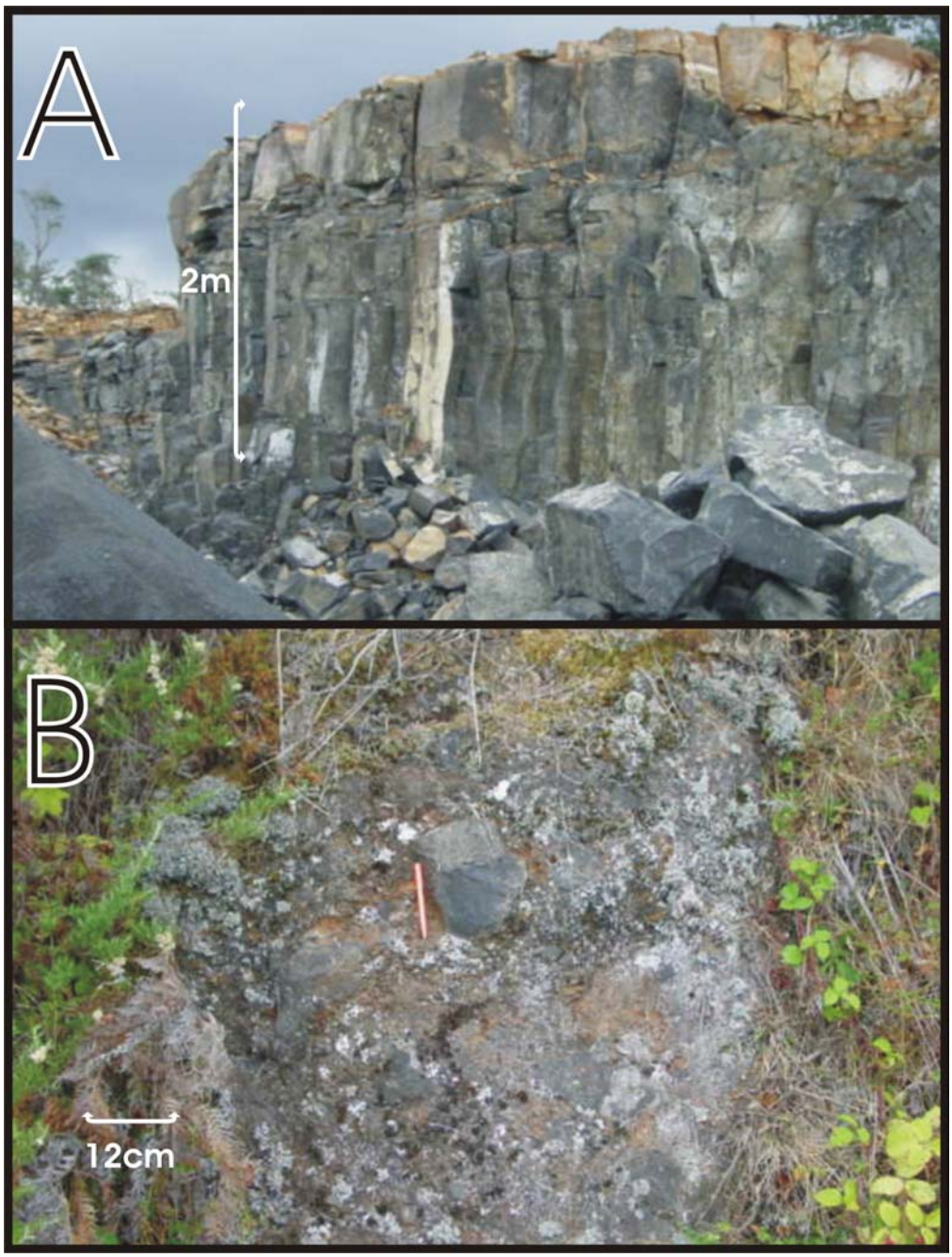

Figure 6 A & B. A - Columnar jointing at Fieldwicks Quarry (FQ1). B – Typical outcrop appearance of the basaltic agglomerate (BA3).

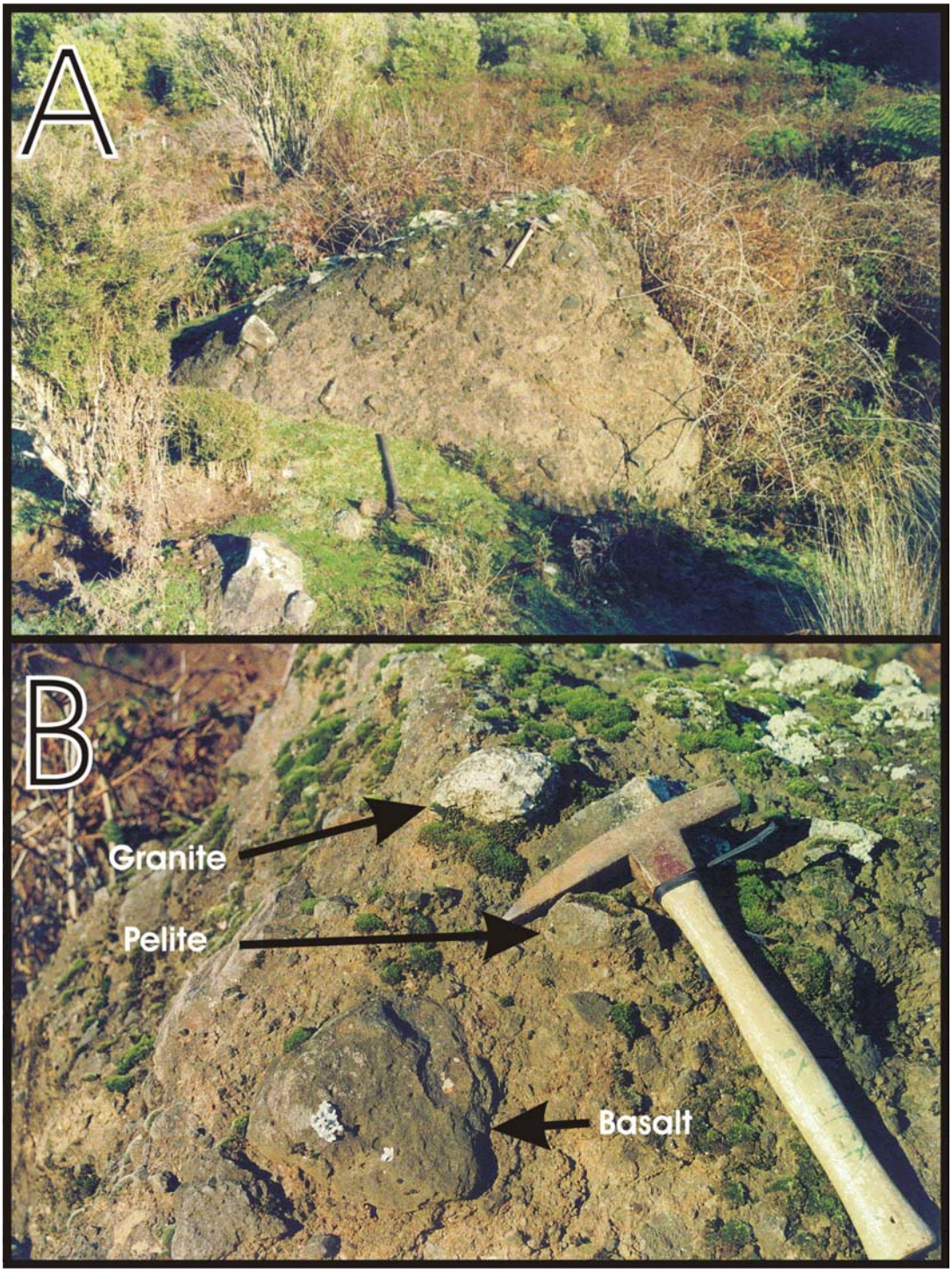

Figure 7A & 7B. 7A - Megaclastic outcrop appearance of polymict conglomerate. B - Obvious polymict appearance in the conglomerate (Figure 5; PC1).

3.2.6 The Gardens

The Gardens basalt is located 30 km east of Weldborough (20 km north of St Helens). Access is via The Gardens road. The Gardens basalt is fine-grained and dark grey. In the specimens sampled, no xenoliths or xenocrysts were present.

3.2.7 Discussion

The mapping of the basalt outcrop at Weldborough supports previous findings Mt. Littlechild, Tower Hill and Forest Lodge are small basaltic shield volcanoes. The underlying agglomerate unit is now known to be more extensive than originally thought. The agglomerate is consistent with being a mass flow deposit. Sapphire (and zircon) are known to occur in the tuffs and breccias associated with basaltic volcanism in NSW (Oakes et al., 1987). Although the agglomerate unit has already been analysed for heavy minerals, sapphire deposits are often localised. For this reason the agglomerate will be re-examined petrographically later in this chapter.

The discovery of a previously unreported polymict conglomerate provides another target for exploration. It is similar in matrix composition to the sapphire bearing breccias of NSW (Dr. Ian Graham, pers. comm., 2005). As a potential sapphire source the conglomerate will be analysed for heavy minerals and undergo thin section analysis for the presence of sapphire and associated minerals (zircon and spinel).

None of the sampled basalts or basaltic units contained visible sapphire. The absence of bauxitic layers makes it difficult to determine if it is one period of volcanism or many. The latter case would suggest that the sapphires might be confined to one flow. Basalts collected from the Weldborough area will undergo petrographical and geochemical analysis to further investigate their suitability as a sapphire host rock.

3.3 Petrography

The purpose of petrographical analysis of the basalts and associated clastic rocks was to detect primary sapphire enrichment. Spinel and zircon xenocrysts also indicate a possible sapphire enrichment and are a petrographical target.

Fifteen basalt, one basaltic agglomerate and one polymict conglomerate were cut to make polished thin sections. The petrography of the basalts and associated clastic rocks will be described broadly in this section. For more detailed descriptions of each thin section refer to Appendix 1. Appendix 2 contains photomicrographs of the studied sections. Sample locations are plotted on Figure 5.

3.3.1 Basalt

The Weldborough basalts are microporphyritic to porphyritic alkali basalts. They typically contain 15 – 35 % phenocrysts of olivine and lesser titanaugite, in a groundmass of olivine,

plagioclase, clinopyroxene and opaque minerals. Phenocrysts of olivine (0.3 mm – 1.2 mm) are typically subhedral to euhedral and in some cases, rimmed by aligned plagioclase laths. Subhedral to euhedral phenocrysts of titanaugite (0.6 – 0.45mm) are typically lavender to brown with a dusty appearance. In some sections, the titanaugite is glomerocrystic. Plagioclase laths (up to 1.5mm) are present (50% of the samples) and exhibit seriate texture, with crystals ranging from groundmass to phenocryst size. Plagioclase had Michel-Levy determined composition ranges of between $An_{38}Ab_{62}$ and $An_{45}Ab_{55}$ classifying them as andesine. Plagioclase laths often show flow alignment.

The groundmass is fine grained and typically contains clear euhedral olivine, brown euhedral clinopyroxene, plagioclase laths and opaque minerals. As mentioned above the plagioclase ranges in size from groundmass to phenocrysts in most samples. The portioning of titanium into clinopyroxene to form titanaugite suggests the basalt magmas were oxidised, and hence the opaque should be magnetite.

Spinel-lherzolite xenoliths and olivine xenocrysts are common in the basalts. Less abundant anorthoclase xenocrysts are found in some samples.

No sapphire, zircon or spinel megacrysts were present in the studied sections.

3.3.2 Agglomerate and conglomerate

Petrographic analysis of the polymict conglomerate and the monomict basalt agglomerate in thin section has recognised four consistent clast types within both rocks. The four clast types are:

- Fine-grained glassy basalt with pseudomorphs of olivine that have undergone hydrothermal alteration. The groundmass consists of plagioclase lathes and opaque minerals. Basalt is vesicular with inclusions of other basaltic clasts possibly included during eruption. Total clast size is <2.4 cm in diameter.
- Fine-grained glassy basalt with few phenocrysts of olivine pseudomorphs. The groundmass consists of plagioclase lathes and is rich in fine-grained magnetite (30%). Total clast size is < 1.6 cm
- Anorthoclase phenocrysts up to 0.9cm. Grains are colourless and light brown along fractures. Grains have been altered and exhibit a cross-thatching twinning under polarised light.

- Coarse-grained plagioclase rich dolerite rock that is the least altered clast present. It exhibits flow foliation and very fine-grained plagioclase, clinopyroxene and magnetite. Clast size is <1.4 cm.

The polymict conglomerate consists of angular to sub-angular clasts and shards of the rock types described above held together by a matrix of carbonate and/or cryptocrystalline silica which forms light brown bands between clasts and in vesicles. Cryptocrystalline silica indicates a fluid rich in silica has cemented these clasts.

The monomict basaltic agglomerate exhibits rounded elongate clasts that align along a foliation. Clasts are distinguished by pseudomorphs of their features that are present in the polymict conglomerate. The cement has now been ferruginised, giving the unit a red colour in outcrop.

The evidence above suggests that the polymict conglomerate is the fresh version of the basaltic agglomerate. The conglomerate has undergone no clast flattening and is likely to reside at the top the volcanic pile. The monomict basalt agglomerate exhibits the same four clast types that have undergone flattening and then been ferruginised. This indicates it sits much lower in the volcanic pile.

No sapphire, zircon or spinel megacrysts were present in the studied sections.

3.4 Geochemistry

Major and trace element geochemistry was carried out on the Weldborough basalts to establish the characteristics of the basalt and the likelihood of it being aluminous enough to crystallise corundum.

For sample selection, analytical procedure and results refer to Appendix 3.

Chapter 4: The characteristics of the Weldborough sapphire

4.1 Introduction

Sapphires can be categorized by their colour, shape, trace element chemistry and their oxygen isotope chemistry. The study of fluid and mineral inclusions is also becoming increasing useful to determine a genetic origin for different sapphire types.

This chapter will describe:

1.1 The general characteristics

1.2 The mineral and fluid inclusions

1.3 The mineral chemistry and

1.4 The oxygen isotope chemistry of the Weldborough sapphire. Section 1.5 discusses geochronology of the sapphires and associated detrital zircons. Section 1.6 will surmise the chapter.

4.1.1 Experimental Techniques

4.1.1.1 Experimental techniques - inclusions

The sapphires were collected from alluvial deposits at ten different localities (Table 4). The selected rough sapphires were prepared for inclusion studies by cleaning the sapphires and preparing them as doubly polished thick sections 0.1-0.3mm in thickness. All samples were optically examined under a petrographic microscope to locate and photograph the inclusions. For heating and freezing of fluid inclusions, the sapphires were removed from their section mounts and analysed as thin chips.

Table 4. Sample locations and characteristics of sapphires for inclusion studies.

Location	No. samples	Colours	Size
Priory 600050mE, 5429950mN	5	Transparent to transparent blue	1-3mm
Frome River 575750mE, 5445523mN	8	Opaque grey, black to transparent blue	>4mm
Ruby Creek 580500mE, 5458350mN	4	Translucent blue to transparent blue	1-2mm
Black Creek 563700mE, 5443000mN	4	Opaque blue to translucent blue	3-4mm
Main Creek 572750mE, 5440850mN	4	Translucent blue to opaque black	2-5mm
Dorset Dredge 581575mE, 5469350mN	4	Translucent blue to opaque black	2-7mm
Moorina 573280mE, 5456200mN	14	Transparent yellow, blue to translucent yellow, blue	2-4mm
Spinel Creek 575950mE, 5438100mN	8	Transparent colourless to translucent blue with banding	2-4mm
Moorina 2 573280mE, 5456200mN	6	One multicolour transparent blue-pink, yellow, brown and green translucent to opaque	2-6mm
Aberfoyle	2	Transparent blue to opaque blue	2mm
Thoreau's Lead 598400mE, 5428550mN	2	Transparent blue to opaque blue	1-2mm

4.1.1.1.1 Heating/Freezing Stages

Fluid/melt inclusions in the sapphires were analysed at the Centre for Ore Deposit Research, University of Tasmania. Microthermometric measurements were carried out on a Linkam MDS600 heating/freezing stage, manufactured by Linkam Scientific Instruments Ltd. The stage has an upper temperature limit of 600ºC. The stage was calibrated using synthetic fluid inclusions supplied by Synflinc Inc. and the precision of the measured temperatures is ±1.0ºC for heating and ±0.3ºC for freezing. The Linkam MDS600 heating/freezing stage is mounted on a Nikon microscope fitted with a long focal length 32x objective lens. To avoid fog covering the sample during the freezing examinations, N_2 gas was blown over the sample chamber.

4.1.1.1.2 Laser Raman Spectroscopy (LRS)

Laser Raman Spectroscopic analysis was undertaken at Geoscience Australia, Canberra using a Dilor SuperLabram spectrometer equipped with a holographic notch filter, 600 and 1800g/mm gratings, and a liquid N_2 cooled, 2000x450 pixel CCD detector (Mernagh, 1988).

The inclusions were illuminated with a 514.5nm laser excitation from a Spectra Physics model 2017 argon ion laser, using 5mW power at the sample, and a single 30-second accumulation. A 100x Olympus microscope objective was used to focus the laser beam and collect the scattered light. The focused laser footprint was 1μm in diameter. Wavenumbers are accurate to ±1cm^{-1} as determined by plasma and neon emission lines. For analysis of CO_2, O_2, N_2, H_2S and CH_4 in the vapour phase, spectra were recorded from 1000 to 3800cm^{-1} using a single 20 second integration time. For analysis of solid phases, spectra were recorded from 200 to 1800cm^{-1} using a single 30 second integration time. The detection limits are dependent on instrumental sensitivity, the partial pressure of each gas and the optical quality of each inclusion. Raman detection limits are estimated to be around 0.1mole% for CO_2, O_2, and N_2, and 0.3mole% for H_2S and CH_4. Errors in gas ratios are less than 1mole%.

4.1.1.2 Experimental technique: trace elements

Sapphires were collected from alluvial deposits at eight different localities (Table 5). The selected rough sapphires were prepared for LA-ICPMS by cleaning and mounting the sapphires in epoxy resin, followed by cutting and polishing. Sapphires to be used for the study of solid and fluid/melt inclusions were cleaned and prepared as doubly polished thick sections 0.1-0.3mm in thickness. All samples were optically examined under a petrographic microscope to locate and photograph the various features.

4.1.1.2.1 Laser Ablation Induced Coupled Mass Spectrometry

5.2.1 Laser Ablation Induced Coupled Plasma-Mass Spectrometry (LA ICP-MS)

A LA-ICPMS system at the School of Earth Sciences, University of Tasmania was used for minor and trace element analysis of sapphires (Table 5). A New Wave UP-213 Nd:Yag Q-switched Laser Ablation System is used as the sampling tool for an Agilent HP4500 Quadrapole ICP-MS. The results were standardised against the NIST612 artificial glass standard. A beam width of 110μm and a pulse rate of 10Hz were used for the analysis of the elements Ti, Cr, Cu, Zn, Ni, V, Ga, Fe, Mg, Be, Nb, Ta and Sn. Al was used an internal standard. The rims and cores of each sapphire grain were selected and areas free of visible inclusions were chosen for analysis.

Table 5. Hand specimen characteristics of sapphires used for trace element analysis.

Location	Colour	Features	Diameter (mm)	Shape
Moorina	Opaque Pale grey to pale blue	No visible inclusions	5	anhedral
Priory	Opaque Pale blue-pale grey to dark blue	No visible inclusions	5	subhedral
Spinel Creek	Translucent Pale grey to white	Star sapphire Brown patches	4	perfect hexagonal section
Thureau's Lead	Transparent Pale blue	Glassy No visible inclusions	1	Anhedral, very rounded
Ruby Creek	Opaque Pale blue to white	Fine black inclusions	2	subhedral
Main Creek	Opaque White domains and dark blue domains	Some blue bands	4	anhedral
Black Creek	Translucent Pale blue to dark blue	Discrete blue bands	4	subhedral
Wyniford River	Opaque Pale blue-grey	Uniform appearance	3	subhedral

4.1.1.3 Experimental technique: oxygen Isotopes

4.1.1.4 CO_2-Laser Fluorination

Sapphires were collected from nine different locations in the Weldborough Region (see Chapter 4.5.1). All samples used were light blue to dark blue and vary from translucent to opaque. The sapphires were weighed, cleaned and crushed for isotopic analysis. In addition to the sapphires, four representative basaltic samples from the Weldborough region were included. Olivine crystals were separated from jaw crushed basalt samples using a combination of sieving, magnetic separation and handpicking. 10mg of both sapphire and olivine was required for each analysis.

O-isotope analyses were performed by the CO_2 laser-fluorination method (Sharp, 1990) at the Institute of Earth Sciences, Academia Sinica, Taipei. A Finnigan MAT 252 mass spectrometer was employed to analyse the CO_2 gas. The results are reported per mil $\delta^{18}O$ values relative to Standard Mean Ocean Water (SMOW). The analytical precision is better than ±0.1 % based on 15 analyses of the UWG-2 garnet standard (Yui, 2000), which was employed to correct for machine drift. The UWG-2 standard has a suggested $\delta^{18}O$ value of +5.8 ‰ (Valley et al., 1995).

4.1.1.5 Experimental technique: Geochronology

4.1.1.5.1 Detrital zircons

A geochronological analysis of alluvial zircons from North Eastern Tasmania was carried out by Khin Zaw et al., (submitted). Five detrital zircons (3-5mm) from alluvial operations in Derby, were analysed for U-Pb by LA-ICPMS. Laser ablation analyses were performed using a Merchantec 213 nm laser at the University of Tasmania. Data was acquired using a 12-micron spot size, pulsing the laser at 5Hz with an energy density of 12mJ/cm^2. The primary standard was Temora 1 and the secondary standard was from the Tyndall Group volcaniclastics. The general procedure and standards used are outlined in Meffre et al., (submitted).

4.1.1.5.2 Zircon inclusions in corundum

A blue hexagonal-prism sapphire crystal (Main Creek 1, MA1) cut parallel to section {0001} was found to contain five clear euhedral zircon inclusions. These zircons ranged from 15µm to 25µm in diameter and were positioned at varying depths in the thick section. The sapphire was repeatedly ground with 6µm diamond paste until one of the zircons appeared close to the surface. The sample was then ground down with 3µm paste until the inclusion was revealed. The sample was cleaned in distilled water and analysed for Pb, U, Nd, Hf, and Th with LA-ICPMS (see method above). The count time varied, as the analysis continued until the zircon signature was lost. This process was repeated until all the inclusions were revealed and analysed.

4.2 General characteristics of the Weldborough sapphire

Around 400 corundum crystals, grains and crystals were examined by binocular microscope to determine their visible properties. The sapphires have an average diameter of 3mm, with the largest being 8mm. The crystals are euhedral and tend to have a barrel or broken-barrel habit (Figure 8 and 9D). Some crystals have cleaved on the {0001} plane and show a perfect hexagonal crystal shape with growth zones. The grains show varying degrees of roundness, but are generally subangular to rounded. All crystals showed signs of magmatic corrosion and small indents due to mechanical abrasion (Figure 9B.). Four sapphires were partially covered in black rims, typical of spinel reactions rims reported elsewhere (Sutherland et al., 2002; Stephenson, 1990).

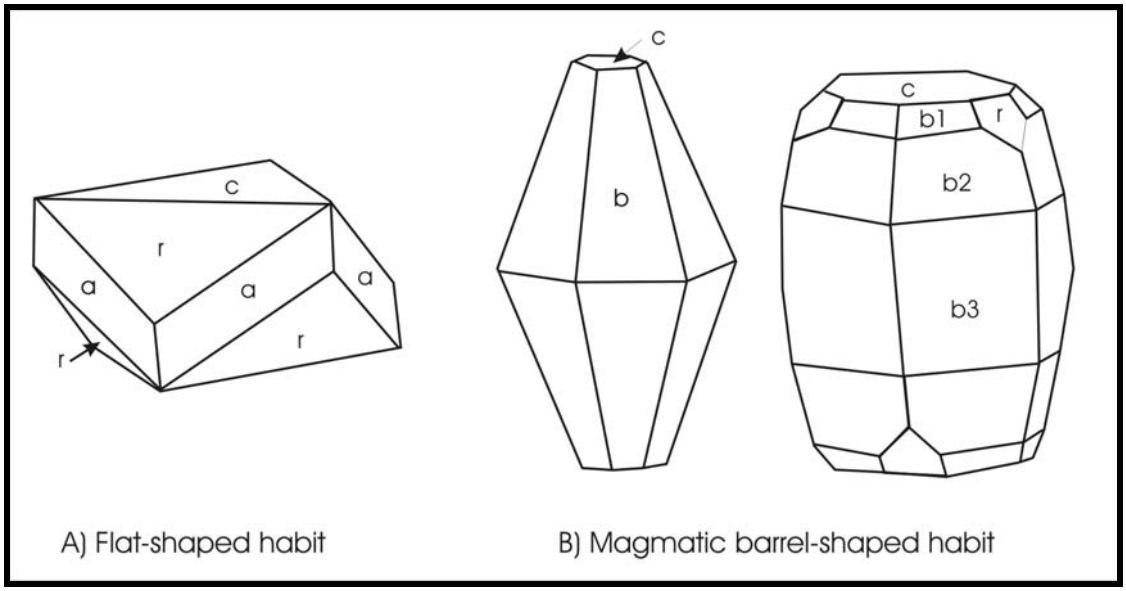

Figure 8. Crystal habit of corundum; A is the metamorphic dominated habit, B is the magmatic dominated habit. Note: Weldborough sapphires are dominated by the barrel-shaped habit. C = pinacoid, r = rhombohedron, a = prism, b = bipyramidal. After Guo (1993).

The sapphires are dominated shades of blue, ranging from almost white to dark blue (Figure 9A). The dark blue opaque sapphires appear black under natural light. Shades of yellow, brown and green make up ~5% of the sapphires. One grain shows a pink core and a blue rim. The sapphires can be multicoloured, with blue-green and blue-yellow and blue-white (Figure 9D) the most common combinations. The multiple colours can have straight boundaries and develop bands with each other, or grade from colour to colour. Multi-coloured sapphires make up ~1% of all sapphires.

These sapphires are typical of the Blue-Green-Yellow (BGY) suite of corundum from basaltic terrain (Sutherland et al., 1996a).

4.3 The mineral and fluid inclusions of the Weldborough sapphire

In comparison to other valuable gemstones, such as diamond and emerald, the nature of the sapphire host rocks remain poorly understood. Unfortunately, the chemistry of corundum is very simple (52.9% aluminium, 47.1% oxygen), and trace element compositions tend to provide very little information in relation to petrogenesis. The presence of various inclusions contained within the sapphire crystals is a potential source of genetic information. These inclusions (fluid, melt and mineral) have potential to preserve valuable information about the chemical environment, physical conditions and the geological processes that affect the host mineral at the time of its deposition (Guo et al., 1996). Inclusion data is therefore critical in

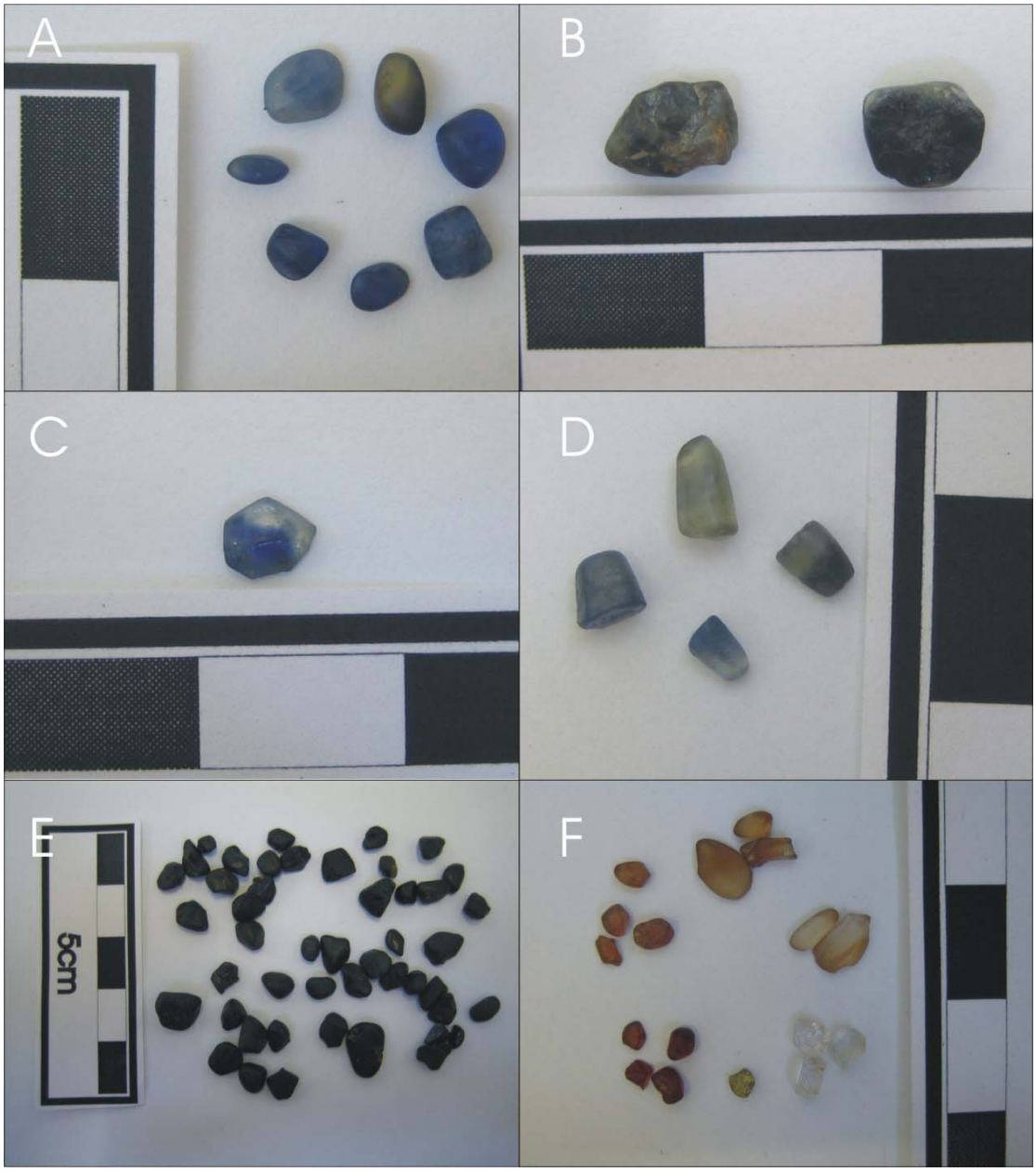

Figure 9. Physical features of the Weldborough sapphires. A. Colour variations, B. Sapphires with spinel reaction rim, C. Blue-yellow zoned sapphire, D. Dominant barrel-shape of the Weldborough sapphire, E. Spinel grains from the Weldborough region, F. Zircon grains from the Weldborough region.

evaluating the genetic models of corundum formation. The aims of this section are to identify various mineral and fluid inclusions within the Weldborough sapphires. Analysis of these inclusions including heating/freezing measurements and zircon inclusion dating will be used to critically analyse contemporary sapphire genesis models and to postulate a genesis model and age of crystallisation for the Weldborough sapphires.

This study will involve the study of 63 sapphire samples from 11 different locations in the Weldborough Region.

4.3.1.1 Mineral inclusions

Mineral inclusions can be classified as protogenetic, syngenetic and epigenetic according to their order of formation relative to the host mineral (Gubelin, 1973). Protogenic form before the host mineral in which it is enclosed, syngenetic inclusions are formed simultaneously with their host mineral and epigenetic inclusions form after the formation of the host crystal. Protogenetic and syngenetic inclusions (primary inclusions) hold most of the genetic information, but are sometimes difficult to tell from one another (Guo et al., 1996).

In this thesis all three types of mineral inclusions will be considered. Relatively recently, studies of sapphires have revealed a wide variety of mineral inclusions (Table 6).

Table 6. Mineral inclusions previously reported in corundum. **B** – sourced from alkali basalt terrains, **M** – sourced from metamorphic rocks. * denotes inclusion is the product of zircon decomposition. References: 1 - Coenraads (1992), 2 - Guo et al. (1996b), 3 - Sutthirat et al. (2001), 4 – Sutherland et al. (1998), 5 – Limutrakun (2001), 6 – Gubelin (1973).

Mineral	Formula	Type	Host	Reference
Pentlandite	$(Fe,Ni)_9S_8$	Sulphide	B	2,4
Pyrrhotite	FeS	Sulphide	B, M	1,2,4,6
Pyrite	FeS_2	Sulphide	M	1
Pyrite	FeS_2	Sulphide	M	6
Sphalerite	ZnS	Sulphide	M	6
Almandine	$Fe_3Al_2(SiO_4)_3$	Silicate	B	1
Pyrope	$Mg_3Al_2(SiO_4)_3$	Silicate	B	1
Alkali feldspar	$(K,Na)(AlSi_3O_8)$	Silicate	B	1,2,4
Albite	$NaAlSi_3O_8$	Silicate	B	1,2,4
Ca-plagioclase	$CaAl_2Si_2O_8$	Silicate	B	1,2,4
Mullite*	$Al_{4.5}Si_{1.5}O_{9.75}$	Silicate	B	2
Thorite	$ThSiO_4$	Silicate	B	2
Sillimanite*	Al_2SiO_5	Silicate	B	2
Nepheline	$(Na,K)AlSiO_4$	Silicate	B	5
Muscovite	$KAl_2(AlSi_3O_{10})(OH)_2$	Silicate	B	5
Zircon	$ZrSiO_4$	Silicate	B, M	1,2,4
Clinopyroxene	$(Ca,Mg,Fe,Al)_2Si_20_6$	Silicate	M	3
Olivine	$(Mg,Fe)_2SiO_4$	Silicate	M	6
Brockite	$(Ca,Th)PO_4.H_2O$	Phosphate	B	2
Apatite	$Ca_5(PO_4)3(OH,F,Cl)$	Phosphate	B, M	1
Columbite	$(Fe,Mn)(Nb,Ta)_2O_6$	Oxide	B	1,2,4
Rutile	TiO_2	Oxide	B	1
Boehemite	AlO(OH)	Oxide	B	1
Hercynite	$FeAl_2O_4$	Oxide	B	1,2,4
Gahnospinel	$ZnAl_2O_4$	Oxide	B	1,2,4
Pyrochlore	$(Na,Ca)_2Nb_2O_6(OH,F)$	Oxide	B	1,2
Uranopyrochlore	$(U,Ca,Ce)_2(Nb,Ta)_2O_6(OH,F)$	Oxide	B	1,2,4
Ilmenorutile	$(Ti,Nb,Fe)_3O_6$	Oxide	B	2,4
Uraninite	UO_2	Oxide	B	2
Hematite	Fe_2O_3	Oxide	B	2
Ilmenite	$FeTiO_3$	Oxide	B	2

Baddeleyite	ZrO_2	Oxide	B	2
Brookite	$Ti(Fe, Ta, Nb)O_2$	Oxide	M	6
Graphite	C	Native	M	6
Dolomite	$CaMg(CO_3)_2$	Carbonate	M	6
Calcite	$CaCO_3$	Carbonate	M	6

4.3.1.2 Fluid inclusions in corundum

Fluid inclusions can be classified as primary, pseudosecondary and secondary (Roedder, 1984). Primary inclusions form during crystal growth and are represented by inclusion trails along primary growth bands. Pseudosecondary inclusions form during the growth of a crystal, but due to the resealing of fractures. Pseudosecondary inclusions cross-cut primary growth bands of a mineral. Secondary inclusions form after crystal growth. Primary and pseudosecondary fluid inclusions therefore record the temperature and pressure conditions at which the enclosing crystal forms. The focus of this study is to find and recognise primary and pseudosecondary fluid inclusions. Some results previously reported are outlined below.

Studies of fluid inclusions in sapphires from Eastern Australia (Barrington and Anakie) and Thailand (Bo Ploi, Thailand) reported two main fluid inclusion types. Types 1 are vapour-rich CO_2 with various densities up to about 0.86 g/cm^3. Type 2 are polyphase (v+l+s) inclusions, which contain several daughter minerals, hypersaline brine and a CO_2 rich vapour phase with a total homogenisation temperature from 920ºC - 1000ºC (Srithai et al., 1999). It was suggested that these inclusions appeared primary, and along with the presence of a silicate melt inclusion, suggested the coexistence of CO_2 vapour, hypersaline NaCl brines (up to 73wt % equivalent NaCl) and silicate melt during the growth of sapphires.

Studies of fluid inclusions in sapphires from northern Thailand (Denchai) also reported two main fluid inclusion types (Limtrakun, 2001): Type 1 are CO_2-rich-dominated inclusions containing three phases (H_2O(l) + CO_2(l) + V) with densities of up to 0.87g/cm^3 and probable trapping temperatures of >550ºC with a minimum pressure of 4 kbars. Type 2 inclusions are polyphase inclusions containing three phases (hypersaline fluid, vapour and halite/sylvite). The fluid contained 58 – 64 wt % NaCl equivalent and indicated minimum trapping temperatures of 7 kbar.

Studies of fluid inclusions in rubies from Vietnam (Luc Yen) provided evidence of CO_2-H_2S-COS-S_8-AlO(OH)-bearing fluids with native sulphur and diaspore daughter minerals without visible water (Giuliani et al., 2003).

4.3.2 The mineral inclusions of the Weldborough Sapphire

The Weldborough sapphires contain a number of different oxide, silicate and sulphide inclusions. Table 7 is a summary of mineral inclusions found in the Weldborough sapphire.

Table 7. Summary of inclusions found in the Weldborough sapphires. Identification method; L=Laser Raman, O=optically, LA=Laser Ablation ICPMS.

Inclusion	Formula	Type	ID method	Figure
Graphite	C	native	L	11A
Diamond	C	native	L	
Rutile	TiO_2	oxide	O, L, LA	11C,D
Columbite	$(Fe,Mn)(Nb,Ta)_2O_6$	oxide	O, LA	11E, F
Hercynite	$MgAl_2O_4$	oxide	L, O	11G
Chromite	$FeCr_2O_4$	oxide	L, O	
Pyrochlore	$(U,Ca,Ce)_2(Nb,Ta)_2O_6(OH,F)$	oxide	O, LA	10, 12C
Apatite	$Ca_5(PO_4)3(OH,F,Cl)$	phosphate	O	12D
Olivine	$(Mg,Fe)_2SiO_4$	silicate	L	12A
Beryl	$Be_3Al_2Si_6O_{18}$	silicate	L	
Zircon	$ZrSiO_4$	silicate	O, L, LA	11H
Anorthite	$CaAl_2Si_2O_8$	silicate	O, L	11B
Oligioclase	$(Na,Ca)(Si,Al)_4O_8$	silicate	L	10A
Quartz	SiO_2	silicate	L	
Molybdenite	MoS_2	sulphide	L	12B
Pyrite	FeS_2	sulphide	L	

The inclusions were identified optically with the assistance of Dr. Ian Graham (Australian Museum) and subsequently tested and identified with Laser Raman Spectroscopy with the assistance of Dr. Terry Mernagh (Geoscience Australia). Some inclusions were detected as part of the LA-ICPMS trace element chemistry determination section of this thesis. It is important to note that the most accepted determination method for inclusions involves exposing the inclusions and using a quantitative device such as the electron microprobe.

Due to the limited number of corundum mineral inclusion spectra available (columbite and pyrochlore not available) and the sampling of minerals with no correlating spectra, some inclusions could only be identified optically.

4.3.3 Inclusions detected by LA-ICPMS

The presence of correlated smooth peaks in the spectra from LA-ICPMS indicates the presence of inclusions within the sapphires (Figure 10). These peaks had to be removed from the spectra before analysis to obtain accurate data on general trends and the rim and core. There are four types of inclusions detected by LA-ICPMS analysis. The possible mineral species that these inclusions represent are discussed below.

Type 1. Nb-Ta-rich inclusions

This type of inclusion is characterised by smooth and correlated peaks between Nb and Ta in the LA-ICPMS spectra (Figure 10A). This type of inclusion is abundant (present in five analyses) and occurs as discrete inclusions or as a series of multiple (and potentially overlapping) inclusions

Type 2. Nb-Ta-Sn-rich inclusions

This type of inclusion is characterised by smooth and correlated peaks between Nb, Ta and Sn in the LA-ICPMS spectra (Figure 10B). It was detected twice in one analysis (H3 – Wyniford River).

Type 3. Nb-Ta-Ti-(Mg-Fe)-rich inclusions

This type of inclusion is characterised by smooth and correlated peaks between Mg and Fe flanked by smooth and correlated peaks between Nb-Ta-Ti in the LA-ICPMS spectra (Figure 10C). This type of inclusion occurred twice in the same analysis (A1 – Moorina).

Type 4. Mg-Ti-rich inclusions

This type of inclusion is characterised by smooth and correlated peaks between Mg and Ti in the LA-ICPMS spectra (Figure 10D). This type of inclusion was detected once (E3 – Ruby Creek) and returned a weak signal compared with the background spectra.

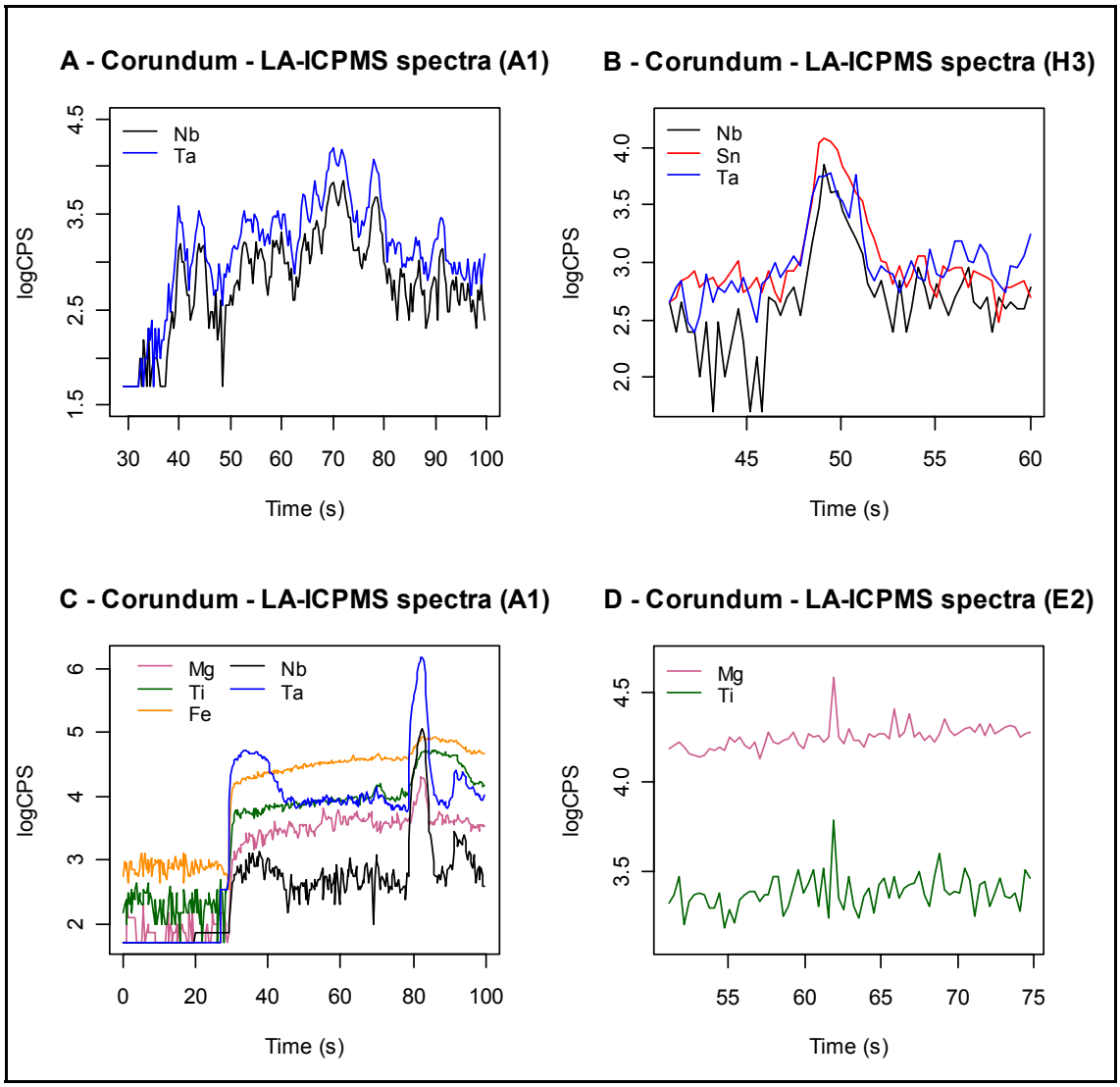

Figure 10A, B, C, D. Corundum LA-ICPMS spectra representative of inclusions. CPS is counts per second. A – Nb-Ta-rich inclusion, B – Nb-Ta-Sn-rich inclusion, C – Nb-Ta-Ti-(Mg-Fe) rich inclusion and D – Mg-Ti-rich inclusion.

4.3.3.1 Mineral Inclusion Descriptions

In Laser Raman Spectroscopy, corundum is typified by fundamental vibrations at 378, 418, 432, 451, 578, 645 and 751cm^{-1} (Griffith, 1987). This spectrum was superimposed on most LRS results. Sapphire tends to have stronger peaks at 451, 578 and 751cm^{-1}. In the following section, optical and LRS studies of mineral inclusions in sapphires will be described. **For Laser Raman spectra of inclusions, refer to Appendix 4.**

Graphite (Sample FR4)

Graphite was detected as an opaque phase inside a clear, euhedral crystal of oligioclase. The graphite inclusion is 10 microns across.

Graphite is characterised by a strong LRS peak at 1574cm^{-1}.

Diamond (Samples MO4 and OC1)

Diamond was detected in three inclusions. In two cases the inclusions were a dark phase within ameboid shaped inclusions that were interpreted to be fluid/melt inclusions. In the final case the diamond signature came from within a possible intergrowth with chromite (MO4). The inclusion was ~15μm deep in the section.

Diamond is typified with a strong peak at 1330cm^{-1} on LRS.

Rutile (Most samples)

Rutile is found in primary growth bands as fine needles or cross cutting primary growth bands as discrete inclusions. Primary rutile (Figure 11C) occurs as fine black needles aligned along the growth planes and are typically up 20 microns long and up to 5 micron wide. The rutile needles that cross-cuts the growth bands are larger, typically up to 200 microns long and 10 microns wide (Figure 11D). This type of rutile was often associated with columbite. Rutile is typified with broad peaks at 440 and 600cm^{-1} in Laser Raman Spectroscopy.

Columbite (Samples MA1 and MO3)

Columbite generally occurs as clear euhedral crystals up to 200 micron in size (Figure 11E and F). However, when occurring as larger crystals, it was submetallic black. Columbite was found in three sapphires. LA-ICPMS data (see Chapter 4.4) indicates that the columbite can be Fe poor (no detected Fe) or Fe rich with varying levels of Sn substitution. The LR spectra produced by the optically identified columbite had distinctive peaks at 353, 1087 and 1465cm^{-1}.

Hercynite (Sample MO2)

Hercynite spinel was detected and is characterised in this sapphire by its grape green colour and cigar-like shape. The spinel was found in an inclusion trail (of spinel) along a primary growth band and is up to 20 microns in length. Hercynite is typified in LR spectra by broad peaks at 610 and 751cm^{-1}.

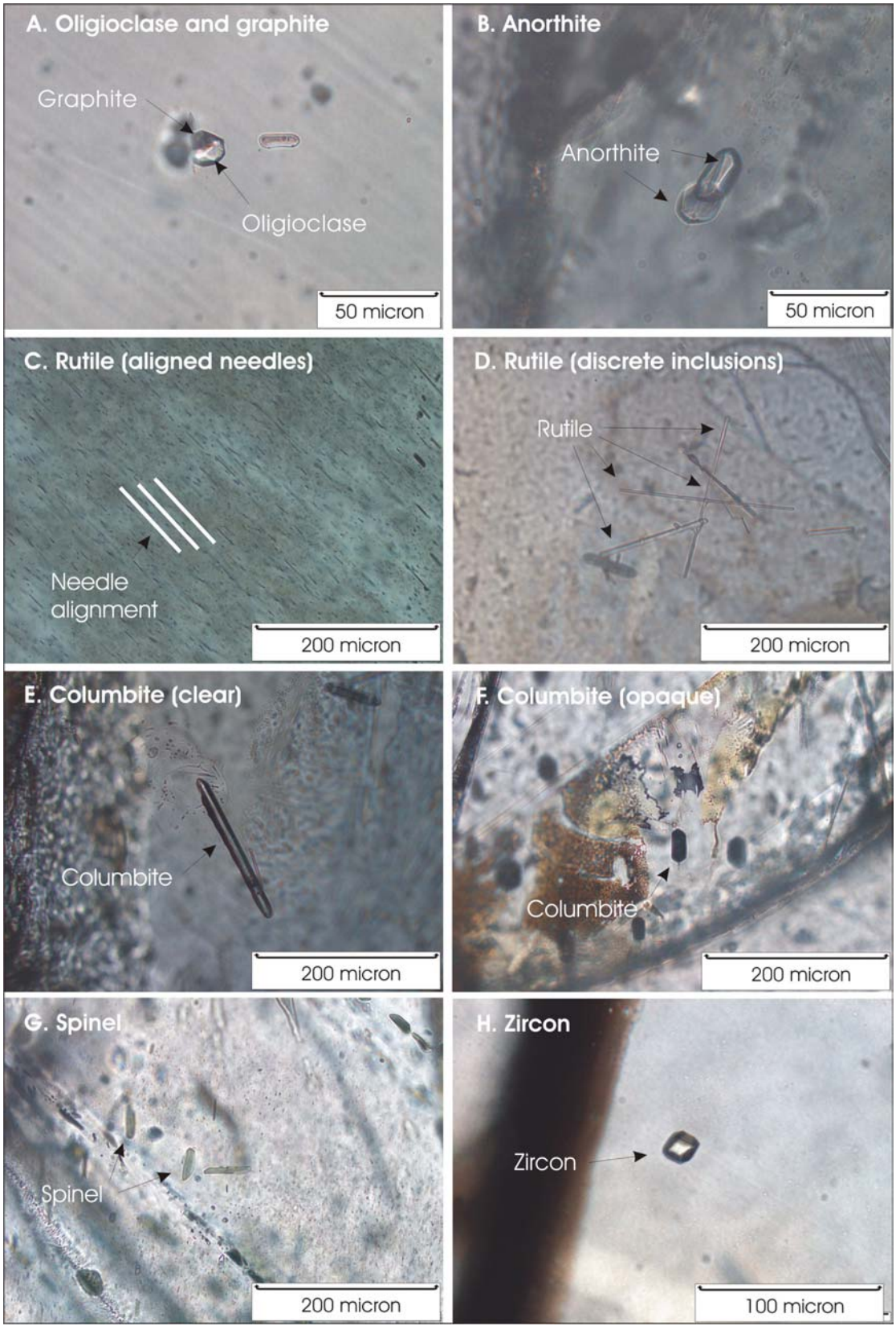

Figure 11A, B, C, D, E, F, G, H. Mineral inclusions in the Weldborough sapphire (plane polarised light).

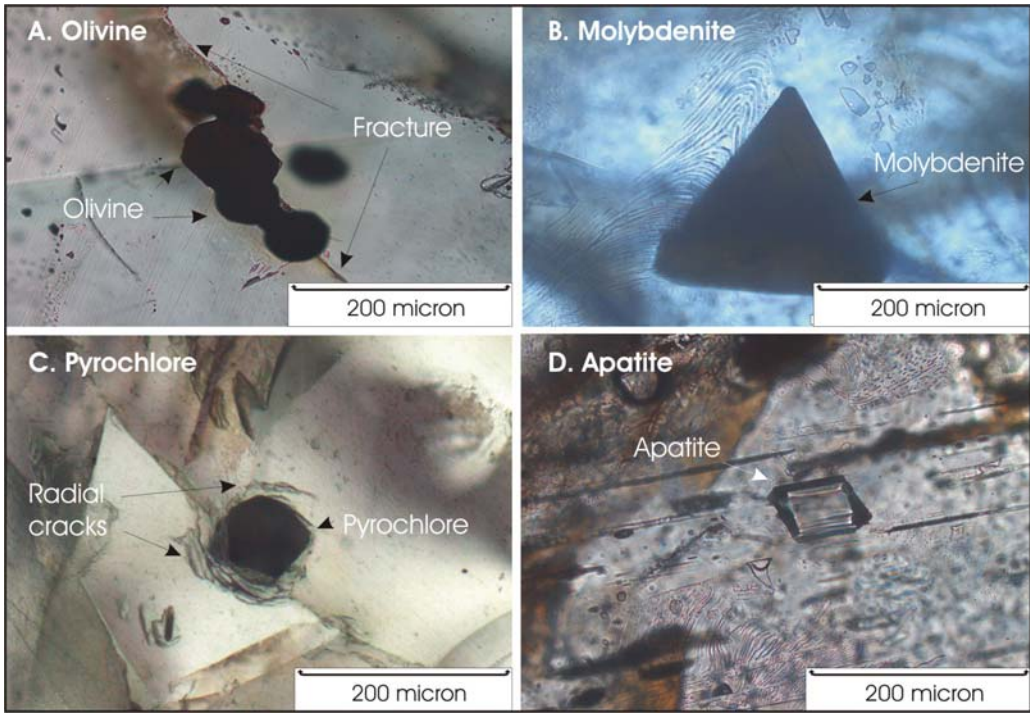

Figure 12A, B, C, D. Mineral inclusions in the Weldborough sapphire (plane polarised light)

Chromite (Sample MO4)

Chromite was detected as a dark red amoeboid centre in an inclusion 25 micron across. The remainder of the inclusion was clear and returned a diamond signal from LRS. Chromite is typified by peaks at 375 and 640cm^{-1} in LR spectra.

Pyrochlore (Sample MO3)

Reddish to brown opaque pyrochlore was identified optically. It has distinctive radial cracks and a faint brown halo due to radiation affects. The hexagonal inclusion is 65 micron in diameter has a LRS spectrum characterised by extreme fluorescence. Fluorescence is a by-product of energetically exciting elements such that they fluoresce. The fluorescence causes major degradation of an LR spectrum, compromising any results. Elements that are notorious for fluorescing are Fe, Ti and U.

Apatite (Sample OC2)

Apatite is present as pleochroic pink-green prismatic crystals. It has a strong square crystal shape and high relief. Apatite inclusions ranged from 30 – 80 micron.

Apatite is typified by a fundamental vibration at 963cm^{-1} in LR spectra.

Olivine (Sample FR1)

Olivine occurs as dark red translucent crystals with a hexagonal shape. These crystals are clustered around a crack suggesting a secondary nature. Although isn't generally hexagonal, the internal structure of corundum is. The shape of this inclusion represents the hexagonally

controlled internal cracks of the sapphire. Individual hexagons are up to 60 micron across. This olivine tends towards a fayalite composition which is typified by peaks at 240 and 850cm^{-1} on an LR spectrum.

Zircon (Sample MA1)

The zircons present are euhedral stubby to elongate crystals with distinct pleochroism. The zircons found are small – up to 25 microns across, with zircons arranged as discrete inclusions or as aggregates of two zircons. Zircon is typified by fundamental vibrations at 437, 356 and 973cm^{-1}.

Four zircons were analysed for Pb, U, Nd, Hf, and Th with LA-ICPMS for U-Pb dating (This chapter, 4.6) but the elemental analysis is presented here (Table 8). The dated zircons have high Hf (1.8wt% HfO_2), high U (1.32wt% UO_2) and moderate Th (0.99wt% ThO_2).

Table 8. Zircon inclusion LA-ICPMS analysis. Results in ppm, numbers in parentheses are weight % oxide.

Sample	U	Nd	Hf	Th	Pb
MA1z1	6461 (0.73)	1.0	14941 (1.76)	4243 (0.48)	35
MA1z2	11626 (1.32)	1.5	15579 (1.84)	8699 (0.99)	75
MA1z3	1262 (0.14)	0.6	12769 (1.51)	713 (0.08)	11
MA1z4	7206 (0.82)	1.5	14327 (1.69)	4961 (0.56)	56

Feldspar (Samples FR4 and MO3)

Anorthite and oligoclase occur as euhedral, clear discrete crystals or intergrowths. One feldspar inclusion consisted of two intergrown feldspar (anorthite) crystals. Another feldspar inclusion (oligoclase) was a composite inclusion with graphite.

All feldspars are typified by fundamental vibrations at 500 and 515cm^{-1}. Mernagh (1991) found that one could discriminate between feldspar minerals on the basis on the peaks in the Si-O stretching region. Anorthite has a distinctive vibration at 503 and 488cm^{-1} whilst oligoclase has distinctive vibrations at 508 and 480cm^{-1}.

Quartz (Sample FR7)

Amethyst was detected as the dominant phase in a dark mineral inclusion suspected to be a melt inclusion. Amethyst is typified by fundamental vibrations at 217, 376 and 460cm^{-1}.

Molybdenite (Samples MA0, MA1 and MA2)

This occurs as large (200µm across) inclusions, with figure 12B exhibiting strong triangular shape and fractures. The molybdenite is dark brown and opaque.

Molybdenite is typified by fundamental vibrations at 381 and 407cm^{-1}.

Pyrite (Sample MO1)

Pyrite is typified by fundamental vibrations at 381 and 407cm^{-1}. Pyrite was identified as an amoeboid dark inclusion <20µm across.

Beryl (Sample MA4)

Beryl is typified by a fundamental vibration at 680cm^{-1}. The strength of the spectra in this study relative to that of typical beryl is poor, and absolute confirmation cannot be given. However, it is likely to be beryl or a beryl-like mineral (Mernagh, 2005).

4.3.3.2 Mineral inclusion discussion

Diamond and Graphite

The presence of diamond in the sample is likely to be due to sample contamination. Diamond paste (used to polish the sample) is probably present on the surface and/or infiltrated cracks in the crystal. The use of the confocal laser system allows the subsurface of the crystal to be sampled with a high spatial resolution (~6µm; (Mernagh, 1988) which suggests that two of the three shallow "diamond inclusions" are a result of diamond polish infiltration.

The third diamond result sits deeper in the section (MO4, ~15µm below the surface) in a relatively flaw free area of the crystal. The diamond is an apparent intergrowth with chromite. Although the infiltration of diamond polish is still a distinct possibility, further investigation to prove that the diamond result is a mineral inclusion is warranted. This would have significant implications for current corundum genesis models.

Graphite has been found as inclusions in metamorphic style corundum from Myanmar (Gubelin, 1973). Carbon can be sourced at all levels in the lithosphere and has little significance other than that the presence of CO_2 (or carbon species such as CO_2, hydrocarbons etc.) can be inferred to be present in the environment.

Rutile

The presence of two different forms of rutile in the same sapphire has significance. The finer rutile needles are clearly primary (oriented with growth planes, FIG 11C) and the larger needles also appear to be primary (no obvious cracks or trails, FIG 11D). This suggests a genetic environment where rutile is co-crystallising with corundum.

(Ferro)columbite and (urano)pyrochlore

Caution must be taken in the discussion of these minerals as they have only been identified qualitatively and their presence is inferred. However their ubiquitous presence as inclusions in sapphires from Australia and Thailand (Sutherland et al., 1998), optical properties and LA-ICPMS data (Chapter 6.1) strongly suggest their presence.

Spinel

The presence of hercynite spinel as an inclusion trail in a primary growth band suggests the hercynite is primary and abundant during corundum genesis.

Chromite and olivine

Chromite and olivine, minerals associated with ultramafic and mafic compositions, are present as inclusions in the Weldborough sapphires. The location of the olivine occurrence along a significant fracture in the sapphire crystal, is good indication that the inclusion is epigenetic (secondary) and related to a later basaltic transportation event.

However, the chromite appears to be primary, which suggests input from a mantle source below the garnet-spinel transition (depending on Cr concentration). As ultramafic rocks tend to be too alumina poor to develop corundum, the Weldborough sapphires are unlikely to have formed in these rocks. The presence of a chromite inclusion indicates that the Weldborough sapphires may have had some level of input from a source compatible with a high Cr mantle during crystallisation.

Zircon

In the literature, zircon inclusions are commonly reported with radial cracks that propagate outwards from the zircon and dark brown haloes in the surrounding corundum. The cracks are due to:

1. differential thermal contraction between zircon and corundum, and/or
2. zircon expansion due to the radioactive decay of Th and U and the brown halo is due to α-irradiation damage from U and Th decay (Guo et al., 1996a).

These affects (cracks and haloes) are thought to accumulate only at low temperature (below 240ºC for zircon) because the temperature of the likely host (basalt, 1200-1250ºC) is high enough to anneal any radiation damage.

These features are not present around any of the five zircons present in the Weldborough sapphires. On this basis it is likely that many zircon inclusions have been overlooked by Guo et al., as indicated by their minimal success (18 zircon inclusions found out of several thousand corundum grains from various sources), compared to this study (five zircon inclusions found out of 25 corundum grains). As Guo et al., was discussing larger inclusions (up to 1000µm compared with this study of <25µm), the absence of radiation affects in the zircons is likely due to the smaller size of the zircons.

Chemically, the Weldborough sapphire zircon inclusions have similar levels of U, Th and Hf enrichment to zircons reported from Australian-Asian sapphires sourced in alkali basalt terrains. Typical zircons inclusions from these terrains have high Hf (up to 3.8wt% HfO_2), high U (up to 1wt% UO_2) and high Th (2.1wt% ThO_2) (Sutherland et al., 1998). The zircon inclusions from this study have slightly higher U, but lower Hf and Th (Table 8).

If the zircon inclusions in the Weldborough sapphires grew from basaltic melt, it is expected that the basalts that host them could contain up to 22000ppm Zr, on the basis that 3% ZrO_2 can dissolve in the melt at 1250ºC-1300ºC (Watson, 1980). The Weldborough basalts contain between 200 and 500pm Zr (This study, Chapter 3) and are therefore not considered to be the source of the zircon inclusions. If the corundum and zircon inclusions are syngenetic, the growth of corundum from a Weldborough basaltic melt composition is unlikely and high levels of U, Hf and Th in the inclusions suggests the parental melt was more highly evolved. If the zircon inclusions are protogenetic (i.e. inherited), caution must be taken before the development of corundum genetic models such as the Guo et al., (1996b) model of interactions between carbonatitic and silicic magmas. In either case (protogenetic or syngenetic) zircon is present in the environment of corundum formation.

Further study to include Zr, U, Hf and Th in corundum trace and minor element analysis is warranted.

Feldspars (oligioclase and anorthite)

The presence of both sodium and calcium rich feldspars are significant given the absence of potassium feldspars. In both recent studies on feldspar inclusions on corundum (i.e. Guo et al., 1996b and Sutherland et al., 1998) indicate the feldspar compositions are generally Na and K-rich with a distinctive absence of Ca-rich feldspars. However Gubelin and Kiovula (1986) detected Na-rich feldspars as inclusions in sapphires and attributed them to basaltic volcanism. This is unlikely for two reasons:

1. The feldspars appear primary
2. Corundum could not crystallise from a basaltic melt.

Crosscut fractures are typical with feldspar inclusions (Guo et al., 1996), but were not observed in association any feldspar inclusions in the Weldborough sapphires.

Molybdenite

This is the first time molybdenite has been identified as a mineral inclusion in sapphires and given the frequency of occurrence (four inclusions in three different sapphires) may be genetically significant. Felsic intrusives such as granites are a good source of Mo, which supports the input of a felsic melt in a corundum genesis model.

As molybdenite may be unique to the Weldborough sapphires, the presence of molybdenite in a sapphire could be used as an authentication indicator. Further work to analyse the sapphires for trace element Mo may indicate that Mo concentration is a powerful tool for the authentification of Tasmanian sapphires.

Other inclusions

The genetic significance of quartz, pyrite, beryl and apatite will not be discussed, as further work is required to confirm these species. However, it is important to note that the potential presence of beryl inclusions can explain the distribution and concentrations of elemental Be found in the Weldborough sapphires.

4.3.3.2.1 Inclusions detected by LA-ICPMS: Discussion

The presence of strong correlating peaks between Nb-Ta associated with Sn or Ti indicates the presence of mineral inclusions containing these elements. Due to the nature of LA-ICPMS sampling, the exact composition of these minerals cannot be obtained. However, the presence of these Nb + Ta-rich inclusions suggests the presence of pyrochlore, ilmenorutile, brookite or columbite (Compositions, Table 9). These four minerals are highly abundant as inclusions in sapphires, making up over 65% of mineral inclusions in one study (Guo et al., 1996b).

Table 9. Elemental chemistry of Nb-Ta bearing phases known to occur in corundum.

Mineral	Formula	Notes
Pyrochlore	$A_{2-m}B_2X_6[(O,OH,F)=Y]_{1-n}.pH_2O$	A=Na, Ca, K, Sn^{2+}, Ba, Sr, REE, Pb, Mn, Fe^{2+}, Bi, Th and U, B=Ta, Nb, Ti, Zr, Fe^{3+}, Sn^{4+} and W^{4+}. Contains essential **Nb, Ta or Ti**. (Lindsley, 1991).
Columbite	AB_2O_6	A = Fe^{2+} or Mn^{2+} and B = Ta^{5+} or Nb^{5+}, (Lindsley, 1991)
Ilmenorutile	(Ti, Fe, Nb, Ta, Sn)O_2	Tetragonal, contains essential **Ti** and **Nb** or **Ta** (Deer et al., 1992).
Brookite	(Ti, Nb, Sb, Sn, Fe)O_2	Orthorhombic, contains essential **Ti** (Lindsley, 1991).

Type 1: Nb-Ta-rich (Figure 10a)
The inclusion does not contain the elements Sn, Ba, Fe or Ti. As ilmenorutile and brookite contain essential Ti, these phases can be ruled out. This is inclusion is likely to be Mn-rich columbite (due to absence of iron) or pyrochlore. However, conclusivity on the exact elemental composition for Type 1 inclusions cannot be determined because:

1. Mn was not analysed

2. Columbite can accommodate many other substitutions, especially tetravalent ions (Lindsley, 1991).

3. The use of LA-ICPMS spectra to determine quantitative elemental abundance of the detected inclusions is not possible.

Type 2: Nb-Ta-Sn rich (Figure 10b)
This inclusion does not contain Ba, Fe or Ti. As ilmenorutile and brookite contain essential Ti, these phases can be ruled out. As mentioned above, tetravalent ions, such as Sn^{4+}, are accommodated in the columbite and pyrochlore lattice. This inclusion is likely to be Sn-rich columbite or pyrochlore.

Type 3: Nb-Ta-Ti-(Mg-Fe) rich (Figure 10c)
If the inclusion was homogenous (monominerallic), the elemental composition strongly indicates that it is pyrochlore. However, the bimodal distribution of the Nb-Ta-Ti correlation indicates that the inclusion is **heterogeneous**. This lack of homogeneity is likely due to either:

1) The inclusion is an intergrowth of two mineral phases or

2) The inclusion consists of a mineral phase with a rim of different composition (eg reaction rim).

If the inclusion was an intergrowth of two minerals, it is unlikely that the resultant spectra would exhibit a smooth bimodal distribution in relation to Nb, Ta and Ti "either side" of the Fe-Mg enrichment.

I conclude that this inclusion consists of an Fe-Mg rich core with an Nb-Ta-Ti rich rim or intergrowth. An Nb-Ta-Ti rich reaction rim on an inclusion suggests an environment rich in incompatible elements, such as a late stage granite pegmatite or carbonatite. Columbite, pyrochlore, ilmenorutile and brookite are equally represented by an Nb-Ta-Ti rich composition.

Type 4: Mg-Ti rich (Figure 10D)

Considering elements such as Ca, Na and Si were omitted from the analysis, it is difficult to identify the type 4 inclusions as a specific mineral. The presence of an Mg- and Ti-rich but Fe-absent inclusion is not represented in the literature as a common inclusion in corundum (eg. Sutherland et al., 1998; Guo et al., 1996) and indicates the presence of a mineral previously unidentified as an inclusion in corundum .

4.3.4 Fluid inclusions in the Weldborough Sapphire

Of the 63 sapphire chips examined, 48 contained primary, pseudosecondary or secondary fluid inclusions. The fluid inclusions have a negative crystal shape, an angular anhedral shape or a rounded amoeboid shape and are between 10-150μm in diameter. Fluid inclusions ranging from 5-20μm are the most abundant (~75% of all fluid inclusions). "Tigers Striping" texture is present in most sapphires and indicates the presence of secondary fluid inclusions, which will not be discussed further.

Based on optical studies, only one type of primary or pseudosecondary fluid inclusion could be distinguished. These inclusions ranged from 10 - 30μm in diameter and consist of a vapour bubble and a liquid phase. These inclusions are isolated and have a negative crystal shape, which indicate that it is primary. No visible daughter minerals are present in the inclusions. These CO_2-rich inclusions are shown in Figure 13.

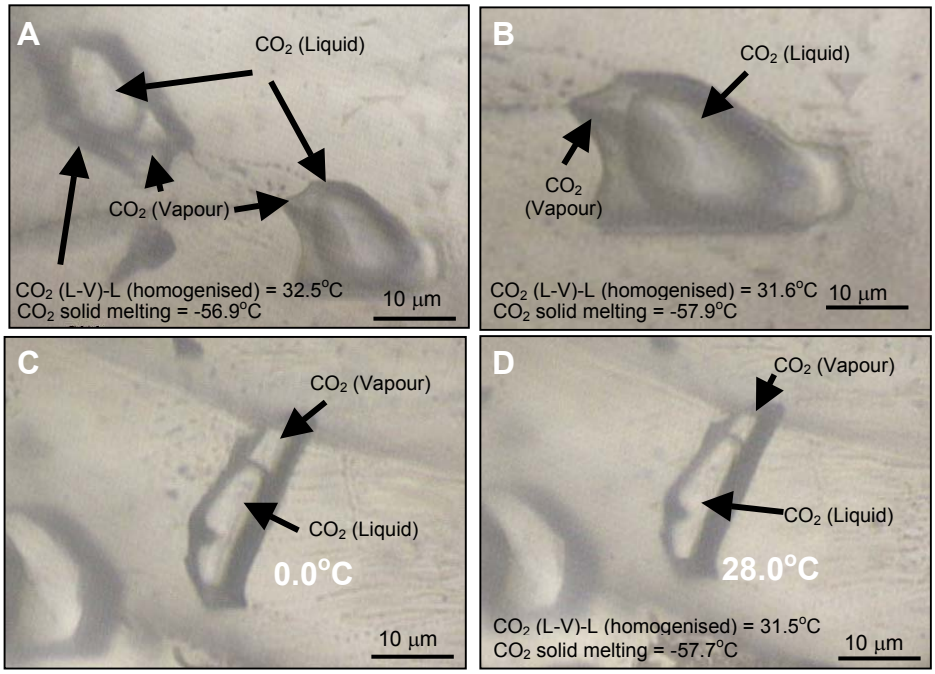

Fig. 13. Photomicrographs of CO_2 liquid bearing fluid inclusions in Weldborough sapphires (Main Creek). **A.** CO_2 liquid-vapour inclusions. **B.** Close-up of second inclusion. **C**. CO_2 liquid-vapour inclusion at room temperature. **D.** CO_2 liquid-vapour inclusion at 28.0°C. Note the CO_2 liquid expands and becomes larger in size, and finally homogenises into the liquid phase at 31.5°C suggesting mid-crustal depths or shallow mantle.

4.3.4.1 Laser Raman results

Laser Raman Spectroscopy was performed on 36 fluid inclusions to determine the compositions of the vapour and gas phases and identify any daughter phases that may be present. In every case only CO_2 liquid and/or vapour was detected (Appendix 4).

4.3.4.2 Microthermometric results

Four sapphires known to contain the two-phase CO_2-rich fluid inclusions were selected for microthermometry. The inclusions were cooled to below -170ºC, causing them to homogenise into a single CO_2-solid phase. No phase transitions were observed in this temperature range, implying that N_2 and CH_4 must either be not present or in low quantities (Limutrakun, 2003). The frozen CO_2 was slowly reheated and had melting temperatures between -56.9ºC and -57.9ºC (4 analyses). These results are slightly higher than the expected value of -56.6ºC, the melting point for pure CO_2 (Roedder, 1984). This confirms the presence of pure CO_2. On slow heating, the homogenisation temperature of CO_2 into the liquid phase ranges from +27.2ºC to +32.5ºC (4 analyses). Using phase relationship from Roedder (1984)

the temperatures can be converted to corresponding inclusion densities given we understand the nature of the phase transition (Figure 14). These temperatures correspond to densities in the range of 0.56 gm/cm^3 to 0.69 gm/cm^3.

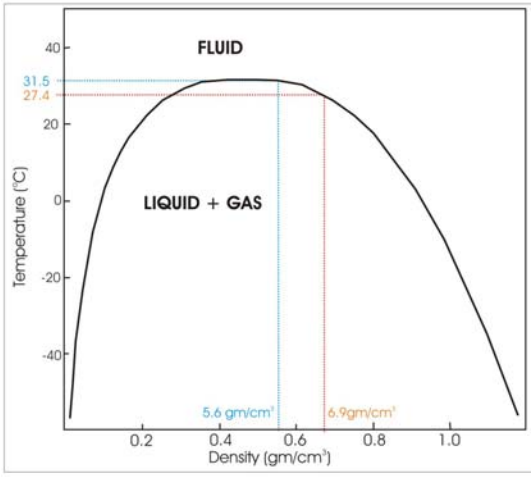

Figure 14. Using CO2 L-V-L range of 27.4 – 31.5ºC the calculated density is 5.6 – 6.9 gm/cm^3 for CO2-rich fluid inclusions in Weldborough sapphire, NE Tasmania. Diagram after Roedder (1984).

4.3.4.3 Fluid inclusion discussion

Fluid inclusions can be used to obtain either temperature or the pressure of trapping, but not both (Roedder, 1984). To obtain T_t or P_t from fluid inclusions requires the pressure or temperature to already be known from independent measurements.

Two studies, producing genetic models for corundum from basaltic terrain, have estimated the temperature and pressure of crystallisation. Guo et al., (1996b) estimated the pressure of sapphire crystallisation to be between 3.7 and 7.5 kbar ("magma mixing" hypothesis, mid-crustal depths) whereas Sutherland et al., (1998a) proposed that sapphire crystallisation occurs between 7 kbar and 11 kbar ("felsic emanations metasomatises hydrous mantle" hypothesis, shallow mantle).

The two models are represented on a P-T diagram (Figure 13). This diagram also shows the field for the densities of fluid inclusions in the Weldborough sapphire. The densities of the inclusions in this study do not overlap with the Sutherland model pressure estimate. Therefore these inclusions are not primary as dictated by the Sutherland model. The densities of the inclusions in this study have a small overlap (above 1200ºC) with the Guo model pressure estimate for sapphire formation. These inclusions could be considered primary as dictated by a Guo model. If the inclusions are primary, and the Guo model of corundum

formation is correct, then these inclusions were trapped at a pressure of ~4 kbar and between 1200 and 1400ºC. In this case, an extreme temperature range was selected to give a broader range of pressures.

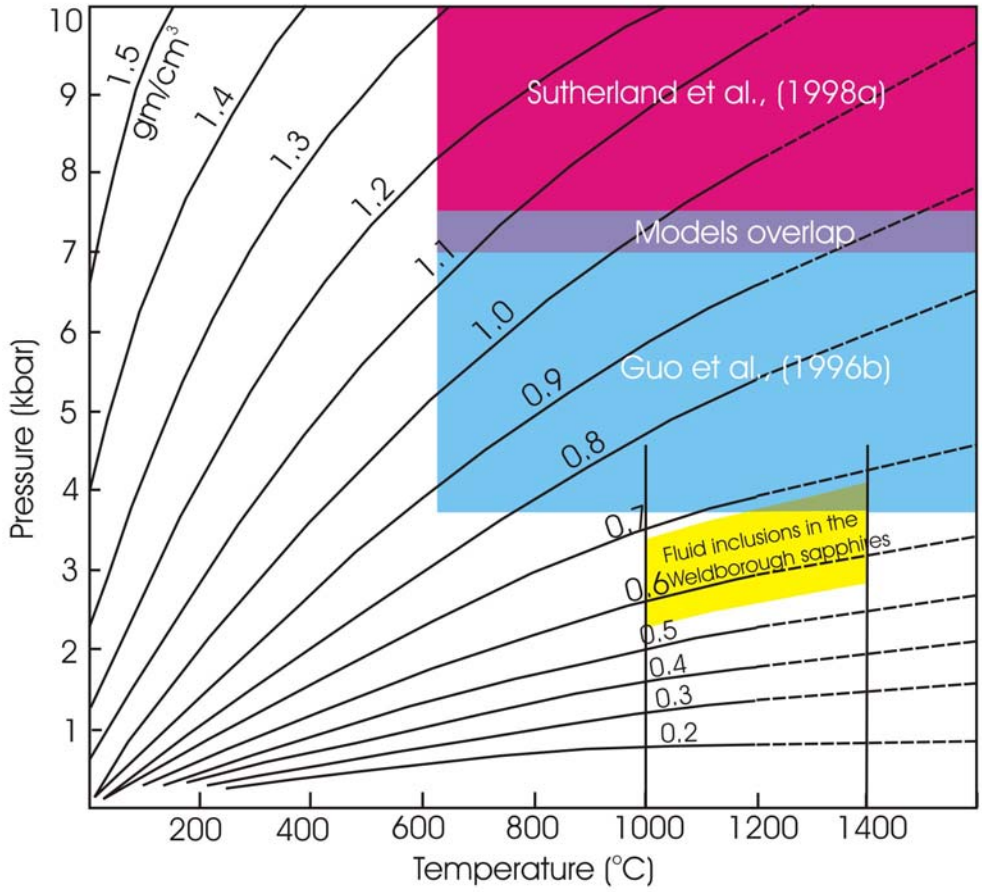

Figure 15. Temperature-Pressure-Density diagram. Purple field represents the Sutherland et al., (1998a) sapphire genesis model. Blue field represents the Guo et al., (1996b) sapphire genesis model. Purple is overlap of two models. Yellow is density range of inclusions in the Weldborough sapphire (this study). Green is overlap between the Guo et al. model and the Weldborough inclusions. Dashed lines indicated extended isochors above 1200ºC. Temperature of basalt from Guo (1993). After Roedder (1984).

The Weldborough sapphires are transported to the surface in basaltic magma. This basaltic magma is another possible source for the studied inclusions. For trapping temperatures of 1000ºC and 1400ºC (realistic temperatures for basaltic magma), a trapping pressure would be between 2.3 and 4.1 kbar. This is equivalent to a depth of between 6 and 11km (density of rock = 2.65 gm/cm^3). The suspected primary inclusions must now be considered to be secondary inclusions. The genetic information obtainable from these inclusions is therefore negligible.

4.4 The mineral chemistry of the Weldborough Sapphire

It has long been considered that corundum occurs as a xenocrystic phase in basalt and associated rocks. Despite petrological evidence (Green et al. 1978; Liu and Presnall, 2000), oxygen isotopic data (Garnier et al., 2005; Zaw et al., 2002) and inclusion evidence (Limutrakun, 2001; Guo, 1996) controversy still exists over the origin of the corundum-bearing xenocrysts and their relationship with alkaline basaltic volcanism. In order to constrain the genetic environment, trace element chemistry of the sapphires will be used to determine the elemental compositions and correlations between elements. Analysis of the rims and cores of sapphires will be used to determine relative enrichment of elements spatially. This will further understanding of the chemical parageneses of sapphires. Finally, the affects of inclusions on analytical procedure will be reviewed. The results will determine the Weldborough sapphires characteristics relative to world sapphires and then used to evaluate popular sapphire genesis models.

4.4.1 Trace element chemistry of corundum

Trace element geochemistry can be used to distinguish between natural and synthetic corundum, differentiate rubies from different localities and to classify corundum derived from basaltic terrains into a metamorphic suite and a basaltic suite in conjunction with mineral inclusions.

Sutherland et al. (1998b) were able to classify corundum derived from basaltic terrains into a metamorphic suite and a basaltic suite on the basis of their trace element contents, mineral inclusions and absorption spectra. They concluded these different types represented different underlying sources tapped by basaltic eruptions. The metamorphic suites were characterised by high Cr/low Ga chemistry with Ga_2O_3 contents <0.01 wt% and Cr_2O_3/Ga_2O_3 ratios above 3. The basaltic (BGY suite) suites were characterised by higher Ga_2O_3 (up to 0.04 wt%) and Cr_2O_3/Ga_2O_3 ratios below 1.

Schwarz et al. (2000) determined that the most useful method for separating corundum of magmatic and metamorphic origin is correlation diagrams that plot Cr_2O_3/Ga_2O_3 against Fe_2O_3/Cr_2O_3 or Fe_2O_3/TiO_2. Magmatic corundum has higher Ga/Cr than metamorphic corundum, with the single exception of some Ga rich metasomatic corundum which can distinguished by Fe_2O_3/Cr_2O_3 ratios of between 20-110.

Sutherland et al. (2002) further used trace element distribution, absorption spectra, geochronology and absorption spectra to characterise the corundum occurrence in the Tumbarumba Basalt field. They divided the corundum into six groups:

1. BGY sapphires with a Fe^{2+}-Fe^{3+} transition (low Cr/Ga, moderate to high Fe)
2. BGY sapphires without a Fe^{2+}-Fe^{3+} transition (low Cr/Ga, moderate to high Fe)
3. BGY related trapiche-like corundum (moderate Cr/Ga, moderate to high Fe)
4. Blue, green, pink diffuse zoned (higher Cr/Ga, moderate Fe)
5. Blue, light blue, white colour zoned (higher Cr/Ga, moderate Fe)
6. Dark pink, purple, red (extreme Cr/Ga, low to moderate Fe)

The BGY and trapiche-like sapphires are considered magmatic, the intermediate sapphires magmatic-metasomatic and the pink to red corundums are metamorphic in origin. This, importantly, classified the Tumbarumba corundums as a polygenetic suite and further research indicates that other gem provinces are also likely to have polygenetic origins.
Saminpanya et al., (2003) assembled trace element data of corundum from different genetic environments in an attempt to classify corundum occurrence and link corundum xenocrysts from alkali basaltic terrain with a distinct parent rock type.

4.4.2 Trace element chemistry of the Weldborough sapphire

Sapphires from eight different localities (Chapter 4.1) were analysed for the minor and trace elements; Be, Mg, Ti, V, Cr, Fe, Co, Ni, Cu, Ga, Nb, Sn, Ba and Ta. These are elements that have been applied in previous studies (Khin Zaw et al., 2002). The analysis was standardised against aluminium (52.9 wt% in corundum).
The apparent rims and cores of each sapphire were sampled using LA-ICPMS and if the resultant spectrum was inhomogeneous, the data was re-sampled in a nearby location. If inhomogenity was apparent in the re-sample, it was inferred that very sharp, short wavelength anomalies (Figure 16) were due to analytical error and that the associated smooth, long wavelength anomalies (Figure 17) were due to the sampling of mineral inclusions within the grain. Samples with abundant inclusions were not included in the comparison of rims and cores.

Magnesium, iron, copper, cobalt, tantalum, beryllium, niobium and vanadium were elements that produced analytical spikes. On more than five occasions the magnesium spectra was seriously affected by spiking.

Element groups involved in inclusions are niobium and tantalum, which commonly occur with tin and/or titanium. A magnesium and iron rich phase was also found on the edges of the Nb-Ta rich phases on the spectra.

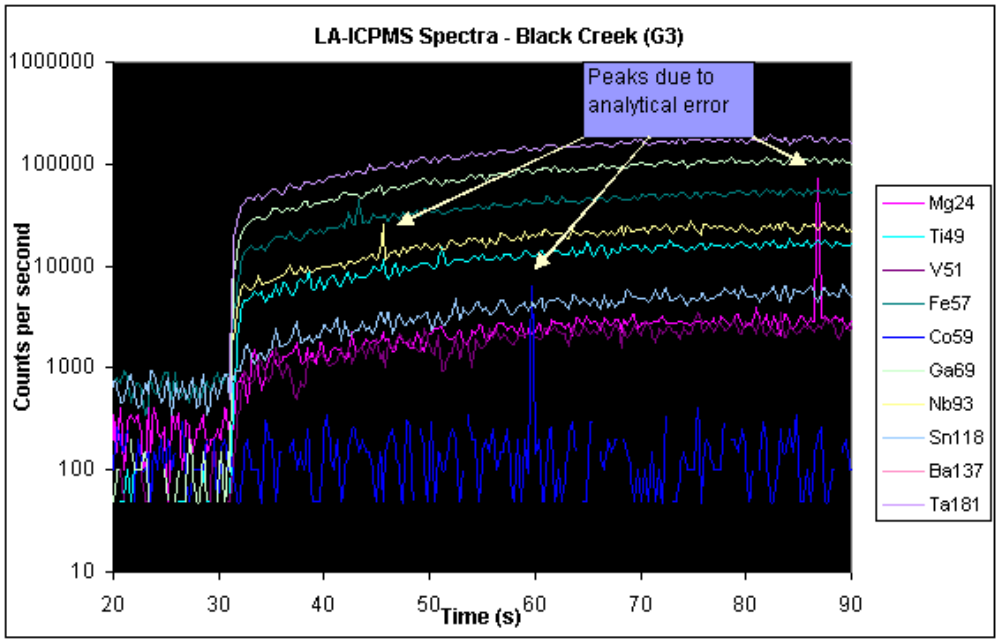

Figure 16. LA-ICPMS spectra showing "spikes" typical of analytical error. The spectra are free of inclusions.

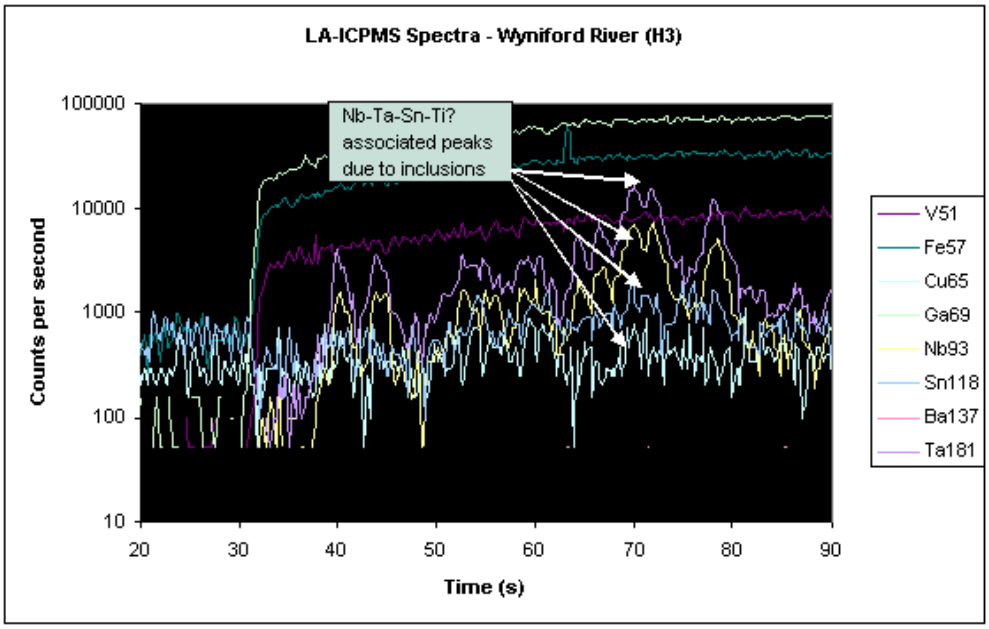

Figure 17. LA-ICPMS Spectra exhibiting the affect of inclusions on data.

4.4.3 Results

The Weldborough sapphires contain <0.02-46ppm Be *(4ppm average)*, 1-90ppm Mg *(23ppm)*, 10-2400ppm Ti *(384ppm)*, 2-16ppm V *(8ppm)*, <0.05-22ppm Cr *(4ppm)*, 1568-4896ppm Fe *(2590ppm)*, <0.025-0.48ppm Co *(0.065ppm)*, <0.05-0.3483ppm Ni *(0.096)*, <0.250-5ppm Cu *(0.5ppm)*, 120-409ppm Ga *(258ppm)*, 0.041-798ppm Nb *(51ppm)*, <0.150-110ppm Sn *(12ppm)*, <0.010-1.951ppm Ba *(0.088ppm)* and 0.028-2570ppm Ta *(187ppm)*.

All the sapphires contained detectable levels of Mg, Fe, Ti, V, Ga, Nb and Ta. Be, Cr, Co, Ni, Cu, Sn and Ba were only present in a limited number of samples with Ba, Ni, Cu and Co often below the detection limit (Table 10). For statistical analysis, any results below the detection limit, were replaced by half the detection limit for that element. This is the case in many other studies (i.e. Saminpanya et al., 2003).

Table 10 - LA-ICPMS results summary (measured isotope shown in brackets)

	Average (ppm)	Maximum (ppm)	Minimum (ppm)	Standard Deviation (ppm)	Detection Limit (ppm)
Be (9)	4.13	46.6	0.02	9.2	0.04
Mg (24)	23.2	90.4	1.1	23.1	0.1
Ti (49)	383	2410	9.9	627	0.6
V (51)	8.52	16.39	2.65	4.7	0.03
Cr (53)	4.5	22.2	0.5	6.8	1.0
Fe (57)	2590	4890	1560	760	6
Co (59)	0.06	0.48	0.03	0.11	0.07
Ni (60)	0.1	0.3	0.1	0.1	0.1
Cu (65)	0.5	5.2	0.3	1.0	0.6
Ga (69)	258	409	121	79.8	0.07
Nb (93)	50	798	0.041	155	0.007
Sn (118)	12.6	109.8	0.2	23.3	0.3
Ba (137)	0.09	1.95	0.01	0.38	0.04
Ta (181)	186	2560	0.028	508	0.004

From the bulk analysis of this data, discrimination plots can be made (Figures 18 and 19).

4.4.3.1 Fe vs. Ga/Mg discrimination

The Fe vs. Ga/Mg discrimination diagram was introduced by Peucat et al., 2005, who noticed that metamorphic and basaltic blue sapphires could be distinguished on iron content and the Ga/Mg ratio. Peucat et al. discovered that blue sapphires from alkali basalts are rich in Fe (2000 to 11000ppm) and Ga (100 to 300ppm) and low in Mg (<10ppm) with Ga/Mg ratios >10, whereas blue sapphires with metamorphic origins have lower Fe contents (300 to 5000ppm), lower Ga contents (<100ppm), but high Mg values (30 to 250ppm) with Ga/Mg ratios <3.

Figure 18 indicates that the Weldborough sapphires have similar Fe contents and Ga/Mg ratios to basalt hosted sapphires in Asia. Slightly lower Fe contents than that of Asian sapphires may be cause for the addition of a "basalt hosted sapphires in Australia" field to this discrimination diagram.

The Weldborough sapphires are likely to be alkali-basalt hosted.

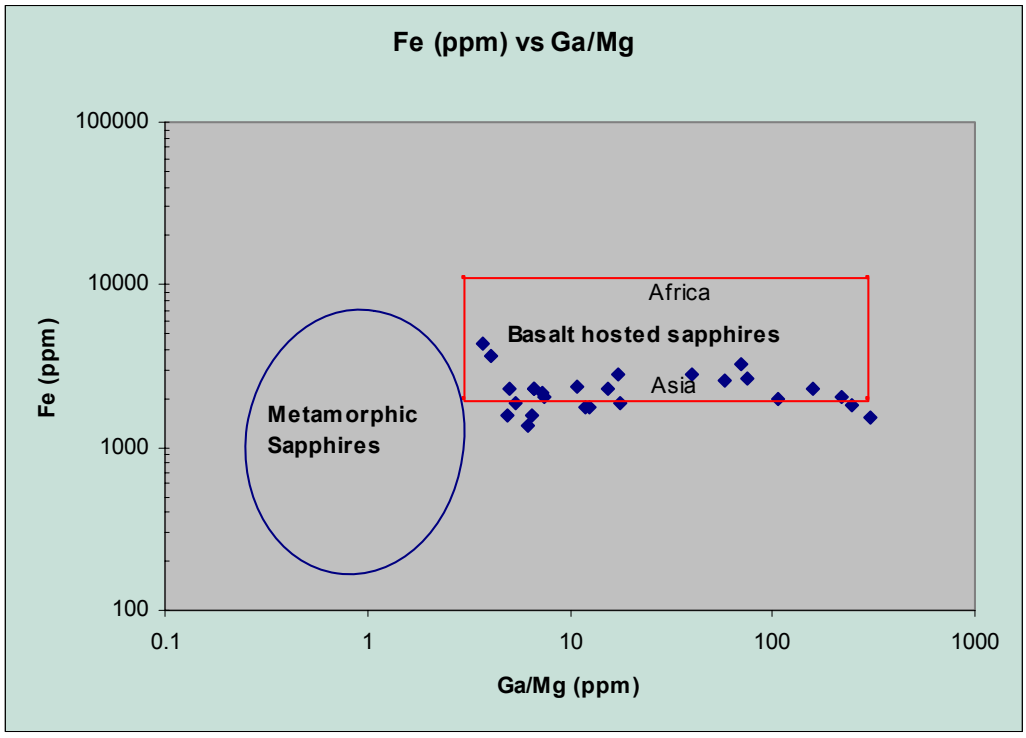

Figure 18. Ga/Mg vs. Fe discrimination diagram. Fields are for blue sapphires only (Peucat et al., 2005). Note that the Weldborough sapphires fall into the basalt hosted field.

4.4.3.2 Fe_2O_3/TiO_2 vs. Cr_2O_3/Ga_2O_3 discrimination

The use of Fe_2O_3, TiO_2, Cr_2O_3 and Ga_2O_3 as parameters in discrimination diagrams was first suggested by Sutherland et al., (1998) and further improved by Saminpanya et al., (2003) to include fields for all varieties of corundum from different terrains (Figure 19).

In Figure 19, the y-axis has been extended to account for the lower levels of chromium detected in Weldborough sapphires by LA-ICPMS (DL=0.75ppm, 0.001wt%). An issue with this diagram is the higher detection limits for other analytical methods. Chromium for the Sampinpanya et al., (2003) study was below or at the detection limit for most samples of sapphires from basaltic terrains. These were still plotted on the diagram, which produces a skewed representation of the true range.

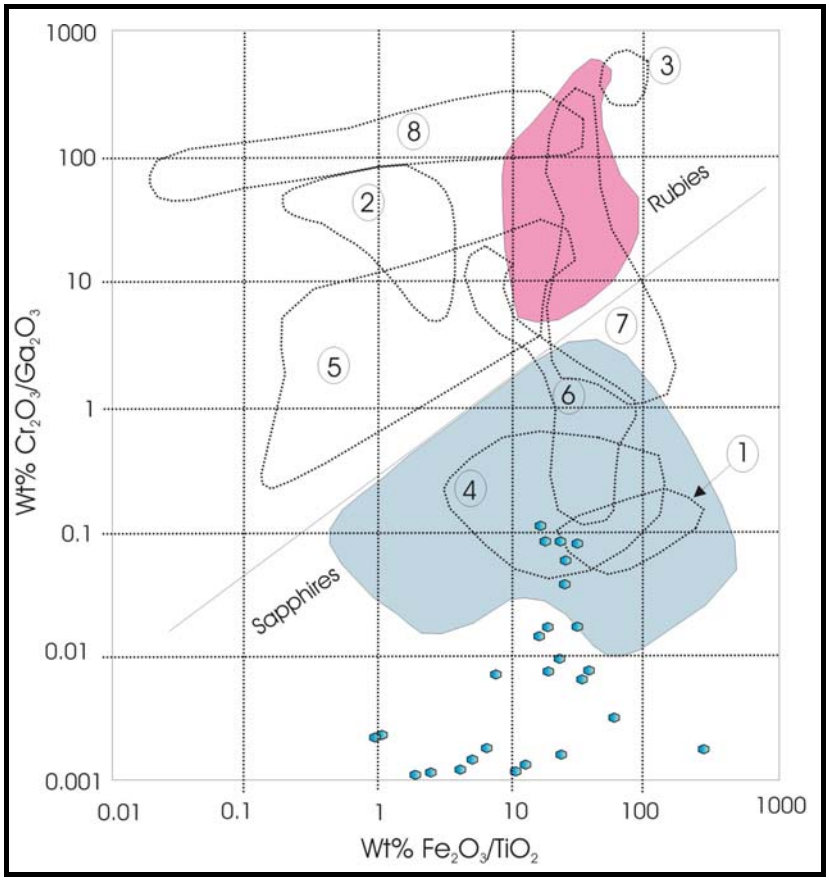

Figure 19. Weldborough Sapphires (blue ovoids). Fe_2O_3/TiO_2 vs Cr_2O_3/Ga_2O_3 discrimination diagram. Fields: Blue - Thai basalt hosted sapphires, pink - Thai rubies, numbered fields are worldwide corundum occurrence from different terrains: 1 – Al-rich diorite, 2 - Al-rich pelite, 3 – ultramafic, 4 – syenitic, 5 – pelitic, 6 – Al,Mg-rich pelitic, 7 – metabauxite, 8 – calcareous. (Saminpanya et al., 2003).

From figure 19 it is apparent that the Weldborough sapphires plot near three recognised fields in corundum study:

1) Thai basalt-hosted sapphires (blue)
2) Corundum in Al-rich diorite (field 1)
3) Corundum in syenitic gneiss (field 4).

It was expected that the Weldborough Sapphires (probably basalt hosted) would have similar Fe_2O_3, TiO_2, Cr_2O_3 and Ga_2O_3 to the Thai basalt-hosted sapphires, based on a similar origin. However, the Weldborough sapphires also plot in and near to corundum hosted in Al-rich diorite (a pegmatitic plumasite from Natal, South Africa) and to corundum hosted in syenite (syenitic gneiss, Bancroft, Ontario, Canada).

A comparison of trace element abundance ranges of the Weldborough sapphire and corundum from these locations is presented in Table 11.

Table 11. Comparison of Weldborough, Thai, South African and Canadian corundum (wt%). Source: Saminpanya et al., (2003).

Locality	Weldborough sapphire	Thai sapphire (Huai Sai)	Al-rich diorite	Syenitic Gneiss
V_2O_5	<DL – 0.0029	<DL – 0.013	<DL – 0.005	<DL – 0.002
Ga_2O_3	0.016 – 0.055	0.013 – 0.10	0.017 – 0.024	0.006 – 0.014
Fe_2O_3	0.22 – 0.69	0.29 – 1.45	1.19 – 1.46	0.20 – 0.35
Cr_2O_3	<DL – 0.0032	<DL – 0.042	0.001 – 0.003	<DL – 0.004
TiO_2	0.017 – 0.40	0.002 – 0.55	0.007 – 0.043	0.002 – 0.060
SnO_2	<DL – 0.013	<DL – 0.075	<DL – 0.004	<DL – 0.003

4.4.3.3 Elemental correlation

The correlation table for the elements is presented as Table 12. This statistical analysis allows us to visualise the level of correlation between individual elements. Two major groups of correlating elements can be observed. A strong positive correlation exists between Nb, Ta, Be and to a lesser degree Ti, Mg and Sn. A weaker Fe, Ga and V correlation is also discussed in this section.

Table 12. Correlation of corundum trace elements. Number after element is isotope measured.

	Be9	*Mg24*	*Ti49*	*V51*	*Fe57*	*Ga69*	*Nb93*	*Sn118*
Be9	1.00							
Mg24	0.46	1.00						
Ti49	0.45	0.25	1.00					
V51	-0.18	0.36	0.03	1.00				
Fe57	0.38	-0.10	0.09	-0.54	1.00			
Ga69	0.10	-0.57	0.20	-0.54	0.34	1.00		
Nb93	0.97	0.44	0.53	-0.10	0.29	0.12	1.00	
Sn118	0.46	-0.08	0.56	0.05	0.09	0.58	0.54	1.00
Ta181	0.93	0.63	0.41	-0.11	0.30	-0.13	0.84	0.26

Yellow highlight is a negative correlation > 0.40 and red is negative correlation < -0.40.

5.5.4 Results: Chemistry variations on rims and cores of the Weldborough sapphires

Analyses confused by inclusions were discarded for the purpose of studying the chemical variation between the rims and cores of the Weldborough sapphires. The spectra for the Priory, Spinel Creek, Thureau's Lead and Black Creek sapphires were free of obvious inclusions. The rim and core data is presented at table 13.

Table 13. The Weldborough sapphires rim and core data. Results are in ppm.

Sapphire	Site	Be	Mg	Ti	V	Cr	Fe	Co	Ga	Nb	Sn	Ta
Black Creek	rim	< DL	13.62	9.9	4.29	< DL	3168	< DL	235	0.076	0.15	0.11
Black Creek	core	0.29	3.49	112	4.58	< DL	3045	< DL	261	0.15	1.36	8.14
Black Creek	core	4.95	7.28	557	4.58	< DL	3204	0.158	293	34.8	19.16	137.2
Black Creek	rim	2.98	5.14	292	5.68	< DL	3650	< DL	355	12.31	15.51	75.4
Thureau's Lead	rim	1.31	1.09	310	2.65	< DL	2304	< DL	237	4.78	8.68	26.17
Thureau's Lead	core	6.80	5.44	204	4.44	< DL	2922	< DL	318	86.1	17.07	87.6
Thureau's Lead	rim	2.13	2.82	33.8	3.63	0.863	2276	< DL	302	19.90	3.35	32.95
Spinel Creek	rim	0.08	10.39	76.7	15.64	1.068	2003	< DL	125	0.757	< DL	0.60
Spinel Creek	core	< DL	10.64	94.7	16.39	2.084	2021	< DL	134	0.041	< DL	0.06
Spinel Creek	rim	< DL	6.86	59.2	11.42	1.875	2114	< DL	121	0.062	< DL	0.03
Priory	rim	0.35	1.14	373	5.08	< DL	1758	< DL	349	2.12	24.53	3.43
Priory	core	0.37	1.52	716	9.14	< DL	2045	< DL	374	3.64	35.59	3.78
Priory	rim	4.76	2.60	1183	11.01	< DL	2597	< DL	409	67.2	109.8	31.9
		Note: Ba, Ni, Zn and Cu below detection limit for all samples										

All samples chosen as inclusion-free have barium, zinc, copper and nickel below detection limits. Cobalt was detected in one analysis, which is probably representative of an inclusion. Chromium is only detected in two sapphires (4 analyses) which is unusual as basaltic hosted sapphires generally have low, but detectable levels of chromium (eg. Tumbarumba gem field, Sutherland et al, 1998a).

5.5.4.1 True core and rim vs apparent core and rim

The recognition of rims and cores was uncertain, that is, arbitrarily the edges of the grain were deemed the rim and the centre of the grain was determined to be the core. For the Spinel Creek sapphire, which was a cross-section through a near-perfect corundum crystal, the data is likely to represent the true rim and core data (Figure 20). The data represents a transect across a corundum crystal for the other three samples, not necessarily crossing the core or reaching any true rim (Figure 20 B and C).

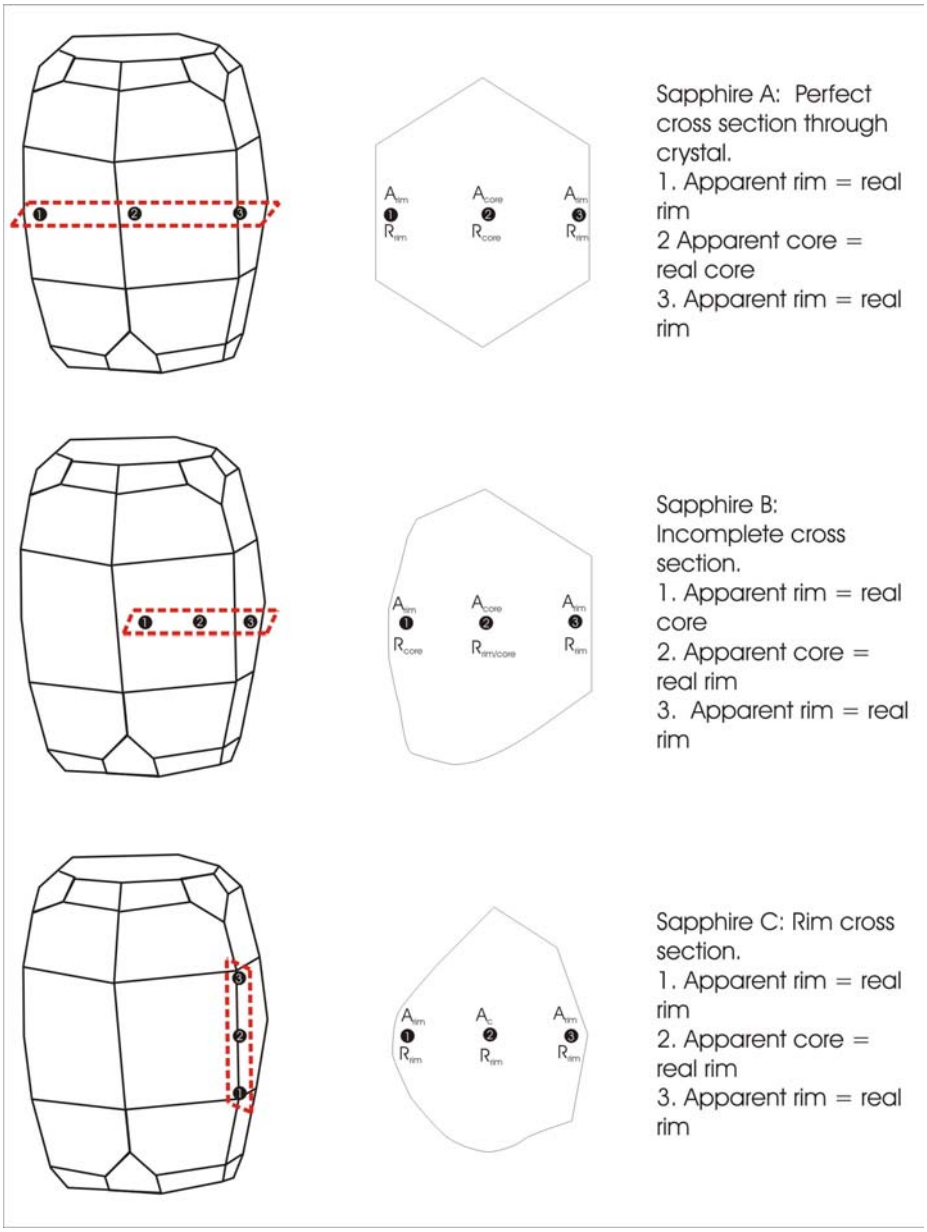

Figure 20. Explanation of considerations for examining the rims and cores of detrital corundum grains. The barrel habit (after Guo, 1993) is used in this example as it is the most abundant form in the study. Detrital grain sections are by dashed red lines. Adjacent to this is a cross section of the grain showing analytical sites represented and actual data achieved. A = apparent, R = real.

Black Creek (Figure 21A)

This sample represents offset rim and core data with the predicted core location represented by an arrow on the graph. In this sapphire Ti, Nb, Ta and Be are enriched in the predicted core. Fe, Mg, Ga and V are constant throughout the sapphire.

Spinel Creek (Figure 21B)

This sample is the best example of true rim and core data. From this data we can see that Cr, V and Ti are enriched in the cores of corundum and depleted at the rims. Nb and Ta are

relatively depleted in the core and enriched in the rims. This may be an affect from very fine-grained inclusions. Fe, Ga and Mg are constant throughout the sapphire.

Thureau's Lead (Figure 21C)

This sample may represent true or near-true rim and core data. This sample has a grain centre enriched in Nb, Ta, Mg and Be. Fe, Ga and V are constant throughout the grain.

Priory (Figure 21D)

The Priory sapphire rim and core data suggests that no true rim and core data was achieved. Fe, Ga, Mg and V are all constant across the sapphire.

4.4.3.4 Summary of rim and core data

The elements Al, O, Fe, Ga,V, Mg, Nb, Ta, Sn, Be and Ti are present in the crystal lattice of the Weldborough sapphires. Fe, Ga, V and Mg are not partitioned preferentially into the core or rim of sapphires (Figure 22). Be and Ti are weakly preferential to the core of sapphires. Nb and Ta tends to be enriched in the cores but some samples exhibit core depletion (Figure 21B). Sn can be either enriched or depleted in the cores of sapphires.

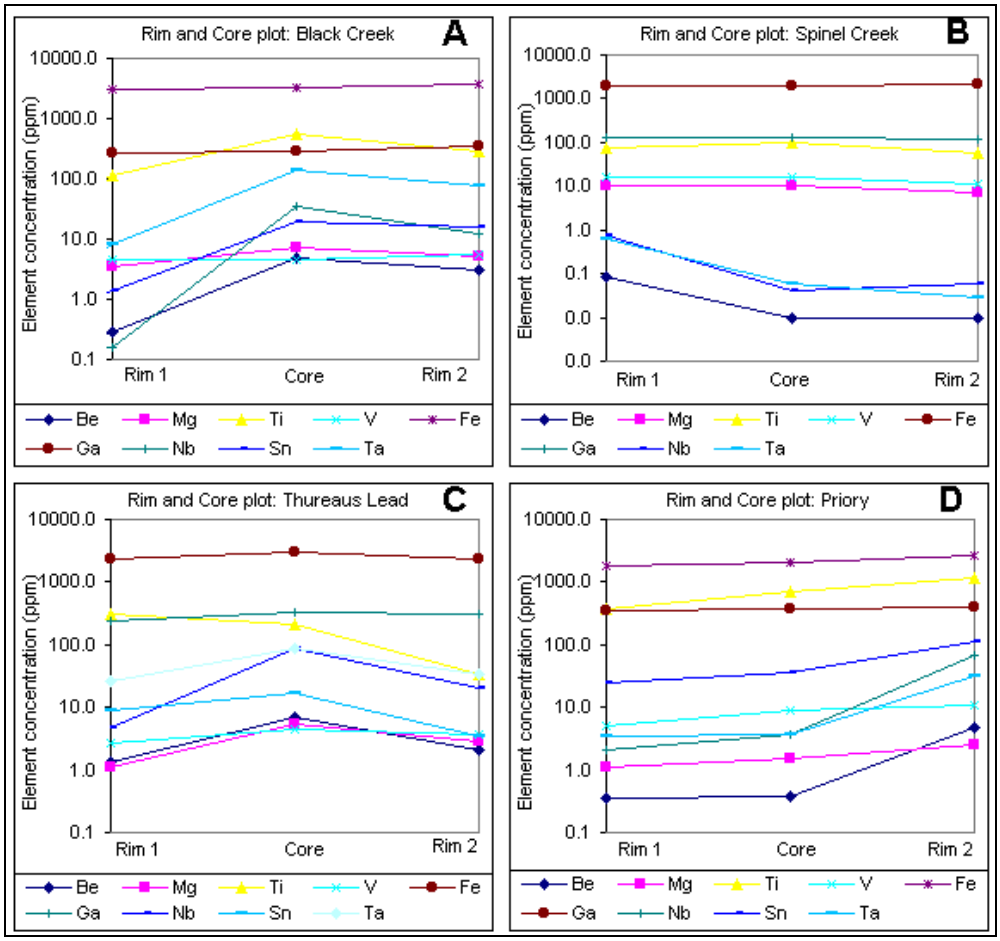

Figure 21A, B, C, D. LA-ICPMS rim and core results for the Weldborough sapphires. A – Black Creek, B – Spinel Creek, C – Thureau's Lead and D – Priory.

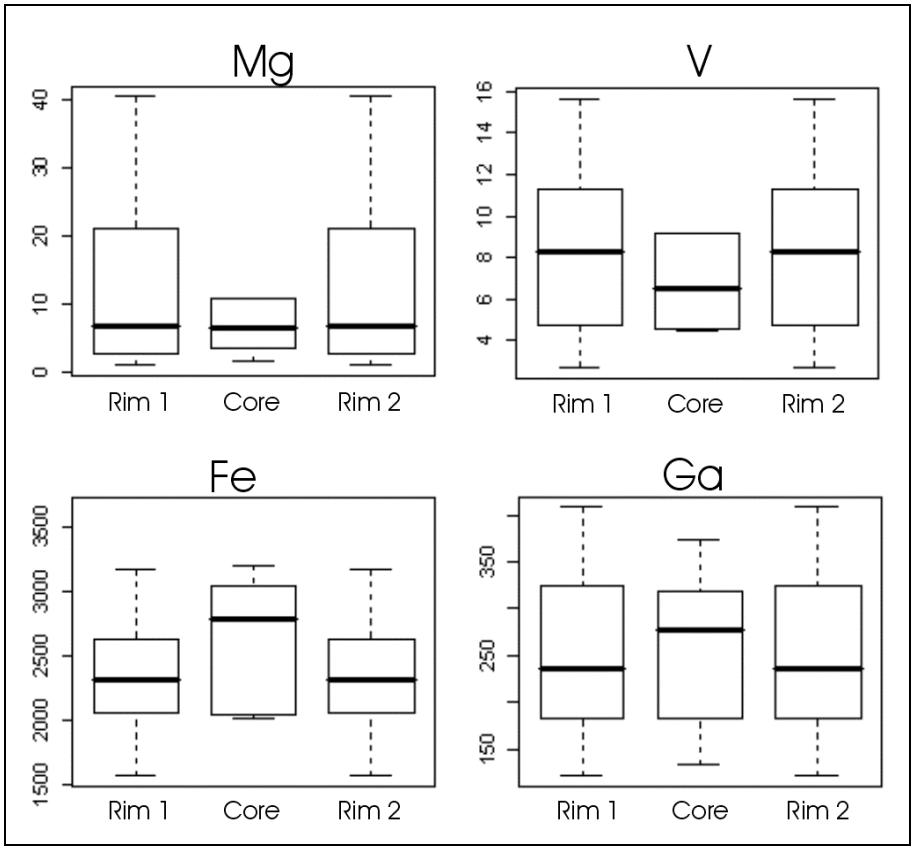

Figure 22. Box & Whisker plot: Average Fe, V, Mg and Ga in the rims and cores of the Weldborough sapphires (ppm)

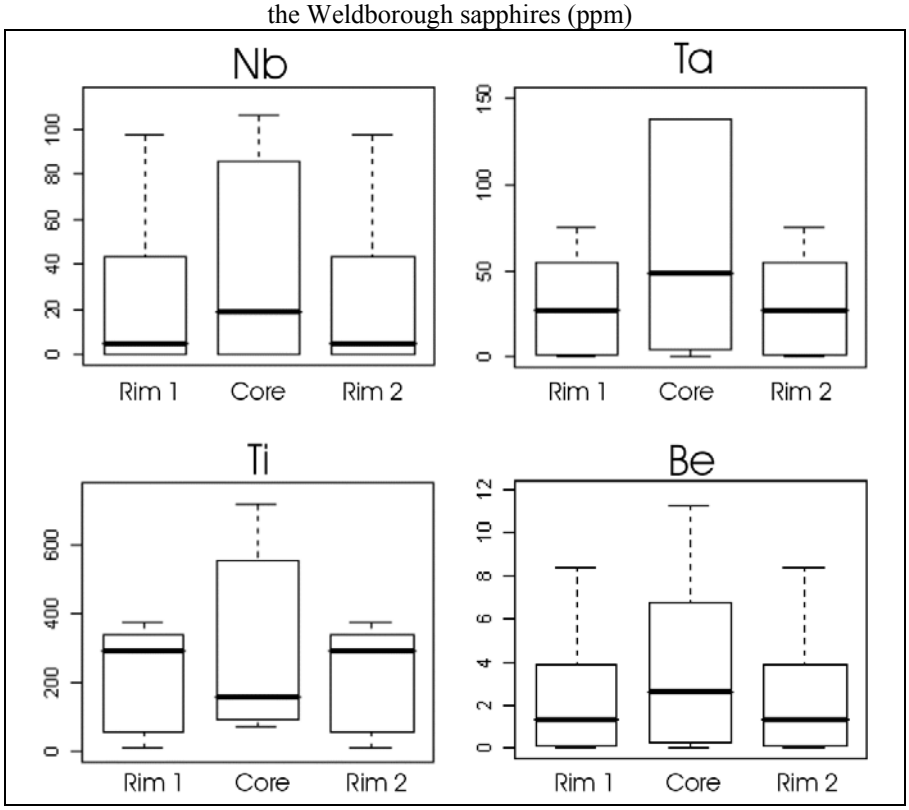

Figure 23. Box and whisker plot: Average Nb, Ta, Ti and Be in the rims and cores of the Weldborough sapphires (ppm)

4.4.4 Discussion

The elements Fe, Ga,V, Mg, Nb, Ta, Sn, Be and Ti are present in the Weldborough sapphires as crystal lattice substitutions for Al. The elements Ba, Cu, Co, Ni and Zn were found to be present only in analyses that were affected by the sampling of inclusions within the sapphire. This suggests that these elements are only present in the Weldborough sapphires as constituents of inclusions.

Chromium (Cr), although used as a discriminatory element for sapphires, was mostly below detection limit, except for one sample (3 analyses, 2ppm, Spinel Creek). Previous studies have utilised other analytical techniques with poorer detection methods (eg. Schwarz et al., (2000) and Saminpanya et al., (2003). Electron probe microanalysis). In these studies, even when no Cr was detected, the sapphires were arbitrarily given a Cr concentration equal to that of the detection limit of the technique. Using the detection limit as the minimum Cr concentration avoids the need to divide by zero when using Fe_2O_3/Cr_2O_3 discrimination (as in Schwarz et al., 2000). However for techniques with better detection limits (i.e. LA-ICPMS), the present discrimination diagrams are unsuitable and requiring modification (eg Figure 5).

Titanium (Ti) is present in sapphires in two forms: as rutile needles and as a lattice substitution (a blue chromophore). Data from this study supports the presence of both forms in the Weldborough sapphires.

Gallium (Ga) tends to be enriched in felsic and intermediate rocks, whereas chromium is enriched in ultramafic and mafic rocks and is generally present with Al (Saminpanya et al., 2003). Levels of chromium are on or below detection limits in most samples, and an ultramafic origin for the Weldborough sapphires is unlikely.

Nb-Ta-Be (Ti-Mg-Sn) element association

There is good positive correlation between Nb, Ta and Be (Figure 24) with an associated lesser correlation including Ti, Mg and Sn (Figure 25).

The presence of strong correlations between incompatible elements Nb, Ta, Be and Sn may indicate that sapphires have formed in a highly evolved melt. The presence of Nb-Ta strongly indicates influence from granitic pegmatites, carbonatites or peralkaline granite (Moller et al., 1989). The associated elements Be and Sn suggest that the sapphires form in a highly evolved melt of syenitic or granitic composition.

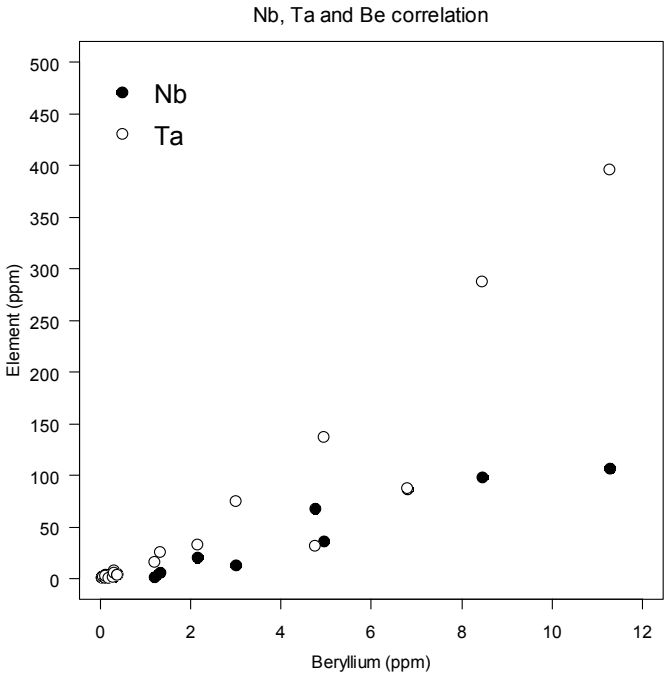

Figure 24. The Weldborough sapphire Be, Nb, Ta correlation plot.

This agrees well with the Sampinpanya et al., (2003) discrimination chart which suggests that the Weldborough sapphires have a chemical similarity to corundum in Al-rich diorite and syenitic gneiss. The low abundance of beryllium in the mantle (probably below detection limits on all available methods; (Grew, 2002) indicates that the genesis of the sapphire must include crustal components.

An important point to note is that this element association is also enriched in the cores of sapphires. I suggest that an Nb-Ta-Be-rich environment was the original crystallisation environment of these sapphires.

Ga-V-Fe element association

Gallium has similar chemical properties to, and is always present with aluminium. Gallium substitutes readily for aluminium in corundum due to similar charge and ionic radius (Al^{3+} = 0.535Å, Ga^{3+} = 0.620Å). Given that in the Weldborough sapphires, Ga:Fe is relatively constant at 1:10, the assumption that iron also substitutes into the lattice for Al^{3+} is strongly supported (Fe^{3+} =0.738Å).

Clearly, gallium is a member of this association only due to thermodynamic similarity with iron and not due to a genetic link with iron and vanadium.

Vanadium correlates negatively with iron (and gallium by-proxy). I propose three possible reasons for this:

1) Vanadium (V^{3+}=0.780Å) substitutes into the crystal lattice at lower concentrations of Fe. This may be explained by a thermodynamic preference for Fe in the corundum crystal lattice. Including V in the corundum lattice is likely to be thermodynamically unfavourable due to its larger ion size.

2) A process of assimilation or fractional crystallisation is changing the melt composition and causing large relative changes in elemental concentrations. Vanadium being added or another vanadium-rich mineral is crystallising (eg rutile).

3) The correlation is redox controlled. Vanadium has 3+ and a 5+ oxidations states and iron has 2+ and 3+. In a reduced system vanadium (III) and Fe (II) will be the dominant species whilst in oxidising environments vanadium (V) and Fe (III) will be the dominant species. As corundum will only accept 3+ valences into the crystal lattice the vanadium: iron ratio may be an oxygen fugacity indicator for the sapphire genetic environment.

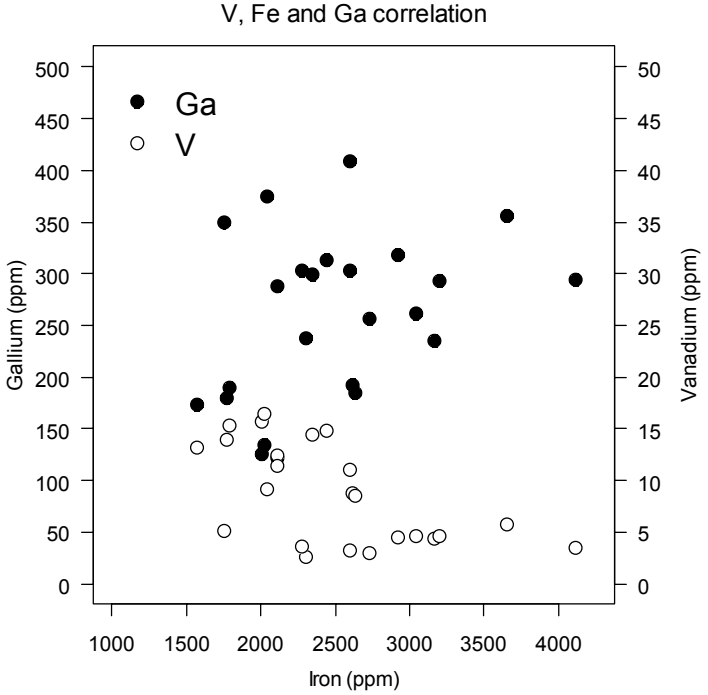

Figure 25. The Weldborough sapphire Fe, Ga and V correlation plot.

Basaltic magma is relatively rich in iron and vanadium. This is a source for the V and Fe found the sapphires. Depending on residence time, elemental diffusion of V and Fe from the basaltic melt to the xenocrystic sapphire is likely responsible for the V-Fe elemental association.

Trace element data indicates that the sapphires begin crystallising in an Nb-Ta-Be-rich environment. V and Fe are diffused into the crystal during subsequent transport as xenocrysts in basaltic magma.

4.5 Oxygen isotopes

Oxygen isotopes are useful to determine the origin of corundum because of the distinct O-isotope difference between mantle and crustal rocks (Yui et al., 2003).

Giuliani et al., (2005) assembled O-isotope data of corundum from economic deposits with different sources (Figure 26). The data shows that the O-isotope value of corundum from each source rock has a specific range (Figure 1B). This can be used as a tool to deduce the likely source of corundum in alkali basalt terrain, especially to differentiate between magmatic and metamorphic origins.

This section will outline the methodology and results of the oxygen isotope study of sapphire and olivine grains from the Weldborough basalts. The results will be used to discuss the potential source rocks and hence a possible genetic origin for these sapphires.

4.5.1 Results

Table 14. Oxygen isotope compositions of sapphires from Weldborough, NE Tasmania. All values relative to VSMOW.

Location	Sample type	$\delta^{18}O$(SMOW)	Analyses
Priory 1 600050mE, 5429950mN	**Sapphire** Light blue opaque, 1mm diameter	**4.4**	1
Priory 2 600050mE, 5429950mN	**Sapphire** Light blue opaque, 2mm diameter	**6.3 ± 0.1**	2
Dorset Dredge 581575mE, 5469350mN	**Sapphire** Blue opaque, 4mm diameter	**5.7**	1
Spinel Creek 575950mE, 5438100mN	**Sapphire** Dark blue, opaque to translucent, 3mm diameter	**5.7**	1
Moorina 573280mE, 5456200mN	**Sapphire** Dark blue transparent, 3mm diameter	**4.4 ± 0.2**	2
Main Creek 572750mE, 5440850mN	**Sapphire** Dark blue opaque, black inclusions, 2mm diameter	**5.1**	1

Black Creek 563700mE, 5443000mN	**Sapphire** Light blue opaque, perfect barrel habit, 4mm	**5.1**	1
Ruby Creek 580500mE, 5458350mN	**Sapphire** Blue opaque 3mm	**6.3 ± 0.1**	2
Thureau's Lead 598400mE, 5428550mN	**Sapphire** Blue opaque 1mm	**4.6**	1
Wyniford River 580740mE, 5449000mN	**Sapphire** Dark blue transparent to translucent, 4mm	**5.1**	1
Mutual Hill 570650mE, 5444450mN	**Olivine from basalt** Olivine-phyric vesicular basalt	**5.1 ± 0.0**	2
Fieldwicks Quarry 581000mE, 5435800mN	**Olivine from basalt** Clinopyroxene-plagioclase microphyric basalt	**4.9**	1
Forest Lodge 575528mE, 5430031mN	**Olivine from basalt** Clinopyroxene-plagioclase microphyric basalt	**4.9**	1
The Gardens 606860mE, 5443280mN	**Olivine from basalt** Flow-aligned-plagioclase phyric basalt	**5.0**	1

4.5.1.1 Sapphires

The oxygen isotope compositions of ten sapphires are shown in Table 14. The sapphires have $\delta^{18}O$ values in the range of +4.4 ‰ to +6.3 ‰ and an average of +5.4 ‰ (see histogram, Figure 26). The lowest and highest values were found in two distinct sapphires from the Priory area (+4.4 ‰ and +6.3 ‰).

4.5.1.2 Olivine

The oxygen isotope values of the four analysed olivine crystals (See Table 14) fall into a very narrow range of +4.9 ‰ to +5.1 ‰.

4.5.2 Discussion

The O-isotope composition of the olivine from basalt is in strong agreement with that reported for olivine from Ocean Island Basalt ($\delta^{18}O$ = +5.0 to +5.4 ‰; Eiler et al., 1997). Mantle olivine has similar O-isotope compositions that vary from +4.8 ‰ to +5.5 ‰ (Mattey et al., 1994). This suggests that the Weldborough basalts are sourced from the mantle with little or no input from other sources with different O-isotope compositions.

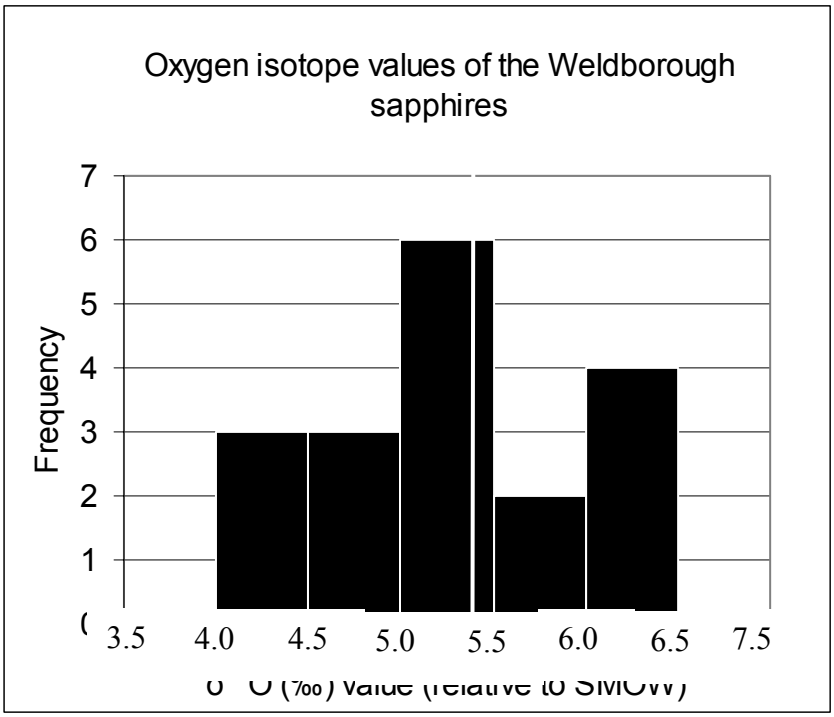

Figure 26. Histogram of O-isotope values for the Weldborough sapphires. Average value for analyses is represented by thick white line at 5.4.

Although corundum and olivine are well known not to be compatible minerals in a basaltic system (Liu & Presnall, 2000), calculations can be made to determine O-isotope fractionation between the minerals. Under the predicted temperature conditions for a basaltic magma (1000-1300ºC), the O-isotope fractionation between olivine and corundum would be between +0.38 to +1.35 ‰ at equilibrium (Zheng, 1993). This suggests the range of variation of the Weldborough sapphires should be between +5.1 and +6.8 ‰, if the sapphires were in equilibrium with the Weldborough basalts or mantle with the same O-isotope character.

Most $\delta^{18}O$ values for the Weldborough sapphires lie within this range (9/13). Four samples have values below expected equilibrium compositions with $\delta^{18}O$ ranging from +4.4 to +4.6 ‰. These lower values are also representative of the mantle. The Weldborough sapphires are therefore considered to be in O-isotope equilibrium with the mantle. Large-scale crustal interactions can be ruled out in the genesis of the Weldborough sapphires.

The longer the corundum has been in the magma (residence time), the more likely it is to represent the predicted $\delta^{18}O$ values. However, long periods of residence in the magma cause corundum xenocrysts to form spinel reaction rims and magmatic corrosion textures and eventually total dissolution of the corundum grain. As the $\delta^{18}O$ values of the sapphires are lower than expected and spinel coatings are rare, it is proposed that the corundum grains had a

short residence time in the magma. This indicates that the entrainment of corundum xenocrysts in the basaltic magma was followed by rapid transport to the surface.

A comparison of the Weldborough sapphire with corundum sourced from different geological environments is shown in Figure 27. The Weldborough sapphires have $\delta^{18}O$ compositions that are also typical of:

1. Corundum sourced from basalt terrains,
2. Corundum from mafic rock,
3. Corundum from lamprophyric rock,
4. Corundum from syenite and
5. Corundum from a desilicified pegmatite in mafic rock.

The O-isotope values are very much lower than that of corundum formed in crustal shear zones, marbles and skarns.

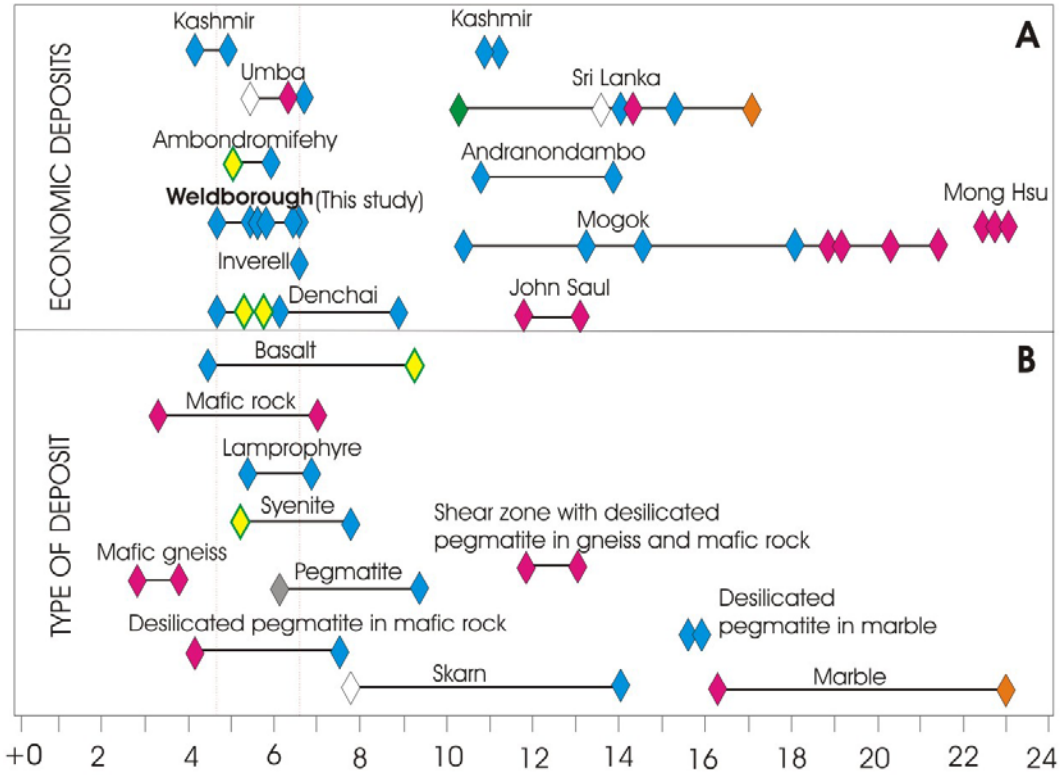

Figure 27A & 27B. Oxygen isotope values of corundum relative to SMOW. Figure **A** shows $\delta^{18}O$ value of economic deposits, note Weldborough sapphires (this study). **B** shows corundum $\delta^{18}O$ range classed by host rock. Colour of diamonds represents colour of corundum found at these deposits. Modified from Giuliani et al. (2005). Note Weldborough is NOT an economic deposit.

The Weldborough sapphires are likely to be sourced from weathered alkali basalts. Because corundum cannot crystallise from a basaltic magma and are considered a xenocryst phase of alkali basalts, other potential genetic sources must be examined. The $\delta^{18}O$ values of the

Weldborough sapphire is similar to that of corundum originating from alkali basalts around the world in Figure 28. The $\delta^{18}O$ composition of sapphires from the Weldborough are very similar to that of Inverell (Australia), Barrington (Australia), Denchai (Thailand), Ambondronifey (Madagascar) and Loch Roag (Scotland). As the sapphires from Weldborough are mainly blue with minor green and yellow stones, sapphires from Denchai and Ambondronifey hold the closest similarity to the Weldborough sapphires. Ambondronfey corundum has the closest range of values and colours. It is interesting to note, that the Barrington polymodal gemfield has an almost identical range of $\delta^{18}O$ compositions to that of the Weldborough sapphires, but a much wider range of sapphire colours.

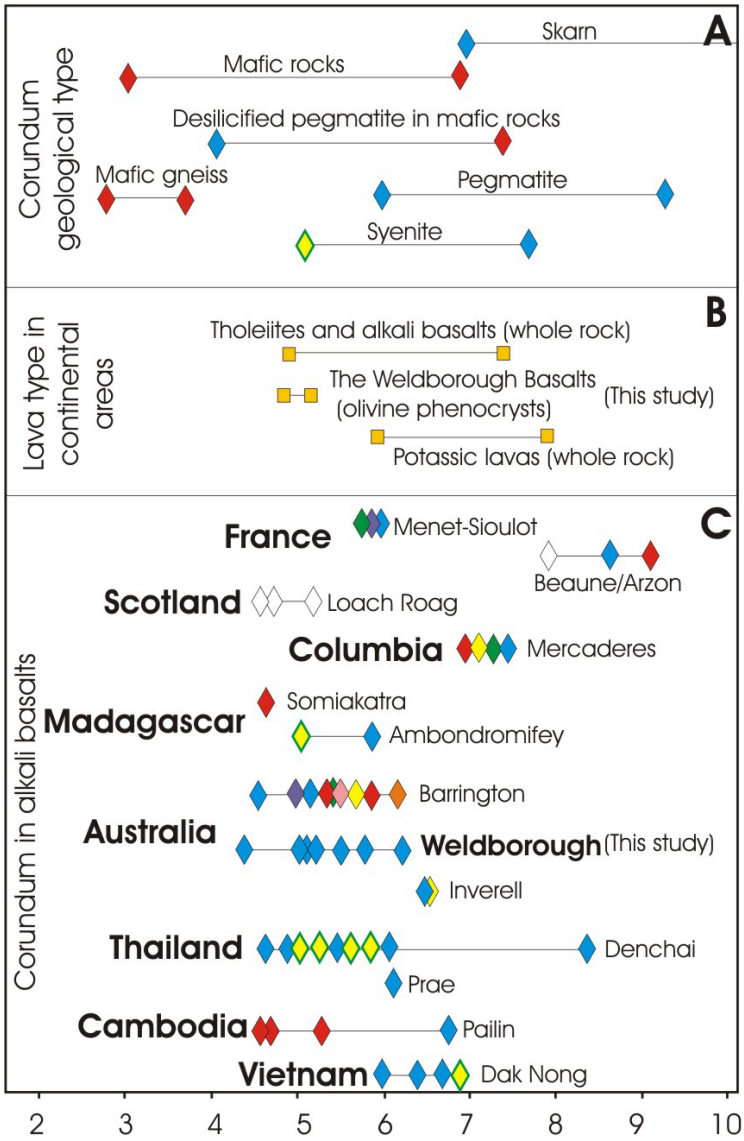

Figure 28A, B & C. Oxygen isotope values of corundum relative to SMOW. **3A** shows $\delta^{18}O$ values for corundum from different host rocks. **3B** shows $\delta^{18}O$ values for basalts in continental areas (includes the Weldborough basalts, this study). **3C** shows $\delta^{18}O$ values of corundum sourced from alkali basalt terrains (includes the Weldborough sapphires, this study). Colour of diamonds represents colour of corundum found at these deposits. Modified from Giuliani et al., (2005).

The lower values of $\delta^{18}O$ ranging from +4.4 to +4.6 ‰ requires a component from another source. These lower values are similar to corundum genesis involving three different geological environments (Figure 28):

1. Mafic rocks (+3.0 ‰ < $\delta^{18}O$ < +7.0 ‰)
2. Mafic gneiss (+2.8 ‰ < $\delta^{18}O$ < +3.9 ‰) and
3. Desilicified pegmatite in mafic rock (+4.0 ‰ < $\delta^{18}O$ < +7.4 ‰).

Of these three environments, only one characteristically produces blue sapphires: the desilicified pegmatite in mafic rock. This corundum genetic type is hosted in amphibolites and serpentinites in Kashmir, Umba and South Africa. The Kashmir locality produces grey to pale blue non-gem corundum with $\delta^{18}O$ compositions ranging from +4.2 to +4.9‰ from amphibolite (Giuliani et al., 2005). This range is slightly lower and narrower than that Weldborough sapphire (+4.4 ‰ to +6.3 ‰), but takes into account the colour of the sapphire. However, the Kashmir locality produces non-gem corundum and other processes must have been involved to produce the gem-quality corundum of Weldborough.

4.5.3 Conclusion

1. The Weldborough sapphires have a $\delta^{18}O$ isotope signature that is compatible with a mantle oxygen source. Little or no crustal oxygen has been incorporated in the sapphire.
2. The Weldborough sapphires have similar $\delta^{18}O$ compositions to that some other alkali basalt sourced corundum (i.e. Denchai and Barrington). They also have similar $\delta^{18}O$ compositions to that of corundum from mafic rock (mafic gneisses), lamprophyre (ouachtite), syenite (syenite or anorthoclasite) and desilicified pegmatite in mafic rock (serpentinite and amphibolite).
3. Sapphire colour and $\delta^{18}O$ composition range indicates the Weldborough sapphires are most closely related to desilicified pegmatites in mafic rock such as the blue-grey corundum found in the amphibolites from Kashmir.

4.6 Geochronology

4.6.1 Introduction

Corundum and zircon commonly occur together as detrital grains sourced from the weathering of alkali basalt terrains. The dating of these minerals can provide us with bounding limits on the age of a potential host rock. U-Pb dating of alluvial zircons is straightforward and well understood. However, conventional methods cannot date corundum

directly. A solution to this dilemma is to date the zircon inclusions known to occur in the Weldborough sapphires (This study, Chapter 4.3).

This chapter describes the analytical methods used to date both detrital zircon and zircon inclusions in corundum for this study. The age of alluvial zircon and zircon included in corundum are discussed and compared with literature results for all dated rocks in the Weldborough area. Finally the implications for the timing of the Weldborough basalt is discussed in reference to the origin of the Weldborough sapphire.

4.6.2 Previous Work

Table 15 is a summary of the relevant dating of north east Tasmanian rocks that was found in published literature:

Table 15. Summary of ages and geochronology techniques for rocks from north eastern Tasmania.

Rock Type	Location	Dating Method	Date	Reference
Pelite	Lefroy	Graptolite	Ordovician	Banks & Smith (1968)
Pelite	Scamander	Graptolite	Devonian	Rickard & Banks in Burret & Martin (1989)
Porphyrite	St Marys	K-Ar	388±1Ma	Turner et al. (1986)
Granite	Scottsdale, Blue Tier, Lottah	Rb-Sr, fission track	368-395 Ma (Rb-Sr), 367±15 Ma (FT)	Rb-Sr: Cocker (1982), FT: Yim et al. (1985)
Sediments (Parmeener Group)	Byatts Razorback	Flora	Triassic	Burret and Martin (1989)
Tuff	Bicheno	K-Ar	214±1 Ma	Bacon & Green (1984)
Basalt	St Marys	K-Ar	233±5 Ma	Bacon et al., in Burret & Martin (1989)
Dolerite	Multiple locations	K-Ar	185.6±1.5 Ma	Williams and Hergt (1998)
Appinite	Cape Portland	Rb-Sr	103±23 Ma	Brooks in McClenaghan et al. (1982)
Basalt	Weldborough	K-Ar, fission track	46.8±0.6 Ma (K-Ar), 46.7±0.6 Ma (FT)	K-Ar: (Sutherland & Wellman, 1986), FT: Yim et al. (1985)
Basalt	Ringarooma	K-Ar	15.6±0.3 to 16±0.3 Ma	Brown (1977)

4.6.3 Results

4.6.3.1 Zircon inclusions in corundum

LA-ICPMS U-Pb isotopic results from the four zircon inclusions are presented in table 16 and are represented by a reverse concordia plot, Figure 29. The range of ages is between 41 ± 5 and 47 ± 4Ma and the zircons have a mean age (weighted by data-point errors only) of 45 ± 4 Ma (95% confidence level).

4.6.3.2 Detrital zircons

LA-ICPMS U-Pb isotopic results from the six detrital zircon grains are presented in Table 17 and are represented by a concordia plot, Figure 30. These detrital zircons represent three age ranges:

- 46.7 ± 0.4 Ma (Tertiary)
- 192 ± 3, 210±4 and 242 ± 1 Ma (Triassic to Early Jurassic)
- 385 ± 5 and 391 ± 3 Ma (Early Devonian).

4.6.4 Discussion

An important issue with U-Pb dating of zircons is that the U-Pb dates represent age of zircon **crystallisation** unless the zircon has undergone Pb loss due to heating. Guo (1993) proved that the U-Pb ages of zircons in basalt may represent the basalts ages because of lead diffusion from the zircons at the high temperature of entrainment. It was demonstrated that heating at 1400ºC would drive all Pb from the zircons of about 100µm in days. However for larger zircon (several mm) and zircon that have been shielded in xenocrysts, diffusion can be limited to the rim of the zircon (Sutherland et al., 2002).

Figure 31 is a diagrammatic summary of the overlap of zircon dates from this study and dated lithologies in NE Tasmania. The ages are represented by bars which represent 1σ error. The shaded area represents the age range of the detrital zircons and zircon inclusions in corundum (this study) within 1σ error.

4.6.4.1 Detrital zircons

Detrital zircon 1 (DZ1) has an identical age range to that of the Weldborough basalt. This zircon crystallised or was reset at this same time of eruption and hence DZ1 is sourced from the Weldborough basalt.

Detrital zircons 5 & 6 (DZ5&6) have geochronological overlap with the Siluro-Devonian Mathinna Beds and Devonian granite. As the Mathinna Beds are unlikely to be able to be involved in a diagenetic zircon age resetting event, the Devonian granites of NE Tasmania are proposed as the source of these zircons.

	U (ppm)	Th (ppm)	Pb (ppm)	206Pb/238U	age	+/-	206Pb/238U age (207corr)	+/-
Z1	6461	4243	35	0.0065	42	4	**41**	**5**
Z2	11626	8699	75	0.0067	43	3	**45**	**3**
Z3	1262	713	11	0.0072	47	4	**46**	**5**
Z4	7206	4961	56	0.0074	47	4	**47**	**4**

Table 16. Summary of LA-ICPMS U-Pb results for zircon inclusions in Weldborough sapphires. Correction was made for common Pb using values from Tera and Wasserburg (1972).

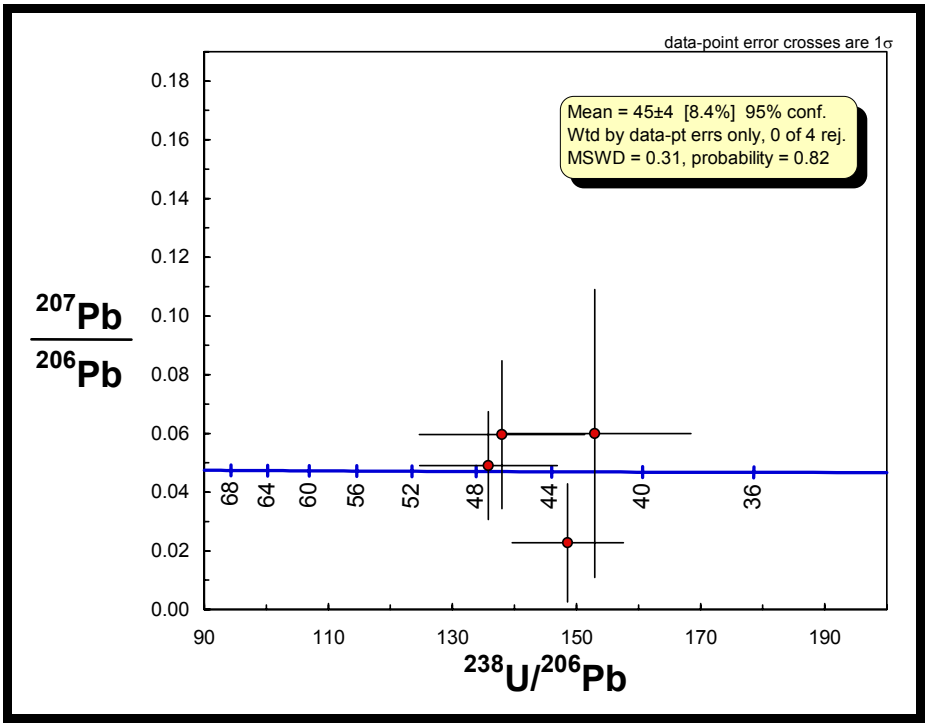

Figure 29. Zircon inclusion U-Pb LA-ICPMS Reverse Concordia plot (this study)

Table 17. Summary of LA-ICPMS U-Pb results for detrital zircons from the Weldborough region. Correction was made for common Pb using values from Tera and Wasserburg (1972).

Zircon	Pb (ppm)	U (ppm)	Th (ppm)	+/-1	207Pb/206Pb	206Pb/238U age (Common Pb corrected)	+/-1s
dz1	6.1	599	594	0.4	0.044	46.7	0.4
dz2	1.6	44	22	3	0.050	192	3
dz3	1.00	25	9.9	4	0.056	210	4
dz4	22.4	434	412	1	0.051	242	1
dz5	69.9	941	108	5	0.057	385	5
dz6	13.3	175	81	3	0.056	391	3

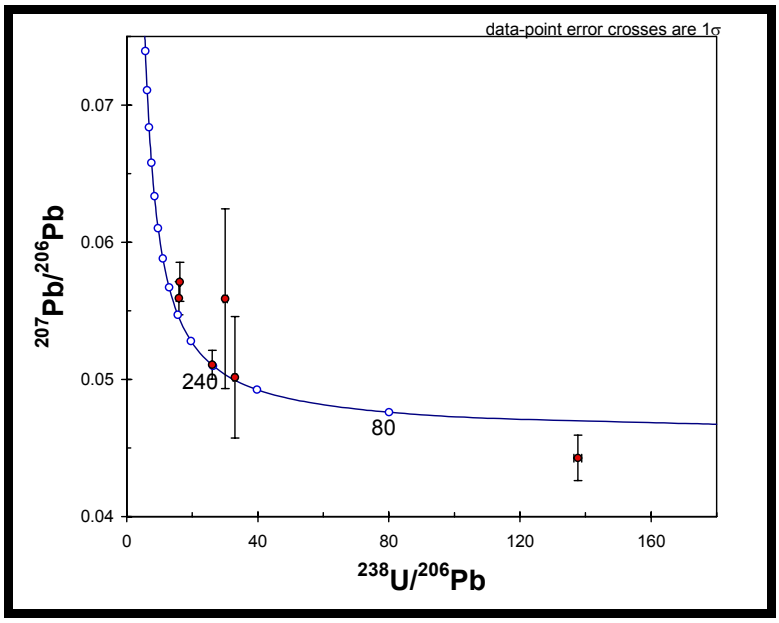

Figure 30. U-Pb LA-ICPMS Concordia plot of detrital zircons from NE Tasmania (Khin Zaw et al., submitted)

Detrital zircons 2, 3 and 4 (DZ2, DZ3, DZ4) represent an unexpected third range of ages. Considering the third association of zircons ages in this study is Triassic-early Jurassic (242 - 192 Ma), source rocks such as Devonian granites and Tertiary basalts can be ruled out as the source of the zircons analytical age. This **does not** imply that the Tertiary basalts cannot be the primary source, as the zircons may be xenocrystic and have had their age preserved despite heating in the magma (see above).

An upper Parmeener Group source for DZ3 (210 ± 4Ma) and DZ4 (242 ± 1Ma) zircons is possible, as early Triassic sandstones are widespread in Tasmania and contain heavy minerals, potassium feldspar and alteration textures indicating a volcanic provenance (Collinson et al., 1990). This source of these volcanic-lithic sandstones is suggested to be a calc-alkaline volcanic arc east of Tasmania along the paleo-Pacific margin.

Detrital zircon 4 (DZ4) also has geochronological overlap with the St Marys basalt. The age of DZ4 (242 ± 1Ma) is slightly younger than the K-Ar date of the St Marys Basalt (233 ± 5Ma). Considering error, the minimum analytical time gap between these ages is 3Ma. Detrital zircon 4 could have been equally sourced from the volcanic-lithic sandstones or the St Marys basalt.

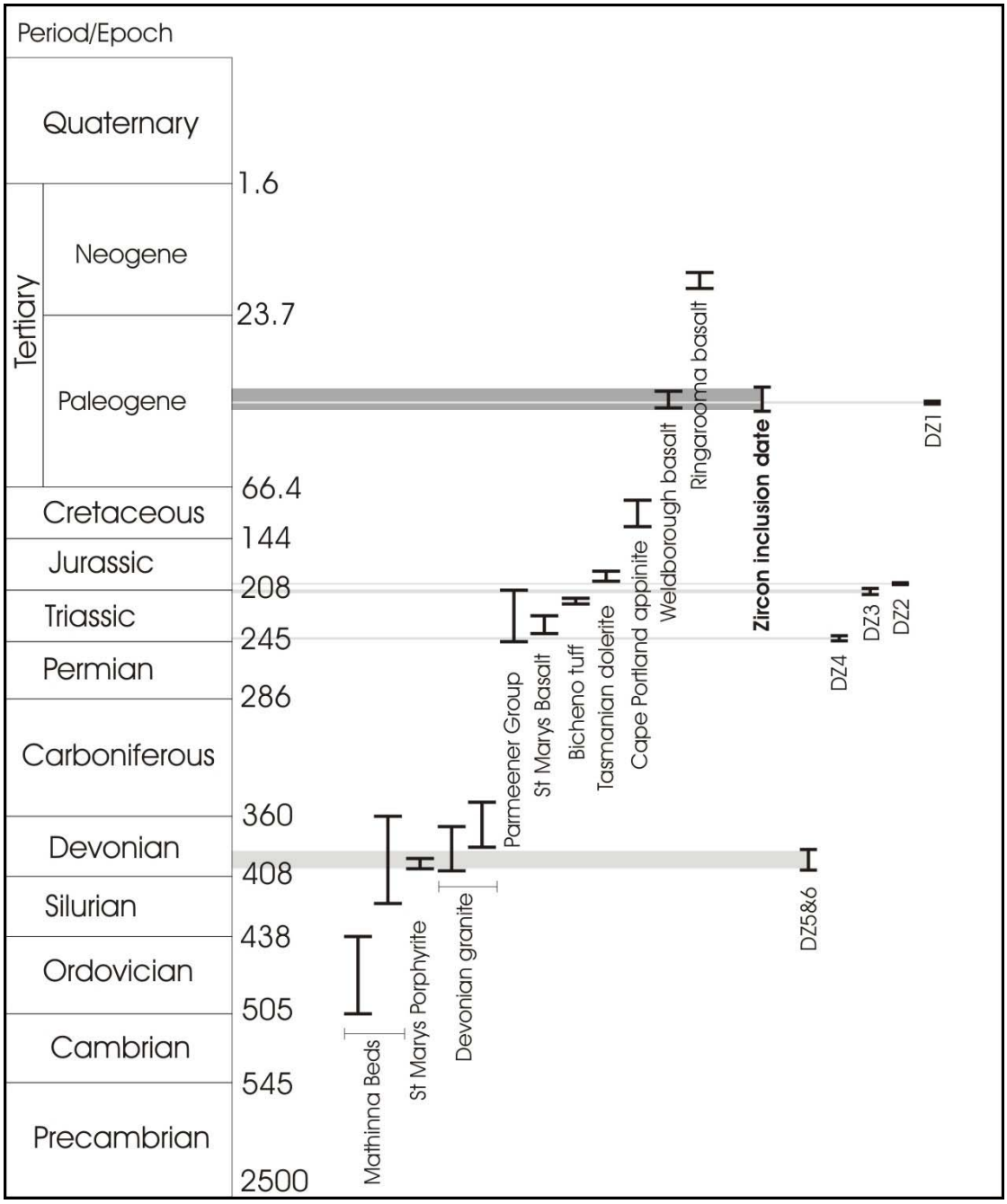

Figure 31. Zircon inclusion in corundum and detrital zircon U-Pb ages compared with known ages of local lithologies. Shading represents age range on analyses. DZ1-6 are the detrital zircons, zircon inclusion date in corundum (this study) in bold. See Table 15 for references.

Detrital zircon 3 (DZ3) also has geochronological overlap with the Bicheno tuff. At 210 ± 4Ma, DZ3 has the age range (within error) of the Bicheno tuff at 214 ± 1 Ma. These tuffs are wide spread in north eastern Tasmania and are usually underlain by volcanic lithic sandstone (Bacon & Green, 1984). Detrital zircon 3 could have been equally sourced from the volcanic-lithic sandstones or the Bicheno tuff.

Detrital zircon 2 (DZ2) doesn't have a discrete geochronological overlap with any lithology. With an age of 192 ± 3Ma, DZ2 is placed ~20My after the Bicheno tuff (214 ± 1 Ma) and between ~2-11My before the intrusion of the Tasmanian dolerite (185.6 ± 1.5Ma). Considering the area that Tasmanian dolerite covers, only a limited numbers of geochronology studies have been undertaken (only one sill has been dated). The potential for wider ranging ages still remains. This zircon is most likely to be sourced from (or reset by) the Tasmanian dolerite.

4.6.4.2 Zircon inclusion in sapphire

The weighted mean age of the zircon inclusions contained within the Weldborough sapphire is 45 ± 4 Ma. This age represents the last high temperature thermal event the zircon inclusions encountered. Considering the sapphires are xenocrysts in basaltic magma, the age of the inclusions may also represent the age of basalt emplacement or the presence of an earlier closure age. The Weldborough basalts have K-Ar cooling ages of 46.8 ± 0.6 Ma. No other lithologies have similar ages in the area. **This is strong evidence to suggest that the Weldborough sapphires were transported to surface by the Weldborough basalts around 47 million years ago.** A much less likely alternative is that the zircon radiogenic clock was reset by the same thermal event that produced the Weldborough basalts, but was transported to the surface later via other means (i.e. Ringarooma basalt, 16 Ma). Considering the affect of lead diffusion on small zircons during heating (see above), the crystallisation age of the sapphire could me much older than 47Ma.

Chapter 5: Summary and Evaluations

5.1 The characteristics of the Weldborough Sapphire

The Weldborough sapphires are dominantly blue (80% of all sapphires). Yellow, green and rare pink sapphires compose the remaining 20%. The sapphires can be colour banded and are commonly combinations of yellow with blue or green. The sapphires show magmatic corrosion and mechanical abrasion surface features.

The Weldborough sapphires contain olivine, feldspar, molybdenite, spinel, zircon and Nb-Ta rich phases as inclusions. Feldspar compositions include anorthite and oligioclase. The zircon inclusions have high hafnium (1.8 wt% HfO_2), and uranium (1.3 wt% UO_2), and moderate thorium (0.99 wt% ThO_2). Nb-Ta-rich phases are suspected to be pyrochlore and/or columbite. Molybdenite is unique to the Weldborough sapphire. Olivine is present as a secondary inclusion.

The Weldborough sapphires are characterised by iron (2590 ppm), titanium (383 ppm), gallium (258 ppm) and tantalum (186 ppm) as trace elements. Niobium, beryllium, magnesium, vanadium, chromium and tin are minor components of all Weldborough sapphires. Barium, zinc, copper and nickel are only present as constituents of inclusions.

There are two groups of elements that correlate. Niobium, tantalum and beryllium positively correlate and there is a more complex vanadium, iron and gallium association. Iron and gallium have a positive correlation whilst iron and vanadium have a negative correlation.
Niobium, tantalum, beryllium and titanium are preferentially enriched in the cores of sapphires. Iron, gallium, vanadium and magnesium have constant values throughout the rim and the core of sapphire grains.

The Weldborough sapphire has oxygen isotope values of + 4.4 ‰ to + 6.3 ‰. The sapphires are therefore considered to be O-isotope equilibrium with rocks of with mantle signatures.

5.2 Evidence for sapphires being basalt hosted

- The sapphires have the same colour to that of other basalt-sourced sapphire deposits

- Magmatic corrosion and spinel reaction rims indicates the sapphires are not in chemical equilibrium with the host rock.
- The sapphires have secondary olivine inclusions suggesting an olivine rich environment, such as basaltic magma.
- Sapphire trace elements have similar compositions to that of other basalt-sourced sapphires.
- Sapphire O-isotope compositions match that of other basalt-sourced corundum.
- Zircon inclusion ages match that of the Weldborough basalt.

5.3 Evaluation of the primary source

Present day drainage patterns and inferred palaeodrainage indicate the Weldborough Region as the primary source of the sapphires. The heavy mineral association of corundum, spinel and zircon indicate a basaltic terrain source. Primary zircon inclusions in corundum have a U-Pb age of 47 ± 4 Ma that is within error of the age of the Weldborough basalts (46.8 ± 0.6 Ma). The zircon inclusions have been reset during entrainment and emplacement of these basalts. **The Weldborough sapphire is sourced from the Weldborough basalts or the associated clastic rocks**. The palaeodrainage extensions presented in Figure 4 allow for the possibility that the Weldborough basalts are the source of **all** sapphire found in NE Tasmania.

The present day location of the primary source is unknown. This study found no sapphire or zircon enrichment in either the basalts or their associated clastic rocks. A considerable amount of weathering has been inferred for the area during the period from 47 Ma to 16 Ma. The primary source may have been totally eroded.

5.4 Sapphire genesis implications

Table 18 is a summary of genetic information obtained as a part of this study:

Table 18. Summary of sapphire genetic environment evidence obtained as a part of this study.

Technique	Chapter	Evidence	Implication (s)
Observations	4.1	Sapphires are predominantly blue, with minor green and yellows.	Similar colour range to that of sapphire derived from basaltic terrains, desilicated pegmatites and syenite.
Observations	4.1	Magmatic corrosion.	Sapphires are sourced from magmatic rock.
Observations	4.1	Spinel coatings	Sapphires are not in equilibrium with magmatic host → sapphires are xenocrysts

Mineral inclusions	4.2	Presence of primary zircon, pyrochlore and Nb-Ta rich inclusions.	Sapphires formed in a highly evolved melt rich in incompatible elements.
Mineral inclusions	4.2	Presence of secondary olivine inclusions	Corundum was transported in olivine-rich magma
Fluid inclusions	4.2	Fluid inclusions containing pure CO_2 that homogenise into liquid phase between 28 and 32ºC.	A CO_2-rich environment of sapphire crystallisation at mid-crustal depths OR, more likely, a secondary inclusion that developed at mid-crustal depths during sapphire transport in magma.
Mineral Chemistry	4.3	Nb-Ta-Be correlating mineral association	Sapphires had input from carbonatite or granite pegmatite
Mineral Chemistry	4.3	Fe-Ga-V correlating mineral association	Sapphires have elemental signatures of both felsic rocks (rich in Ga) and refractory mantle elements (Fe-V).
Mineral Chemistry	4.3	Discrimination diagram: Fe vs. Ga/Mg (ppm)	Sapphires have Fe and Ga/Mg ratios similar to basalt hosted sapphire from Asia
Mineral Chemistry	4.3	Discrimination diagram: Fe_2O_3/TiO_2 vs. Cr_2O_3/Ga_2O_3	Sapphires are most similar to corundum from: 1. Weathered alkali basalts 2. Al-rich diorite 3. Syenitic gneiss
Oxygen isotopes	4.4	Sapphires have O-isotope compositions of between +4.4 ‰ and +6.3 ‰.	Sapphires are in oxygen isotope equilibrium with rocks of mantle O-isotope compositions.
Oxygen isotopes	4.4	O-isotope composition and sapphire colour	Sapphires closely match that of sapphires from alkali basalt terrain, mafic gneiss, lamprophyre, syenite and desilicified pegmatite in mafic rocks.
Geochronology	4.5	Zircon inclusions in sapphires have a U-Pb age of 46 ± 4 Ma.	Zircon inclusions have been reset, and most likely, brought to surface by the Weldborough basalts (K-Ar 46.8 ± 0.6 Ma)

5.4.1 Evaluation of contemporary sapphire genesis models

Guo et al., (1996a) and Sutherland et al., (1998a) have proposed two different, but equally plausible genesis models for sapphire sourced from alkali basalt terrains (Table 19)

Table 19. Characteristics of the Sutherland et al. (1998a) and Guo et al. (1996a) genesis models for corundum from alkali basalt terrains.

	Guo et al., 1996a	**Sutherland et al., 1998a**
Model	Crystallisation of corundum due to a mixing/hybridisation process between a silicic component and an intruding Si-poor magma	Crystallisation of corundum out of partial melts of amphibole-bearing mantle assemblages
Depth	Mid-crustal	Upper mantle
Mechanism of corundum	An advancing thermal plume begins an interaction between a granite/syenite	An advancing thermal plume begins the partial melting of assemblages such as

formation	pegmatite and a carbonatite or similar Si – poor magma. Corundum crystallises due to CO_2 sourced from the carbonatite reducing the solubility of aluminium in the hybrid melt. The plume advances, producing basalts which erupt, entraining the sapphire to the surface.	horneblende-bearing garnet clinopyroxenite and amphibole-spinel websterite. This produces partial melts aluminous enough to crystallise corundum. The plume advances, producing basalts which erupt, entraining the sapphires to the surface.
Reasoning	1. Bimodal geochemical characteristics of mineral inclusions indicate two components are required. The Nb-Ta oxide and low-Ca feldspar mineral inclusions are explained by a syrnite/granite pegmatite source. Fe,Cu-sulphides and Ca,Th-rich phosphates are explained by a carbonatite source 2. Zircon inclusion crystal habit and geochemistry indicate crystallisation from an alkaline-peralkaline and highly evolved silicic melt.	1. The geochemistry of the mineral inclusions suggests that a single silicic source can account for all inclusions (e.g. partial melts of alkaline or syenitic character). 2. Thermodynamic modelling (MELTS Calculation) indicates the above mantle-assemblages can crystallise corundum.

Both models indicate that sapphires are a xenocrysts phase in basaltic magma. The presence of magmatic corrosion and spinel reaction rims on the Weldborough sapphires suggests they are not in equilibrium with the host magma. This indicates they are xenocrysts and supports both models.

The Guo model indicates that Nb and Ta in elemental and mineral inclusion form can be explained by the input of a granite/syenite pegmatite. This agrees well with the Nb-Ta-Be element association, trace element discrimination diagrams and sapphire colour (Table 18). The Sutherland model fails to explain the presence of Nb and Ta. The thermodynamic modelling undertaken for the Sutherland study failed to take into account the elements Nb and Ta, although it is implied that they should be present.

The Guo model fails to explain the abundance of Fe and V in the Weldborough sapphire. Sutherland suggests that the partial melting of mantle pre-enriched with felsic components is favoured to produce corundum-crystallising melts. This type of mantle explains a correlation between a typically felsic source for Ga and a typically mafic source for Fe and V.

Oxygen isotope compositions of the Weldborough sapphires indicate they are in O-isotope equilibrium with rocks of mantle isotopic values. No large scale interaction of rocks with

crustal isotopic values is involved in the formation of sapphires. This is strong evidence in favour of the mantle sourced sapphires of the Sutherland model.

This study indicates that both genetic models can explain most of the features of the Weldborough sapphire. However, the O-isotope composition and Fe, Ga and V concentrations are best accounted for by the Sutherland model.

5.5 Recommendations for future work

- Date the sapphires from the Boobyalla River Catchment to confirm the Weldborough basalts as the source of all sapphire in NE Tasmania.
- Investigate the molybdenite, beryl and diamond inclusions further. The confirmation of these inclusions, especially diamond, would have a significant impact on current genetic models.

Chapter 6: References

Aspen, P., B. G. J. Upton, et al. (1990). "Anorthoclase, Sanidine and Associated Megacrysts in Scottish Alkali Basalts - High-Pressure Syenitic Debris from Upper Mantle Sources." European Journal of Mineralogy **2**(4): 503-517.

Bacon, C. A. and D. C. Green (1984). "A radiometric age for a Triassic tuff from eastern Tasmania." Tasmanian Department of Mines **Unpublished report: 1984/29**.

Banks, M. R. and A. Smith (1968). "A graptolite from the Mathinna Beds, north eastern Tasmania." Australian Journal of Science **31**(3): 118-119.

Bottrill, R. S. (2000). Mineralogy of some basalt xenoliths and xenocrysts, NE Tasmania. Unpublished report for Mineral Holdings Pty Ltd, Mineral Resources of Tasmania**:** 8pp.

Bottrill, R. S. (1996). "Corundum and sapphire in Tasmania." Tasmanian Geological Survey Record **1996**(05): 1-10.

Bottrill, R. S. (1989). "Basaltic agglomerate from near Weldborough." Tasmanian Department of Mines **1989**(10): 1-7.

Brown, A. V. (1977). Preliminary report on age dating of basalt samples from Ringarooma 1:50000 map sheet. Unpublished report, Department of Mines, Tasmania.

Burret, C. F. and E. L. Martin (1989). Geology and Mineral Resources of Tasmania. Hobart, Geological Society of Australia.

Brownlow, A. H. and J. C. Komorowski (1988). "Geology and Origin of the Yogo Sapphire Deposit, Montana." Economic Geology **83**(4): 875-880.

Caine, N. (1983). The mountains of Northeastern Tasmania: A study of Alpine Geomorphology. AA Balkema, Rotterdam.

Clabaugh, S. E. (1952). "Corundum Deposits of Montana." US Geological Survey Bulletin **983**.

Cocker, J. D. (1982). "Rb-Sr geochronolgy and Sr isotopic composition of Devonian granitoids, eastern Tasmania." Journal of the Geological Society of Australia **29**: 139-157.

Coenraads, R. R. (1992). "Sapphires and Rubies associated with volcanic provinces." The Australian Gemmologist August: 70-78.

Collinson, J. W., J. T. Eggert and N. R. Kemp (1990). "Tasmanian Triassic sandstone petrology." Papers of the Proceedings of the Royal Society of Tasmania **124**(1): 61-75.

Deer, W., R. Howie and J. Zussman (1992). An introduction to rock forming minerals. Hong Kong, Longman.

Eiler, J. M., K. A. Farley, J. W. Valley, E. Hauri, H. Craig, S. R. Hart and E. M. Stolper (1997). "Oxygen isotope variations in ocean island basalt phenocrysts." Geochimica et Cosmochimica Acta **61**: 2281-2293.

Garnier, V., D. Ohnenstetter, G. Giuliani, A. Fallick, T. Phan Trong, D. Schwarz, V. Hoang Quang and L. Pham Van (2005). "Basalt petrology, zircon ages and sapphire genesis from Dak Nong, Souther Vietnam." Mineralogical Magazine **69**(1): 21-38.

Gentilli, J. (1977). Climate. In Jean, D.N. ed. Australia: A geography. St Martins Press, New York.

Giuliani, G., J. Dubessy, D. Banks, H. Q. Vinh, T. Lhomme, J. Pironon, V. Garnier, P. T. Trinh, P. Van Long, D. Ohnenstetter and D. Schwarz (2003). "CO2-H2S-COS-S-8-AlO(OH)-bearing fluid inclusions in ruby from marble-hosted deposits in Luc Yen area, North Vietnam." Chemical Geology **194**(1-3): 167-185.

Giuliani, G., A. Fallick, V. Garnier, C. France-Lanord, D. Ohnenstetter and D. Schwarz (2005). "Oxygen isotope composition as a tracer for the origins of rubies and sapphires." Geology **33**(4): 241-336.

Graham, I. (2005). In regards to sapphire hosted tuffs and breccias. B. M. McGee. University of Tasmania.

Grant, J. A. (1985). "Phase euilibria in low-pressure partial melting of pelitic rocks." American Journal of Science **285**: 409-435.

Grew, E. S. (2002). Beryllium - Mineralogy, petrology and geochemistry. Blacksburg, Mineralogical Society of America.

Griffith, W. P. (1987). Advances in Spectroscopy. Advances in Spectroscopy. R. J. H. Clark and R. E. Hester, Wiley & Sons. **14:** 119-186.

Gubelin, E. J. (1973). Internal world of gemstones. Zurich, ABC edition.

Guo, J. F. (1993). Lead diffusion in zircon and its significance to U-Pb geochronology. International Association of Volcanology and Chemistry of the Earths interior, Canberra, Australia.

Guo, J., S. Y. O'Reilly and W. l. Griffin (1996a). "Zircon inclusions in corundum megacrysts; I, Trace element geochemistry and clues to the origin of corundum megacrysts in alkali basalts." Geochimica et Cosmochimica Acta **60**(13): 2347-2363.

Guo, J. F., S. Y. O'Reilly and W. l. Griffin (1996b). "Corundum from basaltic terrains: a mineral inclusion approach to the enigma." Contributions to Mineralogy and Petrology(122): 368-386.

Jordan, W.M. (1975). An assessment of water resources of Tasmania from river gauging and rainfall record 1920 - 1969. Water Resources survey. River and Water Supply Comm. Tasmania.

Kerrich, R., W. S. Fyfe, R. L. Barnett, B. B. Blair and L. M. Willmore (1987). "Corundum, Cr-Muscovite Rocks at Obriens, Zimbabwe - the Conjunction of Hydrothermal Desilicification and Lil-Element Enrichment - Geochemical and Isotopic Evidence." Contributions to Mineralogy and Petrology **95**(4): 481-498.

Leaman, D. E. and P. A. Symonds (1975). "Gravity survey of north-eastern Tasmania." Geological Survey of Tasmania **2**.

Levinson, A.A. and Cook, F.A. (1994) Gem corundum in alkali basalt: origin and occurrence Gems & Gemology, 30, p. 253-262.

Limtrakun, P. (2001). The origin of corundum from alkali basalt terrains. Earth Sciences. Hobart, University of Tasmania**:** 277pp.

Limtrakun, P., K. Zaw, C. G. Ryan and T. P. Mernagh (2001). "Formation of the Denchai gem sapphires, northern Thailand: evidence from mineral chemistry and fluid/melt inclusion characteristics." Mineralogical Magazine **65**(6): 725-735.

Lindsley, D. H. (1991). Stability of Oxide Minerals in Metamorphic Rocks.

Liu, T. C. and D. C. Presnall (2000). "Liquidus phase relations in the system CaO-MgO-Al2O3SiO2 at 2 center dot 0 GPa: Applications to basalt fractionation, eclogites, and igneous sapphirine." Journal of Petrology **41**(1): 3-20.

MacNevin, A. (1972). "Sapphires in the New England district, New South Wales." Records of the Geological Survey Of NSW **14**: 19-35.

Mattey, D., D. Lowry and C. Macpherson (1994). "Oxygen isotope composition of mantle peridotite." Earth and Planetary Science Letters **128**: 231–241.

McClenaghan, M. P., N. J. Turner, P. W. Baillie, A. V. Brown, P. R. Williams and W. R. Moore (1982). "Geology of the Ringarooma - Boobyalla area." Geological Survey Bulletin **61**(1): 187pp.

Meffre, S., R. Scott, R. Glen and R. Squire (2005). "Re-evaluation of contact relationships between Ordovician volcanic belts and the quartz-rich turbidites of the Lachlan Orogen." Australian Journal of Earth Sciences (Submitted).

Mercier, A., P. Debat and J. M. Saul (1999). "Exotic origin of the ruby deposits of the Mangari area in SE Kenya." Ore Geology Reviews **14**(2): 83-104.

Mernagh, T. P. (1988). AGSO's new confocal laser Raman microprobe. AGSO Research Newsletter. Canberra, AGSO**:** 1.

Mernagh, T. P. (1991). "Use of Laser Raman Microprobe for discrimination amongst feldspar minerals." Journal of Raman Spectroscopy **22**: 453-457.

Mernagh, T. P. (2005). Analysis and matching of LRS spectra with that of known LRS spectra. B. M. McGee. Canberra.

Meyer, H. O. A. and R. H. Mitchell (1988). "Sapphire-Bearing Ultramafic Lamprophyre from Yogo, Montana - a Ouachitite." Canadian Mineralogist **26**: 81-88.

Mines, T. D. o., Ed. (1970). Catalogue of the minerals of Tasmania. Record Geological Survey of Tasmania.

Moller, P., P. Cerny and F. Saupe (1989). Lanthanides, tantalum, and niobium mineralogy, geochemistry, processing, and applications, Workshop papers. New York, Springer-Verlag.

Moore, W. R. (1991). Winneleah Geology - 1:100 000 Map sheet. G. J. Dickens. Hobart, Department of Environment & Planning.

Morrison, K. C. (1989). Exploration Licence 48/87 - Weldborough, Annual Report : Year 1 and final report, Totteny Pty Ltd - Unpublished report [TCR 88 - 2901].

Oakes, G. M., W. J. Stroud, S. R. Lishmund, S. R. Pecover, R. E. Brown, L. M. Barron, R. Spencer, D. A. Nicholsonm and G. Rose (1987). Extended Abstracts From a Seminar on Tertiary Volcanics and Sapphires in the New England District. Tertiary Volcanics and Sapphires in the New England District, Department of Mineral Resources, Geological Survey of New South Wales.

Pecher, A., G. Giuliani, V. Garnier and H. Maluski (2002). "Geology, geochemistry and Ar-Ar geochronology of the Nangimali ruby deposit, Nanga Parbat Himalaya (Azad Kashmir, Pakistan)." Journal of Asian Earth Sciences **21**: 265-282.

Peucat, J. J., E. Ruffault, et al. (2005). "A new geochemical tool to separate basaltic from metamorphic blue sapphires." Goldschmidt Conference Abstracts **A287**.

Riesco, M., K. Stuwe, et al. (2004). "Silica depleted melting of pelites. Petrogenetic grid and application to the Susqueda Aureole, Spain." Journal of Metamorphic Geology **22**(5): 475-494.

Roedder, E. (1984). Fluid Inclusions. Reston, Mineralogical Society of America.

Saminpanya, S., D. A. C. Manning, G. T. R. Droop and C. M. B. Henderson (2003). "Trace elements in Thai gem corundums." Journal of Gemmology **28**(7): 319-415.

Schwarz, D., & Stern, W.B., (2000). Chemical finger printing as a tool for characterisation of gem corundums from different genetic environments. Abstracts Volume, 31st International Geological Congress 16-17 August, Rio de Janiero, Brazil.

Sharp, Z. D. (1990). "A laser-based microanalytical method for the in situ determination of oxygen istope ratios of silicates and oxides." Geochimica Et Cosmochimica Acta **54**: 1353-1357.

Smith, D. G. W. (1965). "The chemistry and mineralogy of some emery-like rocks from Sithean Sluaigh, Strachur, Argyllshire." American Mineralogist **50**(11-12): 1982-2022.

Srithai, K. R., asddsa, et al. (1998). "Fluid inclusions in thai sapphires." Abstract from the Geological Society of Thailand: 37pp.

Stephenson, P. J. (1976). "Sapphire and zircon in some basaltic rocks from Queensland, Australia." Abstracts of the 25th International Geological Congress **2**: 602-603.

Stephenson, P. J. (1990). "The geological context of sapphire occurences in the Anakie region, central Queensland." Geological Society of Australia: Abstracts **25**: 232-233.

Sutherland, F. L., G. Bosshart, C. M. Fanning, P. W. O. Hoskin and R. R. Coenraads (2002). "Sapphire crystallization, age and origin, Ban Huai Sai, Laos: age based on zircon inclusions." Journal of Asian Earth Sciences **20**(7): 841-849.

Sutherland, F. L. and P. Wellman (1986). "Potassium-argon ages of Tertiary volcanic rocks, Tasmania." Papers of the Proceedings of the Royal Society of Tasmania **120**: 77-86.

Sutherland, F. L., I. Graham, J. L. Everard, S. M. Forsyth and H. Zwingmann (2004). Cenozoic basalts, Tasmania: Landscapes, exposures, ages, petrography, geochemistry, entrainments and petrogenesis. 17th Australian Geological Convention, Hobart, Tasmania.

Sutherland, F. L., P. W. O. Hoskin, C. M. Fanning and R. R. Coenraads (1998a). "Models of corundum origin from alkali basaltic terrains: a reappraisal." Contributions to Mineralogy and Petrology **133**(4): 356-372.

Sutherland, F. L., Pogson and Barron, B. J. (1998b)."Discussion and reply. Plaeogeothermal gradients in Australia; key to 4-D lithospheric mapping, S.Y. O'Reilly, W.L. Griffin & Gaul, O." Australian Journal of Earth Sciences. **45:** 817-821

Sutthirat, C., S. Saminpanya, G. T. R. Droop, C. M. B. Henderson and D. A. C. Manning (2001). "Clinopyroxene-corundum assemblages from alkali basalt and alluvium, eastern Thailand; constraints on the origin of Thai rubies." Mineralogical Magazine **65**(2(429)): 277-295.

Themelis, T. (1992). The heat treatment of ruby and sapphire. Houston, Texas, Gemlab Inc.

Turner, N.J. (1980). A summary of the geology of north eastern Tasmania. In Abstract. Coal. Tin. Surficial deposits and Geology of North East Tasmania. Geol. Soc. Aus., 1, 2-6.

Upton, B. G. J., R. W. Hinton, P. Aspen, A. Finch and J. W. Valley (1999). "Megacrysts and associated xenoliths: Evidence for migration of geochemically enriched melts in the upper mantle beneath Scotland." Journal of Petrology **40**(6): 935-956.

Vichit, P. (1978). "The distibution and some characteristics of corundum bearing basalts in Thailand." Journal of the Geological Society of Thailand(3): M4.1-M4.38.

Valley, J. W., N. M. Matthew, J. Kohn, C. R. Niendorf and M. J. Spicuzza (1995). "UWG-2, a garnet standard for oxygen isotope ratios: strategies for high precision and accuracy with laser heating." Geochimica Et Cosmochimica Acta **59**: 5223-5231.

Watson, E. B. (1980). "Some experimentally determined zircon/liquid partition coefficients for the rare earth elements." Geochimica Et Cosmochimica Acta **44**: 895-897.

Wells, A. J. (1956). "Corundum from Ceylon." Geological Magazine **93**(1): 25-31.

Wellman, P & MacDougall, I. (1974). Potassium-argon ages on the Cainozoic volcanic rocks of NSW. Journal of the Geological Society of Australia. 21: 247-272.

Williams, I. S. and Hergt, J. M. (1998). "U-Pb dating of Tasmanian dolerites: A cautionary tale of SHRIMP analysis of high-U zircon." Abstract from "New Frontiers in Isotope Geoscience." 185-188.

Yim, W.W.S. (1980). "Heavy mineral studies of stanniferous deeps, north-east Tasmania. Rec. Bur. Min. Res. Geol. & Geophys. Aus., 1980/67, 81.

Yim, W., A. J. Gleadow and J. C. van Moort (1985). "Fission track dating of alluvial zircons and the heavy mineral provenance in Northeast Tasmania." Journal of the Geological Society of London **142**: 351:356.

Yui, T. F. (2000). "Pleminary results on CO_2 laser-fluorination system for O-isotope microanalysis of silicate/oxide grain seperates." Journal of the Geological Society of China **43**: 237-246.

Yui, T. F., Khin. Zaw and P. Limtrakun (2003). "Oxygen isotope composition of the Denchai sapphire, Thailand: a clue to its enigmatic origin." Lithos **67**(1-2): 153-161.

Zheng, Y. F. (1993). "Calculation of Oxygen Isotope Fractionation in Anhydrous Silicate Minerals." Geochimica Et Cosmochimica Acta **57**(5): 1079-1091.

Zaw, Khin, Limtrakun, P., Yui, T.F., Ryan, C.G., Mernagh, T.P. (2002). "Mineral Chemistry, Oxygen Isotopes and Fluid/Melt Inclusion Studies Bearing on the Genesis of The Denchai Sapphires, Northern Thailand", *Proceedings*, Bangkok, Thailand, 309-314

Appendix 1

Basalt Petrography

MLC1 (5437550N, 580490E)

This sample is porphyritic with visible olivine. Phenocrysts make up 35% of the rock and consist of olivine (<10%), plagioclase (10-15%) and clinopyroxene (titanaugite, 5%). The euhedral olivine crystals (0.9-1.2mm) display a wide range of serpentinisation; no alteration, at the rims only, or total serpentinisation and zeolite replacement of the olivine ghost. This serpentinisation produces fine grained opaque magnetite within the crystal. Plagioclase laths (up to 1.5mm) have strong flow alignment and have a Michel-Levy composition of $An_{60}Ab_{40}$. The pink-brown euhedral pyroxene crystals (<1.5mm) exhibit high dispersion at extinction and are typical of titanaugite phenocrysts.

The groundmass is much finer grained (<0.03mm) and consists of plagioclase (35%), clinopyroxene (30%), olivine (10%) and opaques (magnetite or ilmenite, 20%). The plagioclase laths (<0.05mm) are not oriented. The brown clinopyroxene crystals (0.3mm) are tabular and all even in size and shape. Euhedral to subhedral olivine microphenocrysts (0.04mm) have high birefringence. The opaques are ubiquitous in the thin section with no obvious arrangement or alignment (<0.4mm).

Highly serpentinised anhedral olivine xenocrysts (4mm) exhibit embayment by the magma, some reaction rimming and infilling of zeolites.

MLC2(X) (5437200N, 580460E)

This sample is microporphyritic. Phenocrysts make up 15% of the rock and consist of olivine (>7%), plagioclase (<4%) and clinopyroxene (titanaugite?, 7%). The subhedral-euhedral olivine crystals (0.3-0.8mm) display heavily serpentinised rims. This serpentinisation produces fine grained opaque magnetite at the edges of the crystal. Plagioclase laths (up to 0.3mm) have no flow. Brown euhedral pyroxene crystals (0.2-0.4mm) are present.

The phenocrysts range into the groundmass (0.05-0.08mm) and consists of plagioclase (35%), clinopyroxene (35%), olivine (10%) and opaques (magnetite or ilmenite, 20%). The altered plagioclase laths (<0.05mm) are not oriented. The brown clinopyroxene crystals (0.8mm) are

tabular and all even in size and shape. Euhedral to subhedral glassy olivine microphenocrysts (0.04mm) have high birefringence. The opaques are ubiquitous in the thin section with no obvious arrangement or alignment (<0.4mm).

Highly serpentinised anhedral olivine+feldspar xenocrysts (<2mm) are present along with a large (8mm) anhedral clinopyroxene+plagioclase xenocryst with brown (chromite/sphene) inclusions.

MLC2X (same location) is porphyritic to microphenocrystic and contains a large (>10cm) plagioclase+clinopyroxene+orthopyroxene xenolith. It has a gabbroic texture and a CPX+OPX intergrowth. Plagioclase in this xenolith has a Michel-Levy composition of $An_{60}Al_{40}$. The xenolith has a knife edge contact with enclosing basalt.

MLC3 (5436983N, 580412E)

This sample is porphyritic to microporphyritic. Phenocrysts make up 25% of the rock and consist of olivine (<10%) and clinopyroxene (titanaugite, 15%). Euhedral-subhedral olivine crystals (<0.9mm) are present. Plagioclase is not present as phenocryst. Abundant pink-brown euhedral pyroxene crystals (0.06-0.45mm) exhibit high dispersion at extinction and are typical of titanaugite phenocrysts. This CPX
is also present as **glomerocrysts** in this slide.

The groundmass is much finer grained (<0.04-0.08mm) and consists of plagioclase (40%), clinopyroxene (30%), olivine (5%) and opaques (magnetite or ilmenite, 20%). The plagioclase laths (<0.08mm) are oriented to "mantle" the phenocrysts. The brown clinopyroxene crystals (0.03-0.08mm) are tabular and all even in size and shape. Euhedral to subhedral olivine microphenocrysts (0.04mm) have high birefringence. The opaques are ubiquitous in the thin section with no obvious arrangement or alignment (<0.4mm).

Heavily altered and cracked euhedral olivine xenocrysts (<2.0mm) are present.

MLC4 (5436738N, 580459E)

This sample is microporphyritic to aphanitic. Phenocrysts make up 10-15% of the rock and consist of olivine (10-15%), plagioclase (5%) and clinopyroxene was not recognised in this slide. The anhedral-subhedral olivine phenocrysts (0.2-0.4mm) display an iddingsite weathering rim and a degree of serpentinisation. Some olivine shows zoning. Plagioclase laths (0.1-0.2mm) have little flow alignment.

The groundmass is of similar size (<0.02-0.1mm) and consists of plagioclase (35%), clinopyroxene (20%), opaques (magnetite or ilmenite, 10%) and olivine is not present. The plagioclase laths (0.1mm) are not oriented. The brown clinopyroxene crystals (0.02-.1mm) are tabular and all even in size and shape. For an alkali basalt, olivine is not present in the groundmass. The opaques are ubiquitous in the thin section with no obvious arrangement or alignment (<0.4mm).

The sample is vesicular, with infilling zeolite minerals.

MLC5 (5436325N, 580490E)

This sample is porphyritic with visible olivine. Phenocrysts make up 20% of the rock and consist of olivine (15%), plagioclase (<1%) and clinopyroxene (titanaugite, <1%). The euhedral-subhedral olivine crystals (0.35-4mm) are altered and have iddingsite+magnetite rimming. Plagioclase laths (up to 0.35mm) exhibit little alignment. The brown euhedral pyroxene crystals (<0.5mm) are rare.

The groundmass is much finer grained (<0.06-0.1mm) and consists of plagioclase (60%), clinopyroxene (20%), olivine (10%) and opaques (magnetite or ilmenite, 10%). The plagioclase laths (<0.1mm) are not oriented. The brown clinopyroxene crystals (0.06mm) are tabular and all even in size and shape. Euhedral to subhedral olivine microphenocrysts (0.04mm) have high birefringence. The opaques are ubiquitous in the thin section with no obvious arrangement or alignment (<0.4mm).

Heavily altered and cracked euhedral olivine xenocrysts (<2.0mm) are present.

THB1a, b (5433854N, 579347E)

This sample is porphyritic with visible olivine. Phenocrysts make up 25-35% of the rock and consist of olivine (20%), plagioclase (5-10%) and clinopyroxene (titanaugite, <5%). The euhedral-subhedral olivine crystals (0.8-3mm) display serpentinised rims. Seriate plagioclase laths (0.2-0.8mm) have no flow arrangement. The dirty brown euhedral pyroxene crystals (<1.4mm) exhibit high dispersion at extinction and are typical of titanaugite phenocrysts. Some CPX shows zoning and formation of aggregates (**glomerocrysts**)

The groundmass is fine grained (<0.1mm) and consists of plagioclase (45%), clinopyroxene (25%), olivine (<10%) and opaques (magnetite or ilmenite, 10%). The plagioclase laths (<0.05mm) are not oriented. The brown clinopyroxene crystals (0.3-0.6mm) are tabular and all even in size and shape. Euhedral to subhedral olivine microphenocrysts (0.08mm) are altered to green chlorite. The opaques are ubiquitous in the thin section with no obvious arrangement or alignment (<0.4mm).

Highly serpentinised anhedral olivine xenocrysts (<4mm) exhibit embayment by the magma, some reaction rimming and infilling of zeolites.

THB2a, b, c (5434820N, 579038E)

This sample is microporphyritic to aphanitic. Phenocrysts make up 5-10% of the rock and consist of olivine (5%), plagioclase (5%) and clinopyroxene (titanaugite, <1%). The euhedral-subhedral olivine phenocrysts (0.2-0.9m) display an iddingsite weathering rim on the larger phenocrysts. Seriate plagioclase laths (0.2mm) have little flow alignment. The cloudy brown euhedral pyroxene crystals (<0.2mm) exhibit high dispersion at extinction and are typical of titanaugite phenocrysts.

The groundmass is fine grained (<0.1-0.2mm) and consists of plagioclase (35%), clinopyroxene (35%), olivine (10%) and opaques (magnetite or ilmenite, 10%). The plagioclase laths (<0.05mm) show alignment in some areas of the slide. The brown perfectly euheral clinopyroxene crystals (<0.5mm) are tabular and all even in size and shape. Euhedral to subhedral olivine microphenocrysts (0.08mm) are in some places altered to chlorite. The opaques are ubiquitous in the thin section with no obvious arrangement or alignment (<0.4mm).

Serpentinised anhedral olivine xenocrysts (<4mm) exhibit reaction rimming.

A clinopyroxene xenocryst (1.8mm) is present in the rock and show a thin reaction rim on the edge as well as zonation within the crystal. A large opaque (spinel, magnetite, ilmenite?) cube (8x8mm) was found with plagioclase laths mantling the grain edge. An anhedral olivine cumulate xenolith with minor interstitial clinopyroxene (>3cm) was found in the slide. A euhedral to subhedral olivine xenocryst (0.8mm) was identified in this slide.

THB3, c (534441N, 579285E)

This sample is porphyritic to microporphyritic. Phenocrysts make up 25-30% of the rock and consist of olivine (10%), clinopyroxene (titanaugite, 5-10%) and plagioclase (10-15%). Euhedral-subhedral olivine crystals (0.4-0.5mm) are present with some being totally altered to chlorite with serpentinite rims. Seriate plagioclase laths and some euhedral crystals (0.2-1.8mm) exhibit no flow alignment and yellow birefringence (anorthite). Brown euhedral pyroxene crystals (0.4-1.8mm) exhibit high dispersion at extinction and are typical of titanaugite phenocrysts.

The groundmass (<0.02mm) consists of abundant plagioclase (40%)clinopyroxene (10-30%), olivine (<5%) and opaques (magnetite or ilmenite, 20%). The plagioclase laths (<0.2mm) have no alignment. The brown clinopyroxene crystals (0.2mm) are tabular and all even in size and shape. Euhedral to subhedral olivine microphenocrysts (0.6-0.9mm) are almost totally chloritised. The opaques are ubiquitous in the thin section with no obvious arrangement or alignment (<0.4mm).

Clinopyroxene xenocrysts (1.8-2mm) are present in the rock and show a thin reaction rim on the edge. **THB3c** contains a large (>3cm) rounded feldspar xenolith which shows little reaction rimming with enclosing basalt. The edge does however appear to contain minimal chlorite alteration.

FQ1 (5435800N, 581000E)

This sample is porphyritic to microporphyritic. Phenocrysts make up 10-15% of the rock and consist of olivine (10-12%), clinopyroxene (titanaugite, <2%) and seriate plagioclase (<3%). Euhedral-subhedral olivine crystals (0.3-1.8mm) are present, and some suffer from

serpentinisation. Seriate plagioclase laths (0.3mm) exhibit strong flow alignment. Pink-brown euhedral pyroxene crystals (0.2-0.3mm) are typical of titanaugite phenocrysts.

The groundmass (<0.1mm) consists of abundant plagioclase (30-40%), clinopyroxene (30%), olivine (<5%) and opaques (magnetite or ilmenite, 20%). The plagioclase laths (0.04-0.1 mm) have some alignment. The brown clinopyroxene crystals (0.05mm) are euhedral. Euhedral to subhedral olivine microphenocrysts (0.3mm) are present. The opaques are ubiquitous in the thin section with no obvious arrangement or alignment (<0.4mm).

There is a large rounded **feldspar cumulate** xenocryst (6cm) present in the rock. Individual feldspar crystals are up to 1cm. The xenocryst has a fine opaque reaction rim.

FQ2 (5435800N, 581000E) –Zeolite structure

This sample is locally porphyritic to microporphyritic and heavily altered. This level of alteration is related to the vesicularity and is also represented by the extensive zeolite infillings. Phenocrysts make up 20% of the rock and consist of olivine (10%), clinopyroxene (titanaugite, 5%) and seriate plagioclase (<2%). Euhedral olivine crystals (bimodal: 0.4mm, 1.8-2.0mm) are present, and some suffer from severe serpentinisation. Seriate plagioclase laths (0.2mm) exhibit patchy flow alignment and range in size down to the matrix. Heavily altered pink-brown euhedral pyroxene crystals (0.3mm) are typical of titanaugite phenocrysts.

The groundmass (<0.1mm) consists of abundant plagioclase (30-40%), clinopyroxene (30%), olivine (<5%) and opaques (magnetite or ilmenite, 20%). The plagioclase laths (0.04-0.1 mm) have some alignment. The brown clinopyroxene crystals (0.05mm) are euhedral. Euhedral to subhedral olivine microphenocrysts (0.3mm) are present. The opaques are ubiquitous in the thin section with no obvious arrangement or alignment (<0.4mm).

BSW1 (5437416N, 574700E)

This sample is porphyritic with visible olivine. Phenocrysts make up 40% of the rock and consist of olivine (15%), plagioclase (5-10%) and clinopyroxene (titanaugite, 10-15%). Euhedral clear to brown olivine crystals (0.7-1.2mm) display serpentinised rims and where

alteration has destroyed the crystal, zeolites have filled the cavity. The clear olivine crystals have higher birefringence than the dirty brown crystals. Seriate textured plagioclase laths (0.1-0.7mm) have no flow arrangement. The brown euhedral pyroxene crystals (0.4-1.8mm) exhibit zonation and some twinning and are typical of titanaugite phenocrysts.

The groundmass is fine grained (0.04-0.1mm) and consists of plagioclase (40%), clinopyroxene (~10-20%), olivine (<10%) and opaques (magnetite or ilmenite, 20%). The plagioclase laths (0.04mm) are not oriented. The brown clinopyroxene crystals (0.3-0.6mm) are tabular and all even in size and shape. Euhedral to subhedral olivine microphenocrysts (0.08mm) are altered to green chlorite. The opaques are ubiquitous in the thin section with no obvious arrangement or alignment (0.8-1mm).

Anhedral olivine xenocrysts (0.8-4mm) with iddingsite rims are present. In one xenocryst, a **symplectite (myrmikite)** texture is present with elongate ovoid replacement of olivine to plagioclase and glass?

BSW2 (5436679N, 574082E)

This sample is weakly porphyritic with visible olivine. Phenocrysts make up 20% of the rock and consist of olivine (15%), plagioclase (<5%) and clinopyroxene (titanaugite, <5%). Euhedral-subhedral clear olivine crystals (0.4-0.9mm) display serpentinised rims (20% are serpentinised) and some have been totally replaced by chlorite. Elongate plagioclase laths (0.3-0.6mm) have flow alignment in some areas of the slide and no arrangement in the other areas. The brown euhedral pyroxene crystals (0.7mm) are heavily cracked.

The groundmass (0.04-0.1mm) consists of plagioclase (60%), clinopyroxene (5%), olivine (<5%) and opaques (magnetite or ilmenite, 20%). The plagioclase laths (0.01-0.3mm) are not oriented. The brown clinopyroxene crystals (0.3-0.6mm) are tabular and all even in size and shape. Euhedral to subhedral olivine microphenocrysts (0.02mm) are present but rare. The opaques are ubiquitous in the thin section with no obvious arrangement or alignment with two sizes: <0.2mm and 0.6-0.8mm.

A rounded feldspar phenocryst (8-9mm) is present in this sample. It has undulose extinction on the broad twinning. There is some reaction rimming.

BSW3 (5439331N, 574645E)

This sample is porphyritic with visible olivine. Phenocrysts make up 30% of the rock and consist of olivine (12%), plagioclase (10%) and clinopyroxene (titanaugite, 8%). The euhedral olivine crystals (0.8-1.6mm) can show cracking and calcite? infills these cracks. Plagioclase laths (0.6-1mm) have no flow alignment and have a Michel-Levy composition of $An_{45}Ab_{55}$. The pink-brown euhedral pyroxene crystals (0.4-0.9mm) exhibit twinning and concentric and lamellar zoning.

The groundmass is much finer grained (<0.1mm) and consists of plagioclase (40%), clinopyroxene (15%), olivine (10%) and opaques (magnetite or ilmenite, 20%+). The plagioclase laths (<0.1mm) are not oriented. Small clinopyroxene crystals (<0.1mm) are tabular and all even in size and shape. Euhedral olivine microphenocrysts (0.06mm) have high birefringence. The opaques are ubiquitous in the thin section with no obvious arrangement or alignment (<0.4mm).

Highly fractured and irregular olivine cumulate xenocrysts (9mm) exhibit some reaction rimming. Interstitial clinopyroxene (10%) is present in the cumulate. An unusual **irregular quartz xenocryst** (10mm) is present in the slide. This xenocryst has its boundaries breaking down to glass (radial needles) as the reaction rim.

FL4 (5430031N, 575528E)

This sample is porphyritic with visible olivine. Phenocrysts make up 40% of the rock and consist of olivine (15%), plagioclase (15%) and clinopyroxene (titanaugite, 5%). The euhedral-subhedral olivine crystals (0.7-4mm) exhibit varying degrees of serpentinisation. Seriate plagioclase laths (0.3-0.8mm) have areas of flow alignment. The pink-brown euhedral pyroxene crystals (0.5-0.9mm) exhibit some twinning. Some of the CPX forms as aggregates **(glomerocrysts).**

The groundmass is much finer grained (<0.1mm) and consists of plagioclase (40%), clinopyroxene (20%), olivine (<2%) and opaques (magnetite or ilmenite, 20%). The plagioclase laths (<0.1mm) are not oriented. Small clinopyroxene crystals (<0.1mm) are

tabular and all even in size and shape. Euhedral olivine microphenocrysts (0.02mm) have high birefringence. The opaques are ubiquitous in the thin section with no obvious arrangement or alignment (<0.4mm).

A euhedral to subhedral cracked olivine xenocryst (0.8mm) was identified in this slide.

SVD (MH1) (5444450N, 570650E)

This sample is porphyritic with visible olivine. Phenocrysts make up 15-20% of the rock and consist of olivine (5-10%) and clinopyroxene (<2%). The euhedral-subhedral olivine crystals (0.4-1mm) display little or no serpentinisation. Plagioclase phenocrysts are absent in this sample. The clear euhedral clinopyroxene microphenocrysts (<0.6mm) are not is titanium rich as others and is probably just augite. The pyroxene also shows a rare stripy birefringence.

Nepheline is probably present and further techniques will determine this.

The groundmass is much finer grained (<0.03mm) and consists of clinopyroxene (70%), plagioclase (10%), olivine (10%) and opaques (magnetite or ilmenite, 10%). The plagioclase laths (<0.04mm) are not oriented. Abundant brown clinopyroxene crystals (0.05mm) are tabular and all even in size and shape. Euhedral to subhedral olivine microphenocrysts (0.04mm) have high birefringence. The opaques are ubiquitous in the thin section with no obvious arrangement or alignment (<0.2mm).

Anhedral olivine xenocrysts (0.3-7mm) exhibit concentric zonation and have brown inclusions (**sphene, chromite?).**

GH1a (5439915N, 564743E)

This sample is microporphyritic. Phenocrysts make up <15% of the rock and consist of olivine (10-12%), plagioclase (3-5%) and clinopyroxene is absent. The euhedral-subhedral olivine phenocrysts (0.09-0.9m) display an iddingsite weathering rim on the larger phenocrysts with opaque inclusions. Seriate plagioclase laths (0.1-0.8mm) have little flow alignment.

The groundmass is fine grained (<0.1mm) and consists of plagioclase (60%), clinopyroxene (<10%), olivine (<5%) and opaques (magnetite or ilmenite, 10+%). The plagioclase laths (0.02-0.1mm) show partial flow alignment in some areas of the slide. The brown euhedral clinopyroxene crystals (<0.01mm) are difficult to identify due to their fineness. Euhedral to subhedral olivine microphenocrysts (0.02mm) have heavily altered rims. The opaques are ubiquitous in the thin section with no obvious arrangement or alignment (<0.4mm).

Serpentinised anhedral olivine xenocrysts (<1mm) are present.

An irregular feldspar xenocryst (0.6mm) is heavily altered although still recognizable from twinning and birefringence.

GH1b (5439915N, 564743E)

This sample is porphyritic with visible olivine. Phenocrysts make up 15-20% of the rock and consist of olivine (8-10%), plagioclase (<1%) and clinopyroxene (titanaugite, 2-5%). The euhedral olivine crystals (0.1-0.7mm) are altered and have iddingsite+magnetite rimming. The seriate brown euhedral pyroxene crystals (<0.4mm) are present and some occur as elongate twinned crystals. Plagioclase is a rare phase.

The groundmass is much finer grained (0.18mm) and consists of plagioclase (10%), abundant clinopyroxene (70%), olivine (10%) and opaques (magnetite or ilmenite, 10%). The plagioclase laths (<0.1mm) are not oriented. The brown clinopyroxene crystals (0.18mm) are tabular and all even in size and shape. Euhedral to subhedral olivine microphenocrysts (0.18mm) have high birefringence. The opaques are ubiquitous in the thin section with no obvious arrangement or alignment (<0.4mm).

An anhedral olivine xenocryst (9mm) is present. It has zoning and a cpx inclusion which shows segmented extinction.

An anhedral orthopyroxene (hypersthene?) xenocryst (1.4mm) is present in the slide. It is heavily altered to fine grained olivine. It has large brown linear intergrowths (exsolution lamellae – sphene or chromite?).

TG1 (5443280N, 606860E)

This sample is aphanitic. Microphenocrysts make up 10% of the rock and consist of olivine (10%) and clinopyroxene (5%). The euhedral-subhedral olivine phenocrysts (0.18-1.4m) display a wide range of serpentinisation with some grains totally serpentinised with magnetite associated magnetite growth. The long edges of the olivine grains are aligned with the aligned feldspar laths. The dusty euhedral clinopyroxene microphenocrysts (0.4mm) are not is titanium rich as in other slides, also the maximum dispersion is low. The pyroxene is probably augite.

The groundmass is very fine grained (0.01-0.5mm) and consists of flow aligned plagioclase (70%), clinopyroxene (<10%), olivine (<10%) and opaques (magnetite or ilmenite, 10+%). The seriate plagioclase laths (0.02-0.5mm) show flow alignment and have a Michel-Levy composition of $An_{44}Ab_{56}$. The brown euhedral clinopyroxene crystals (<0.05mm) are difficult to identify due to their fineness. Euhedral to subhedral olivine microphenocrysts (<0.2mm) are present. The opaques are ubiquitous in the thin section with no obvious arrangement or alignment (<0.4mm).

Anhedral (rounded) olivine xenocrysts (1-4mm) are present. They have little serpentinisation, minor reaction rims and contain other olivine inclusions. The plagioclase laths mantle the grain boundaries and after one layer are perpendicular to the grain boundaries. Opaques are also present as exsolved? inclusions.

Appendix 2

Photomicrographs of basalt

Appendix 3
Geochemistry

Appendix 4
LRS Spectra

Appendix 5
LA-ICPMS results

Appendix 6
Literature Review: "Corundum Occurrence"